FTIR-ATR spectroscopic and FTIR-FPA microscopic investigations on panel board production processes using Grand fir (*Abies grandis* (Douglas ex D. Don) Lindl.) and European beech (*Fagus sylvatica* L.)

DISSERTATION

In Partial Fulfillment of the Requirements for the Doctoral Degree (Dr. forest.)
of the Faculty of Forest Sciences and Forest Ecology of the
Georg-August University of Göttingen, Germany

Submitted by

Günter Stefan Müller
Born in Oberviechtach, Germany
Göttingen, April 2008

Referee: **Prof. Dr. Andrea Polle**

Co-referee: **Prof. Dr. Stefan Schütz**

Table of contents

Summary

Global warming and climate change affect the composition of German forests and require the reconstruction of domestic forest stands. As a consequence, long-term goals of forestry are the reconstruction of monospecific forests into mixed stands with an increase of broad leaved tree species. Therefore, the ratio of European beech (*Fagus sylvatica* L.) is continuously increasing. Furthermore, there is rising demand of woody biomass, which requires introduction of species with high growth potential and stress tolerance to enable sustainable cultivation in a changing climate.

Grand fir (*Abies grandis* (Douglas ex D. Don) Lindl.) is a fast growing but nation-wide still unknown tree species. Since it is ecologically compatible with the domestic tree species and is known to be drought tolerant, it offers the potential to being introduced into sustainable forest stands with beech. However, there is little to no experience of industry in processing wood of Grand fir to derived timber products. Especially for industrial wood use, knowledge on the chemical composition of raw materials, intermediate and final products is of great importance.

The overarching goal of this thesis was to contribute information on wood properties and chemical changes during the development of innovative wood-based panels of Grand fir and European beech using Fourier transform infrared (FTIR) attenuated total reflectance (ATR) spectroscopy and FTIR microscopy combined with a focal plane array detector (FPA).

For this purpose, different types of lignin and cellulose were characterized by means of FTIR spectroscopy. FTIR-ATR analyses of chemical modifications of Grand fir and beech wood during processing to novel derived timber products were accomplished to enable the control of production processes. A further goal was to introduce FTIR microscopy as a novel method for illustrating the spatial distribution of chemical components in wood tissue.

To address these goals, novel wood-based panels, such as medium density fiberboards (MDF), insulating wood fiberboards and particleboards, composed of beech and Grand fir solid wood were produced and analyzed by FTIR-ATR spectroscopy. This held true for solid wood as raw material and fibers and particles as intermediate wood products. Furthermore, binders, such as potato pulp and potato starch, melamine-urea-formaldehyde (MUF) - and urea-formaldehyde (UF) -resin, both admixed with paraffin, were investigated with ATR. To characterize chemically different types of lignin and cellulose, technical and acid-insoluble Klason lignin as well as industrial produced cellulose were analyzed by means of FTIR-ATR.

The obtained spectra were evaluated in two different ways; first, the bands of the FTIR spectra were interpreted directly and tentatively assigned to chemical compounds, based on published data. Subsequently, the FTIR-ATR spectra were investigated with multivariate methods. Cluster analysis as an unsupervised and unbiased statistical method was used to analyze the intrinsic relationships of the samples, based on their spectral heterogeneity. Furthermore, principle component analysis (PCA) was applied to identify wavenumbers of the main spectral components responsible for differences between the spectra.

FTIR microscopy combined with a focal plane array (FPA) detector was used to analyze the localization of chemical components in wood sections of Grand fir and European beech. The obtained spectral data were evaluated with two independent methods. To image lignin and cellulose a wavenumber range typical for lignin (1530-1490 cm^{-1}) or for cellulose (1390-1350 cm^{-1}) was integrated. The second method, called correlation method, was applied as novel method for evaluating the FPA data set. The spectra of one FPA measurement were correlated with a pure ATR reference spectrum of the chemical component of interest. For both evaluation methods, the resulting FTIR-FPA images were illustrated in color coded images, respectively, revealing the spatial distribution of the component of interest. Subsequently, the FPA images were validated by Scanning transmission electron microscopy (STEM) combined with Energy dispersive X-ray spectroscopy (EDX) as an independent optical method. Lignin was labeled with mercury (Hg) and detected indirectly by determining Hg in early and latewood cells of Grand fir solid wood sections with STEM-EDX. EDX-mappings were recorded for the similar sample area as for the FPA measurements, but with much higher resolution. Furthermore, TEM-EDX point measurements were generated to analyze the lignin content in different cell compartments.

Spectroscopic analyses on the processing of Grand fir and beech solid wood to different types of wood-based panels revealed changes in the recorded ATR spectra, depending on the particular production step. In general, differences in the absorbance units, band positions or number of bands were identified and tentatively assigned to lignin and holocellulose.

In the medium dense fiberboards (MDF) and particleboards, the added binder and heat treatment during the pressing process modified the chemical compounds in the plates compared to the intermediate wood products. This was visible e.g. in significant deviations of the methyl- and methylene groups (2938, 2882 cm^{-1}) caused by the admixed paraffin. Secondary amides as derivatives of the MUF- and UF resin were identifiable in MDF and particleboards. Spectra of the insulating wood fiberboards revealed chemical modifications especially at the O-H association band of carbohydrates, which enabled the differentiation of

conventional and microwave drying of the fiber mats. Additions of plant-based renewable adhesives diminished the spectral absorbance of the resulting products and were significantly correlated with the amount of added binder. Cluster analysis and PCA as multivariate methods enabled a differentiation between hard- and softwood, raw material and final product.

Based on the results obtained during the investigations on panel board processing of beech and Grand fir, it is concluded that FTIR spectroscopy combined with multivariate data analysis can be used to support the optimization and control of production processes. Petro-chemical and bio-based additives can be determined and separated, as well as the influences of the particular production processes on the chemical composition of wood. Thus, the technique enables quality control of innovative wood-based panels as well as that of other wood products.

Furthermore, the FTIR-ATR technique was used to identify significant deviations in the spectra of different lignin types, visible in different band positions and a varying number of bands. This enabled the separation of technical and acid-insoluble lignin by direct spectra interpretation. FTIR-ATR measurements of the different types of cellulose resulted in similar spectra. Despite very low spectral heterogeneity evaluation by cluster analysis enabled a separation of the lignin and cellulose, respectively.

FTIR-FPA microscopy was used to investigate the localization of chemical components in solid wood sections of Grand fir and European beech. The spatial distribution of cellulose was homogenously. However, areas with slightly higher accumulation of cellulose were identifiable. This held true for both tree species. High lignin contents were detected especially in the area of the middle lamellae, the angles of the cells and in the wood rays. STEM-EDX mappings, used for illustrating the spatial distribution of lignin in woody cell walls at high resolution, confirmed the results obtained by FTIR microscopy. This held true for the TEM-EDX point measurements, which identified the highest lignin content in the compound middle lamellae.

The results of this thesis contribute to widen the application of FTIR spectroscopic techniques in wood processing and for quality control. This opens new fields of FTIR application, particularly in investigating the processing of conventional and bio-based wood products. The results support that Grand fir is suitable for utilization in derived timber products industry for novel products and may contribute to stimulate an increased cultivation of this tree species in domestic forestry.

Zusammenfassung

Die globale Erwärmung und der Klimawandel beeinflussen die Zusammensetzung der Wälder in Deutschland und erfordern den Umbau heimischer Waldbestände. Daraus ergeben sich als langfristige Ziele im Hinblick auf die Forstwirtschaft unter anderem der Umbau von Monokulturen zu nachhaltig bewirtschafteten Mischbeständen und die Erhöhung des Anteils von Laubgehölzen. Damit verbunden ist das kontinuierliche Anwachsen des Anteils der Buche (*Fagus sylvatica* L.). Des Weiteren gibt es eine wachsende Nachfrage für Biomasse aus Holz, was die Einführung schnell wachsender Arten mit hoher Stresstoleranz erfordert, mit dem Ziel, nachhaltigen Waldbau während des Klimawandels zu ermöglichen.

Die Küstentanne (*Abies grandis* (Douglas ex D. Don) Lindl.) ist eine schnell wachsende, aber in Deutschland noch immer unbekannte Baumart. Da sie ökologisch mit heimischen Baumarten gut verträglich und bekannt für ihre Trockenheitstoleranz ist, hat sie das Potential, um in nachhaltig bewirtschaftete Forstbestände von Buche eingebracht zu werden. Es besteht jedoch wenig bis keine Erfahrung der Industrie in der Verarbeitung des Holzes von Buche und Küstentanne zu zusammengesetzten Holzwerkstoffen. Besonders für die industrielle Verwendung des Holzes ist das Wissen um die chemische Zusammensetzung von Rohmaterial, Zwischen- und Endprodukten von großer Wichtigkeit.

Das übergreifende Ziel dieser Arbeit war es, unter Verwendung der Fourier transform infrarot (FTIR) attenuated total reflectance (ATR) Spektroskopie und der FTIR-Mikroskopie kombiniert mit einem Focal plane array Detektor (FPA) zur Information über Holzeigenschaften und chemische Veränderungen während der Entwicklung neuartiger Holzwerkstoffe aus Küstentanne und Buche beizutragen.

Zu diesem Zweck wurden unterschiedliche Arten von Lignin und Cellulose mit Hilfe der FTIR-Spektroskopie charakterisiert. FTIR-ATR-spektroskopische Analysen von chemischen Veränderungen von Küstentanne und Buche während der Produktion zu neuartigen Holzwerkstoffen wurden durchgeführt, um die Kontrolle des Produktionsprozesses zu ermöglichen. Ein weiteres Ziel war es, die FTIR-Mikroskopie als neue Methode zur bildlichen Darstellung der räumlichen Verteilung von chemischen Komponenten in Holz einzuführen.

Um diese Ziele zu erreichen wurden neuartige Holzwerkstoffe wie mitteldichte Faserplatten (MDF), Holzfaserdämmstoffplatten und Spanplatten aus Küstentanne und Buche zur Verfügung gestellt und mit FTIR-ATR-Spektroskopie analysiert. Dies galt auch für Vollholz als Rohmaterial und Fasern und Spänen als Zwischenprodukte. Des Weiteren

wurden die verwendeten Bindemittel wie Kartoffelpülpe und Kartoffelstärke, Melamin-Urea-Formaldehyd (MUF) und Urea-Formaldehyd (UF) -Harz, beide mit beigemischtem Paraffin, mit ATR untersucht. Um chemisch unterschiedliche Typen von Lignin und Cellulose zu bestimmen, wurden technisches und Klason Lignin ebenso wie industriell hergestellte Cellulose mit Hilfe von FTIR analysiert.

Die erhaltenen Spektren wurden auf zwei unterschiedliche Arten ausgewertet. Zunächst wurden die Banden der FTIR-Spektren direkt interpretiert und, basierend auf veröffentlichten Daten, den mutmaßlichen chemischen Komponenten zugeordnet. Nachfolgend wurden die FTIR-Spektren mit multivariaten Methoden untersucht. Die Clusteranalyse wurde als unabhängige statistische Methode verwendet, um die intrinsischen Verhältnisse der Proben aufgrund ihrer spektralen Heterogenität zu analysieren. Des Weiteren wurde die Hauptkomponentenanalyse (PCA) verwendet um die Wellenzahlen der spektralen Hauptkomponenten zu identifizieren, die für die Unterschiede zwischen den Spektren verantwortlich sind. Die FTIR-Mikroskopie mit einem Focal plane array (FPA) Detektor wurde verwendet, um die Verteilung der chemischen Komponenten in Holzschnitten von Küstentanne und Buche zu untersuchen. Die erhaltenen spektralen Daten wurden mit zwei unabhängigen Methoden ausgewertet. Um Lignin und Cellulose im Image darzustellen, wurde der typische Wellenzahlbereich für Lignin (1530-1490 cm^{-1}) oder für Cellulose (1390-1350 cm^{-1}) integriert. Die zweite, so genannte Korrelationsmethode, wurde als neue Methode zur Auswertung des FPA Datensatzes angewandt. Die Spektren einer FPA Messung wurden mit einem ATR Referenzspektrum der jeweilig interessierenden chemischen Komponente korreliert. Für beide Auswertungsmethoden wurden die resultierenden FTIR-FPA Images als farbkodierte Bilder dargestellt, welche die räumliche Verteilung der jeweiligen Komponente zeigten. Nachfolgend wurden die FPA Images mit der Raster-transmissionselektronenmikroskopie (STEM) als einer unabhängigen optischen Methode validiert. Lignin wurde mit Quecksilber markiert und indirekt durch die Bestimmung des Quecksilbers in Früh- und Spätholzzellen von Vollholzschnitten der Küstentanne mit STEM-EDX bestimmt. EDX-Mappings wurden für eine ähnliche Fläche der Probe aufgenommen wie für die FPA-Messungen, aber mit wesentlich höherer Auflösung. Des Weiteren wurden TEM-EDX Punktmessungen durchgeführt, um den Ligningehalt in den einzelnen Zellabschnitten zu analysieren.

Spektroskopische Analysen des Produktionsprozesses von Rohholz der Küstentanne und der Buche zu unterschiedlichen Holzwerkstoffplatten zeigten Veränderungen in den ATR-Spektren in Abhängigkeit vom jeweiligen Produktionsschritt. Unterschiede in den

Absorbance Units, der Position der Banden und der Bandenzahl konnten nachgewiesen und Lignin und Holocellulose zugeordnet werden.

Verglichen zu den Zwischenprodukten modifizierte das zugegebene Bindemittel die chemischen Verbindungen in den MDF und Spanplatten. Dies war z.B. in signifikanten Abweichungen der Methyl- und Methylengruppe (2938, 2882 cm^{-1}) sichtbar, die durch das beigegebene Paraffin verursacht wurden. Sekundäre Amide wurden als Derivate von MUF und UF-Harz in MDF und Spanplatten identifiziert.

Spektren der Holzfaserdämmstoffplatten enthüllten chemische Veränderungen besonders in der O-H Bande der Kohlenhydrate, was die Unterscheidung konventioneller Trocknung von Trocknung durch Mikrowellen ermöglichte. Die Zugaben von Klebern auf erneuerbarer Pflanzenbasis verminderte die spektrale Absorption der daraus resultierenden Produkte, was signifikant mit der Höhe des zugegebenen Bindemittels korrelierte. Clusteranalysen und PCA als unabhängige Methoden ermöglichten die Unterscheidung von Laub- und Nadelholz, dem Rohstoff Holz und dem Endprodukt.

Aus den Untersuchungsergebnissen zu den Produktionsschritten von Holzwerkstoffplatten aus Buche und Küstentanne kann man schließen, dass die FTIR-Spektroskopie kombiniert mit multivariater Datenanalyse verwendet werden kann, um die Optimierung und Kontrolle von Produktionsprozessen zu unterstützen. Des Weiteren ermöglicht die Technik die Qualitätskontrolle neuartiger Holzwerkstoffplatten, wie auch die von anderen Holzprodukten. Zusätze auf petrochemischer und biologischer Basis können spektroskopisch bestimmt und voneinander getrennt werden. Einflüsse auf das Holz, verursacht durch den jeweiligen Produktionsprozess, sind nachweisbar.

Des Weiteren wurde die beschriebene Technik dazu verwendet, signifikante Abweichungen in den Spektren der unterschiedlichen Typen von Lignin zu identifizieren, die in unterschiedlichen Positionen der Banden und deren Anzahl sichtbar wurden. Dies ermöglichte die Unterscheidung von technischem und säureunlöslichem Lignin durch direkte Spektreninterpretation. FTIR-ATR Messungen der unterschiedlichen Typen von Cellulose resultierten in ähnlichen Spektren. Trotz dieser sehr geringen spektralen Heterogenität war es mit Hilfe der Clusteranalyse möglich, innerhalb der Lignin- und Celluloseproben die Spektren getrennt darzustellen.

Die FTIR-FPA-Mikroskopie wurde zur Lokalisierung der chemischen Komponenten in Vollholz von Küstentanne und Buche verwendet. Die räumliche Verteilung der Cellulose war homogen, jedoch wurden Bereiche mit etwas erhöhtem Cellulosegehalt identifiziert. Dies galt für beide Baumarten. Hohe Ligningehalte wurden besonders in der Mittellamelle, den

Zellecken und den Holzstrahlen nachgewiesen. Die STEM-EDX-Mappings, verwendet um die räumliche Verteilung von Lignin in holzigen Zellen mit hoher Auflösung darzustellen, bestätigten die durch die FTIR-Mikroskopie erhaltenen Ergebnisse. Dies traf auch für die TEM-EDX Einzelpunktmessungen zu, mit denen der größte Ligningehalt in der Mittellamelle nachgewiesen werden konnte.

Die Ergebnisse dieser Arbeit tragen zur erweiterten Anwendung der FTIR-spektroskopischen Techniken in der Holzverarbeitung und zur Qualitätskontrolle bei. Dies eröffnet neue Felder der Anwendungsmöglichkeiten der FTIR-Technik, besonders für Untersuchung von Holzprodukten auf herkömmlicher und biologischer Basis.

Die Ergebnisse befürworten, dass die Küstentanne für die Verwertung in neuartigen Holzprodukten geeignet ist und können dazu beitragen, ein Anreiz für die Forstwirtschaft zum vermehrten Anbau dieser Baumart zu sein.

CHAPTER I

1   Introduction

1.1 Changes of environmental conditions, wood demand and effects on forestry and wood supply

Forests have always been subjected to natural disturbances. Global climate change is expected to influence plant growth and forestry. As a result of storms, heat, drought and insect infestation harming the forests there will be a profound change in forest management followed by changes in wood marketing (Behrendt and Rupp 2006). Corresponding to the new conditions, sustainable forestry will lead to mixed forests containing stands of different species, ages and structures.

Globalization and economic changes in developing countries are causing rising costs for fossil fuels, thereby, affecting the demand on wood as bioresource for energy (Wolf 2005; Reich 2008). In the face of a dramatically growing world population, there is a strong and increasing demand for wood (Dohrenbusch and Bolte 2008). Even in Germany, the present stock of timber will be insufficient to meet the needs of industry in the next decades (Behrendt and Rupp 2006).

1.2 Changes in domestic forestry, future trends and measures for reconstruction of forests and wood supply in the next decades

Germany is one of the leading nations in forestry and forest industries in Europe (Spellmann and Kehr 2008). Coniferous forest stands with Norway spruce (*Picea abies* L.) as main tree species still dominate the growing stock, followed by pine (*Pinus sylvestris*) and beech (*Fagus sylvatica* L.) (Spellmann and Kehr 2008). However, spruce is very sensitive to the environmental stress caused by the change of climate (Borchert and Kölling 2004; Horn 2006). Due to the silvicultural goal to enlarge the portion of broad-leaved tree species up to 60 %, the long-term supply of wood for processing will change (Behrendt and Rupp 2006). The increased planting of beech as the potentially natural dominant species in Germany (Ellenberg 1996) will be followed by a noticeable loss of supply in coniferous wood and a rising assortment of lower wood qualities of deciduous trees (Behrendt and Rupp 2006). Furthermore, beech is also sensitive to the expected climate change (Rennenberg 2004).

Since wood processing industries need a long term supply, various measures have already been suggested to accommodate the demand. The utilization of wood from deciduous

tree species, the mobilization of round wood potential in privately owned forests and an enlargement of plantations with conifers in short rotation cycles (Behrendt et al. 2007; Spellmann and Kehr 2008) are promising measures. Douglas fir (*Pseudotsuga menziesii)* and Grand fir (*Abies grandis* (Douglas ex D. Don) Lindl.) have already been introduced into Germany's forestry from North America and are considered being of high potential (Röhrig 1981; Nörr 2004). Grand fir, which seems to be particularly well suited because of its drought tolerance, its ecological compatibility (Röhrig 1981) and an outstanding growth could enrich nature-oriented forest stands of beech in some silvicultural areas. Furthermore, due to its promising properties, solid wood of Grand fir as raw material is of high potential for domestic sawnwood, panel board, pulp and paper industries. This suggests that Grand fir could be cultivated increasingly in beech-dominated nature-oriented mixed forest stands.

1.3   Grand fir (*Abies grandis* (Douglas ex D. Don) Lindl.) - a novel tree species and beech (*Fagus sylvatica* L.) - a rediscovered tree species

The natural occurrence of Grand fir is on the American continent in British Columbia, Washington State, Oregon, the north-east of California, Idaho and the west of Montana, at an altitude between 400 and 2200 m (Röhrig 1981; Stratmann 1988). A low demand on nutrients enables growth on granite, gneiss and bunter (Riebel 1994) and shows the high potential of this fir species for cultivation in different areas (Kleinschmitt and Svolba 1979; Stratmann 1988). In contrast to the shallow root system of spruce, Grand fir develops a tap-root system, allowing high stability against environmental impacts (Röhrig 1981; Stratmann 1988). Though fiber length, bending strength and modulus of elasticity are comparable to spruce (*Picea Abies* L.*)* or Silver fir *(Abies Alba* Mill.*),* the durability, raw density and compressive strength are significantly lower, as well as the machining resistance (Müller 1935; Schwab and Stratmann 1983; Alden 1997; Wagenführ 2000). However, the wood of Grand fir has outstanding gluing abilities (Sachsse 1991; Alden 1997). Due to its low strength values, utilization is limited to applications where strength is of minor importance (Wagenführ 2000). Wood and wood products of Grand fir are mainly traded on the American market and are mostly used in pulp- and paper industry, for doors, boxes, windows and partly as building and construction timber (Wagenführ 2000).

Since two thousand years, beech (*Fagus sylvatica* L.) has been the most dominant tree species in Central Europe by nature (Ellenberg 1996). However, it was replaced by fast-growing and highly profitable conifers such as spruce (*Picea abies* L.) and only used to serve for protective or recreational purpose in forests (Dertz 1996). In recent years, beech was

increasingly cultivated due to the goal of ecological silviculture enlarging the portion of broad-leaved tree species.

Between 1999 and 2002, beech wood has been subjected to conditions of the global market. The China business pushed the prices of premium quality of beech timber, whereas prices for little and small sized qualities decreased by weak demand (Spellmann and Kehr 2008). Spellmann and Kehr (2008) estimate the German growing stock of beech with 583 million m^3. This species is sensitive to increasing impacts of environmental changes such as nitrogen stress, acid soils, rising ozone concentrations, aridity and therefore under risk of the expected climate change (Rennenberg et al. 2004). Additionally, these stress factors make the trees sensitive to insects, fungi, bacteria and viruses (Schober 1972; Roloff 1996). However, juvenile trees up to an age of about 50 years can be considered as fast-growing (Wagenführ 2000) and therefore, the species will become very interesting for future forest management and wood industries. Beech solid wood is diffuse-porous, of high density, tensile strength, compression strength and bending strength. Its homogenous structure makes it easily machineable. Due to its low natural durability it is not weather resistant and must be protected when used in exterior (Wagenführ 2000). Less distinctive annual rings than in softwood lead to an excellent chipping quality (Thole 2006). Beech wood is poor of volatile organic compounds (Thole 2006), however, its dust is supposed to be risky in causing allergies and cancer (Mohtashamipur et al. 1989; Nelson et al. 1993; Naaralla et al. 2003).

The tough, strong wood of beech is e.g. used for construction, furniture and flooring. About 250 commercial sectors of beech wood utilization are known; even the red heart wood is in great demand for individual furniture (Wagenführ 2000). Hitherto, because of its high density and the potentially dangerous dust, beech wood is not used as raw material for derived timber products.

1.4 Wood - an inhomogeneous material

Wood properties depend on the particular timber species, the provenance and the conditions of growth (Fengel and Wegener 2003; Kloeser et al. 2008). As naturally grown raw material for a plenty of different products, wood shows high variability in its chemical, biological and physical properties (Fengel and Wegener 2003; Kloeser et al. 2008). Wood color, number and dimension of knots, fiber length and dimensions, resinousness and extractive contents are just some of the variations, which can be detected in solid wood (Wagenführ 2000; Fengel and Wegener 2003). Wood is hygroscopic, its swelling and shrinkage leads to the so called working of wood (Chauhan and Aggarwal 2003; Sonderegger and Niemz 2006). In addition,

wood is anisotropic with different material properties and changes in the mechanical strength, dependent on the particular fiber orientation (Fengel and Wegener 2003). Due to these facts, processing of timber products with unchanging material properties is difficult or quite impossible (Holzwirtschaft Schweiz 2000). However, the development of derived timber products made it possible to eliminate most of the disadvantages mentioned above.

1.5 Wood-based panels - definition and development

The most important type of forest product in Germany is sawnwood followed by derived timber products (Marutzki 2004). Derived timber product industry processes with rising trend approximately 16 million m^3 or about 40% of domestic annual felling (Marutzki 2004). Germany is the most important panel board manufacturer in Europe (Kloeser et al. 2008).

The production of panel boards always follows the same production process:

Wood is mechanically chipped, milled or grinded to homogenized material, such as fibers, particles or strands. These intermediate wood products are usually bond by adhesives with further additives and pressed under heat and high pressure to final products.

Therefore, panel board industry has the potential to process wood-based panels out of large quantities and qualities of different wood material, having better strength properties and reduced swelling-shrinking anisotropies, compared to solid wood (Kloeser et al. 2008). Waste timber, thinning material, by-products of saw-milling like saw dust, splinters or wood chips are largely used as raw material for panel production (Deppe and Ernst 2000; Kloeser et al. 2008).

The intermediate wood products are most likely glued with synthetic adhesives, such as urea-formaldehyde, phenol-formaldehyde, or organic isocyanates and further additives, such as paraffin (Youngquist et al. 1997; Kües et al. 2008). However, many attempts have already been made to replace these synthetic binders, based on petro-chemical products, by bio-based adhesives (Kharazipour and Hüttermann 1998; Pizzi 2006). Thereby, binders from renewable resources could be used, based on cellulose, starch, dextrins, mechanically-enzymatically decomposed potato pulp, proteins, tannins, and lignins (Müller et al. 2008), enabling the degradability of the final products (Smok 1999; Müller 2005).

The most important types of panel boards are particleboards, medium density fiberboards (MDF), plywood and oriented strand boards (OSB). A particleboard is defined as a wood-based panel, manufactured under pressure and heat from particles or chips of wood, usually under the addition of adhesives (Kloeser et. al 2008). MDF is made from lignocellulosic fibers, combined with a synthetic resin in a dry process by hot-pressing

(Bolton and Humphrey 1988; Thoemen and Humphrey 2003). A further wood-based panel is the low-density fiberboard or softboard, produced in a wet- or dry-process (Moser et al. 2003) and mostly used for insulation (Sedlbauer 2004). The dry-process requires an admixture of adhesives (Moser et al. 2003). Applying the wet-process, adhesives can be added, but depending on fiber length they may not be essential, since cross linking occurs due to the plastification of lignin and formation of hydrogen bonds (Makas 2006).

At present, particleboard production is the largest of all panel board productions in Europe, of which one fourth of it is assumed to be located in Germany (Kloeser et al. 2008). Mantau et al. (2003) predicted for the German particleboard industry an increase in capacity of about 10 %.

MDF represent the second largest amount of panel boards produced in Europe (Kloeser et. al 2008). To date, spruce and pine are the main resources for derived timber products (Wagenführ 2000) but in future, other tree species, such as beech and Grand fir, could alternatively be introduced into the production processes.

1.6 Chemical composition of wood and analyzing wood

To utilize wood most efficiently, an understanding of product properties, requiring laboratory analysis of the anatomy and chemical components, is necessary.

Wood is primarily composed of cellulose, lignin, hemicelluloses and minor amounts of extractives, such as resin, fatty acids, triglycerides, sterols and steryl esters (Johansson et al. 1999).

Cellulose $(C_6H_{10}O_5)_n$, the major component in wood (40-50 %), consists of anhydroglucopyranose units, which are joined to form a molecular chain and stabilized by hydrogen bonds (Fengel and Wegener 2003). Cellulose is a linear polymer, consisting of (1-4) ß-linked glucose monomers. The cellulose molecules are arranged into fibrils, which are organized into elements that make up the cell wall of wood fibers, forming the structurally strong framework in the cell walls. Most of the cell wall cellulose is crystalline (Sjöström 1998; Fengel and Wegener 2003).

Lignin is, after cellulose, the second most abundant terrestrial biopolymer (Boerjan et al. 2003; Fengel and Wegener 2003). It is a complex aromatic heteropolymer, mainly derived from the three hydroxycinnamyl alcohol monomers *p*-coumaryl, coniferyl and sinapyl alcohols (Freudenberg and Neish 1968). These monolignols produce, respectively, *p*-hydroxyphenyl (H), guaiacyl (G) and syringyl (S) phenylpropanoid units when incorporated into the lignin polymer (Boerjan et al. 2003). Conifer lignin is largely G-lignin, whereas

hardwood is mostly composed of G- and S-units (Donaldson 2001). Lignin makes up approximately one-fourth to one-third of the dry mass of wood (Fengel and Wegener 2003), is accumulated particularly in the middle lamellae of tracheids and vessels and in the secondary cell wall for stabilization (Donaldson 2001; Fengel and Wegener 2003; Teeri et al. 2007).

Additionally, a number of various polysaccharides called polyoses or hemicelluloses are present in wood. They differ from cellulose by a composition of various sugar units and acid- or carboxy groups, by much shorter molecular chains and by branching of the chain molecules. The sugar units, making up the polyoses, can be subdivided into groups, such as pentoses, hexoses, hexuronic acids and deoxy-hexoses (Rowell 1984; Fengel and Wegener 2003).

It is of great importance for technical wood use that wood properties of a species match product requirements. Therefore, efficient utilization of wood products is possible through an understanding of product properties, requiring laboratory analysis of wood anatomy and composition by different methods. Established standard methods are e.g. the quantitation of cellulose (Tappi T 203 om-93), lignin (Tappi T 222 om-98), hemicelluloses (Tappi T 203 om-93), extractives (Tappi T 264 cm-97) and ash content (Tappi T 264 cm-97). In addition to these methods, there are many other techniques in use. However, since they are labor and time intensive procedures, they are not appropriate for screening the material involved (Pandey and Nagveni 2007).

1.6.1   FTIR spectroscopy

FTIR spectroscopy is a modern technique for determination of molecular structures, identification of compounds in biological samples and investigation of complex polymers (Arndt et al. 1999; Kacuráková and Wilson 2001). It is well-established for analysis of the chemical composition of wood (Faix 1991; Pandey 1999; Pandey and Pitman 2003). It is suitable for the analysis of bonds between wood, wood components and glues (Fabo 2004).
 The technique is widely used in both, research and industry, for quality control and dynamic measurements. The detected vibrations of the molecules in the wood sample, caused by IR-light, enable drawing conclusions on its chemical composition (Naumann et al. 2008). Absorption bands of substances are generated during each analysis and can directly be assigned to a certain molecular bond (e.g. C=O) or to frequencies of functional groups (e.g. G/S lignin) (Gottwald and Wachter 1997).

FTIR spectroscopy offers a large potential for wood analysis, because it is a fast and quite simple method for determination of the chemical composition of complex samples. The

changes in crystalline structures of cellulose in cell walls, the composition of the chemical structures of various tree species as well as the chemical composition of wood, its primary, composed and degradation products can be analyzed (Naumann et al. 2008). The method allows the detection of the influence of binders on wood quality and the accumulation of additives (Fabo 2004). FTIR spectroscopy enables quick analysis of wood components. Due to qualitative differences in the spectra it is possible to assign the chemical structures of timber to a single wavenumber, as e.g. that for lignin, extractives or polysaccharides. It is possible to distinguish e.g. soft- or hardwood due to their different composition of lignin and holocellulose (Faix 1991; Pandey 1999).

FTIR spectroscopy was used e.g. for classification of lignins from different botanical origins (Faix 1991), for the detection of adhesives on wood particles (Körner et al. 1992), for screening of cell-wall mutants and differentiation of wood from different habitats and proveniences of *Eucalyptus* spp. (Chen et al. 1998) or for comparison of soft and hardwood trees (Pandey 1999). Another example for the use of FTIR spectroscopy is the quality control of pulp and paper (Böttcher 1993).

Until recently it was necessary to produce potassium-bromide (KBr) pellets for sample analysis with FTIR spectroscopy. This required time-consuming sample preparation. The sample had to be milled to a fine powder. Afterwards, it had to be pressed into small pellets, mixed with a defined amount of KBr powder. This chemical substance served as background for the spectroscopic measurements.

Innovative units, such as the attenuated-total-reflectance (ATR)-unit, have been developed recently. Now, spectroscopic measurements are possible with little to no sample preparation. It is possible to measure e.g. wood blocks with plane surface and wood powder to determine different wood components like lignin and cellulose. The ATR technique as a universal sampling accessory to FTIR provides reproducible qualitative and quantitative analysis of samples (Bukowski and Monti 2007) and is a non-destructive method for detection of the molecular composition of a sample. Therefore, a sample can be analyzed several times. FTIR-spectra of solid, liquid or gaseous samples are generated in a few minutes. A deuterium-triglycine-sulfate (DTGS) -detector, frequently used in modern FTIR spectroscopes, allows analyzing measurements of spectra within a frequency range from 600-4200 cm^{-1}. However, especially in the wave number area between 1800 and 600 cm^{-1}, the so-called fingerprint-region, the bonds can be directly interpreted and ascribed to a particular chemical composition in the sample. The spectra can be analyzed quantitatively (quantities of components in the sample), qualitatively (educt-product comparison to follow reactions; direct interpretation of

spectra, comparison with a reference spectrum) and semiquantitatively (calculation e.g. of the lignin or cellulose-ratio). A FTIR-ATR spectrum of beech solid wood powder is given as an example in Fig. 1. The peaks have been assigned tentatively to the particular chemical components (Tab. 1).
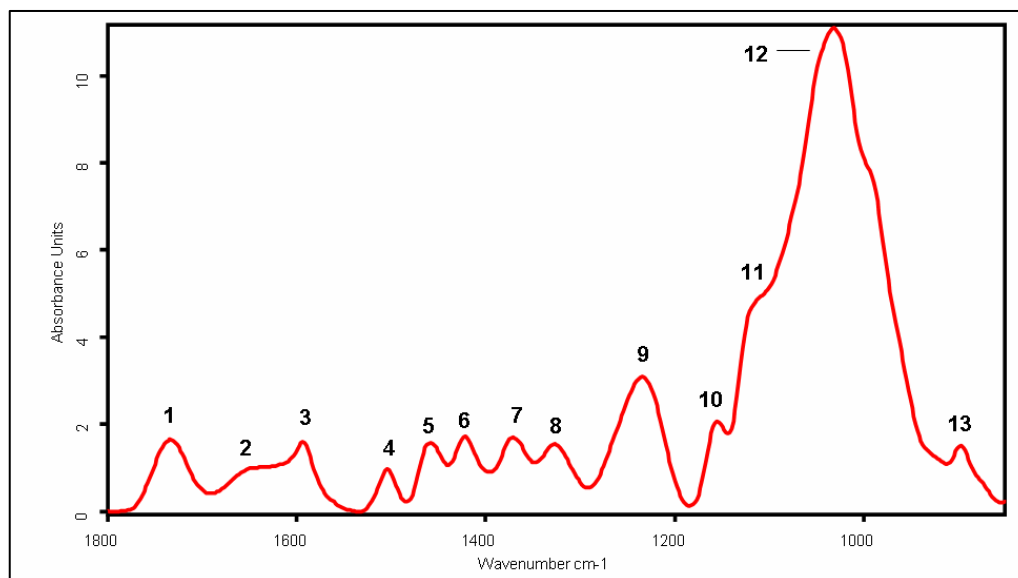
Fig.1: Mean FTIR spectrum of beech (Fagus sylvatica L.) wood in the fingerprint region (1800-850 cm^{-1}). For explanations of numbers at wavenumber maxima, see Table 1.

Table 1: FTIR band assignments in the mid-infrared region of beech (Fagus sylvatica L.) wood powder (wavenumber maxima are given) and tentative assignments to wood components (according to Hergert 1971; Usmanov et al. 1972; Parker 1983; Faix 1991; Fengel and Wegener 2003; Pandey and Pitman 2003).

Wavenumber [cm^{-1}]	Assignment	Number in Fig. 1
1732	C=O stretch in xylans (hemicelluloses)	1
1649	Absorbed O-H and conjugated C-O	2
1593	Aromatic skeletal vibration in lignin	3
1505	Aromatic skeletal vibration in lignin	4
1460	C-H- deformation in lignin and carbohydrates	5
1424	C-H- deformation in lignin and carbohydrates	6
1372	C-H deformation in cellulose and hemicelluloses	7
1328	S ring plus G ring condensed	8
1235	Syringyl ring and C= stretch in lignin and xylans	9
1157	C-O-C vibration in cellulose and hemicelluloses	10
1122	Aromatic skeletal vibration and C-O stretch	11
1031	C-O vibration in cellulose and hemicelluloses	12
897	C-H deformation in cellulose	13

The combination of FTIR spectroscopy and multivariate methods, such as principal component analysis (PCA) and cluster analysis, is in common use for analysis of spectral data. It enables the investigation of the intrinsic relationship of samples, according to their spectral heterogeneity (Everitt 1993), or the determination of very slight spectral changes (McCann et al. 1997). Chen et al. (1998) detected small changes in cell wall properties using a combination of infrared spectroscopy and discriminant analysis. Zanetti et al. (2005) separated spectra of Southern Yellow pine (*Pinus palustris*) boards of declining surface quality, as affected by weathering, using NIR spectroscopy combined with PCA. Using MIR and NIR spectroscopy combined with PCA, Fackler et al. 2007 developed regression models for prediction of weight loss on fungal decayed wood, investigating white and brown rot fungi on beech (*Fagus sylvatica* L.). NIR spectroscopic investigations combined with PCA on Yellow poplar (*Liriodendron tulipifera* L.), chemically modified with acetic anhydride, enabled the separation of the samples according to the esterification level (Çelen et al. 2008).

1.6.2   FTIR microscopy

A relatively new technique used for sample analysis is FTIR microscopy. It is a combination of Fourier transform infrared (FTIR) spectroscopy and imaging techniques, which enables the illustration of the spatial resolution of the chemical composition of organic compounds (Salzer et al. 2000; Naumann et al. 2005; Naumann and Polle 2006). The result of a measurement is a color coded image, which reflects the localization of the intensity of the bonds of the scanned area. High and low intensities are encoded by different colors, producing a so-called false color image.

A focal plane array (FPA)-detector can be used to obtain high resolution chemical images from a defined sample area. To characterize wood and wood products, woodcuts of about 10µm of thickness or less are used. Thicker samples prevent sufficient transmission of infrared radiation, reducing the quality of the recorded spectra (Naumann and Polle 2006).

The FPA-detector contains 64 x 64 (4096) detector elements and thus, generates 4096 independent spectra per scan. The measured sample area is 256 µm x 256 µm, because there are 64 detector elements on each detector side with a longitude size of 4 µm. The resolution of the image is dependent on the size of a single detector element out of the 4096 elements, which has an area of 4 µm x 4 µm. Depending on the wavelength, a maximum resolution of 4 µm is possible; in the fingerprint region the resolution decreases from 4 µm (at 1500 cm^{-1}) to 7.5 µm (at 800 cm^{-1}) (Naumann and Polle 2006; Naumann et al. 2008). FPA is a true imaging technique, acquiring both, spatial and spectral information. The huge gain of

measurement speed in imaging is based on the simultaneous detection of several thousand spectra by individual pixels across the detector array in 1 to 15 data sets.

The 4096 single spectra of an image can be evaluated with two methods: the first integrates the 4096 spectra in a selected wave number range, which is considered to be typical for a chemical component in the sample. 18 different types of integration can be selected with the OPUS 6.5 software (Bruker Optics, Ettlingen, Germany). The result of the evaluation is e.g. the area below each single spectrum for a selected wave number area. Thus, for an image, 4096 single areas are received and illustrated in the image with different colors, depending on the particular values of the areas. A color scale indicates the semiquantitative content, ranging from blue (no content) to pink (high content).

The second evaluation method requires a reference sample of the chemical component of interest, e.g. lignin or cellulose. FTIR-ATR spectra of the sample are recorded and averaged to a mean reference spectrum. The so-called correlation method calculates the correlation of the reference ATR spectrum as first parameter and the 4096 spectra of the FPA data set as second parameter. The obtained values are illustrated in a color coded image, ranging from blue (no content) to pink (high content), semiquantitative illustrating the spatial distribution of lignin and cellulose in the sample. Figure 2 exemplarily shows the lignin distribution in a FTIR-FPA image of a Grand fir solid wood cross-section, evaluated with integration and correlation method.
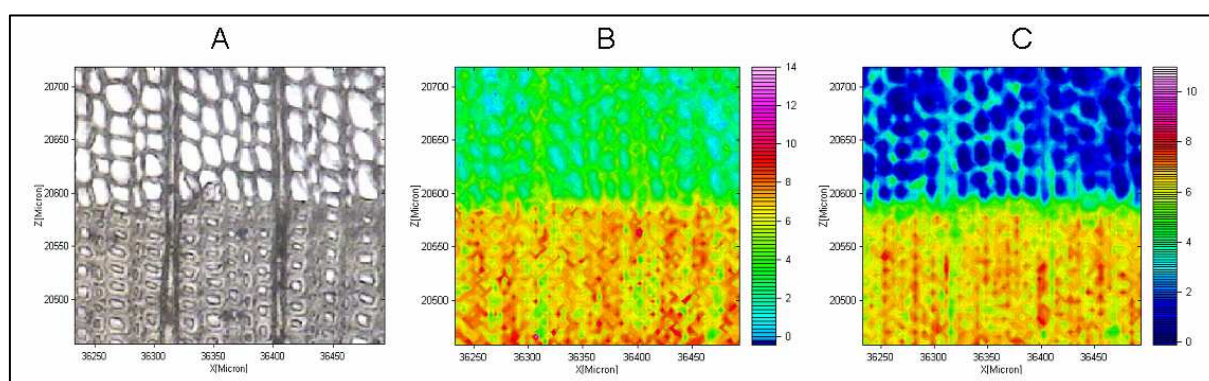
Fig. 2: Fourier transform infrared (FTIR) microscopic FPA images of a Grand fir solid wood cross-section. Fig. 2 A illustrates the light microscopic image of the investigated wood area with early and latewood top down. Fig. 2 B gives the corresponding color coded image, illustrating the spatial distribution of lignin. The FTIR-FPA data-set was evaluated by integrating the range between 1530-1490 cm^{-1}, tentatively assigned to lignin (Faix 1991). Fig. 2 C gives the corresponding color coded image, illustrating the spatial distribution of lignin, evaluated with the function "trace-computation" of the OPUS 6.5 software (Bruker Optics, Ettlingen, Germany).

1.7 Main goals

There is little to no experience in processing panel boards based on beech or Grand fir. Besides the mechanical and technological properties, the knowledge of the chemical compounds of raw material, intermediate and final products is of great importance.

To obtain information of the materials involved and their processing to wood-based panels, FTIR spectroscopy and microscopy techniques were employed for sample analysis to achieve the following goals:

i.   to investigate the potential of FTIR spectroscopy in identifying different types of lignin and cellulose;

ii.   to investigate changes in wood properties during particle-, fiber- and hybrid board production of Grand fir and beech;

iii. to investigate changes in fiber properties during their processing to insulating wood fiber mats, based on beech wood;

iv.   to investigate and validate the distribution of wood compounds in Grand fir and beech, using FTIR imaging and electron microscopy;

To achieve the above goals the following chapters will be treated independently. In the chapter *"FTIR spectroscopy in combination with cluster analysis as tool for analysis and control of wood properties and production processes"*, different types of lignin and cellulose were investigated with FTIR-ATR spectroscopy and the obtained data were additionally evaluated by cluster analysis.

In the chapter *"FTIR-ATR spectroscopic analysis of changes in wood properties during particle- and fiberboard production of hard- and softwood trees"*, FTIR-ATR spectroscopy combined with cluster analysis and principle component analysis was used to illustrate the chemical changes in wood properties during the whole production process of Grand fir and beech wood into wood composite panels.

In the chapter *"FTIR-ATR spectroscopic analysis of changes in fiber properties during insulating fiberboard manufacture of beech wood"*, FTIR-ATR spectroscopy was applied to trace changes in chemical fiber properties during processing to different types of insulating fiber mats. Cluster analysis was used to control the homogeneity of the products.

Finally, in the chapter *"Imaging of lignin and cellulose in soft and hardwood species using Fourier transform infrared microscopy and Scanning transmission electron microscopy"*, FTIR microscopy combined with a focal plane array (FPA) detector was used

for illustration of the distribution of lignin and cellulose in early and latewood of Grand fir. Two independent visualization methods for FPA imaging were applied and compared. Scanning transmission electron microscopy combined with Energy dispersive X-ray spectroscopy (STEM-EDX) was used as independent method for comparison of the obtained data with EDX-mappings.

References

Alden, H. A. (1997). Softwood of America. US Department of Agriculture, Forest Service, Forest Products Laboratory, Madison, Wisconsin, Gen. Tech. Rep. FPL-GTR-102.

Arndt, K. F., Richter, A., Ludwig, S., Zimmermann, J., Kressler, J., Kuckling, D., Adler, H. J. (1999). Poly(vinylalcohol)/poly(acrylicacid)hydrogels: FT-IR spectroscopic characterization of crosslinking reaction and work at transition point. Acta Polymerica. 50: 383-390.

Behrendt, S., Rupp, J. (2006). Perspektiven der Holzmobilisierung zur Stärkung nachhaltiger Zukunftsmärkte der Forst- und Holzwirtschaft. Institut für Zukunftsstudien und Technologiebewertung, Berlin.

Behrendt, S., Henseling, C., Erdmann, L., Knoll, M., Rupp, J. (2007). Trendreport: Zukunftstrends für das Bauen mit Holz. Institut für Zukunftsstudien und Technologiebewertung, Berlin.

Boerjan, W., Ralph, J., Baucher, M. (2003). Lignin biosynthesis. Annual Review of Plant Biology. 54: 519-546.

Bolton, A. J., Humphrey, P. E. (1988). The hot-pressing of dry-formed wood-based composites. A review of the literature, identifying the primary physical processes and the nature of their interaction. Holzforschung 42: 403-406.

Borchert, H., Kölling, C. (2004). Waldbauliche Anpassung der Wälder an den Klimawandel jetzt beginnen. LWF aktuell. 43: 28-30.

Böttcher J. H. (1993). Quantitative Analyse von Holz und Holzkomponenten mittels FTIR-Spektroskopie unter Anwendung multivariater statistischer Verfahren. Dissertation, Fachbereich Biologie der Universität Hamburg.

Bukowski, E. J., Monti, J. A. (2007). FTIR-ATR spectroscopy for identification of illicit drugs seized from clandestine laboratories. American Laboratory. 20: 16-19.

Çelen, I., Harper, D., Labbé, N. (2008). A multivariate approach to the acetylated poplar wood samples by near infrared spectroscopy. Holzforschung. 62 (2): 189-196.

Chauhan, S. S., Aggarwal, P. (2003). Effect of moisture sorption state on transverse dimensional changes in wood. Holz als Roh- und Werkstoff. 62: 50-55.

Chen, L., Carpita, N. C., Reiter, W., Wilson, R., Jeffries, C. McCann, M. (1998). A rapid method to screen for cell-wall mutants using discriminant analyses of Fourier transform infrared spectra. The Plant Journal. 16(3): 385-392.

Dertz, W. (1996). Buchenwälder im Zielkatalog der Forstwirtschaft. In: ABS C. (Hrsg.). Stiftung Wald in Not. Buchenwälder - Ihr Schutz und ihre Nutzung, Bonn. pp. 2-8.

Donaldson, L. A. (2001). Lignification and lignin topochemistry - an ultrastructural view. Phytochemistry. 57: 859-873.

Dohrenbusch, A., Bolte, A. (2008). Forest plantations. In: Wood production, wood technology and bio-technological impacts. Ed. Kües, U. Universitätsverlag, Göttingen. pp. 73-83.

Deppe, H.-J., Ernst, K. Taschenbuch der Spanplattentechnik. DRW Verlag, Leinfelden-Echterdingen, 2000.

Ellenberg, H. (1996). Vegetation Mitteleuropas mit den Alpen in ökologischer Sicht. Eugen Ulmer Verlag, Stuttgart, 1996.

Everitt, B. S. Cluster analysis. John Wiley, Toronto, 1993.

Faix, O. (1991). Classification of lignins from different botanical origins by FT-IR spectroscopy. Holzforschung 45: 21-27.

Fabo, A. (2004). Untersuchungen zur Wechselwirkung von Polyethylenimin (PEI) mit Holzkomponenten. Dissertation, Universität Hamburg, Hamburg.

Fackler, K., Schwanninger, M., Gradinger, C., Hinterstoisser, B., Messner, K. (2007). Qualitative and quantitative changes of beech wood degraded by wood-rotting basidiomycetes monitored by Fourier transform infrared spectroscopy methods and multivariate data analysis. FEMS Microbial. Letters. 271:162-169.

Fengel, D., Wegener, G. (2003). Wood - chemistry, ultrastructure reactions. Kessel Verlag, Remagen. 613 pp.

Freudenberg, K., Neish, A. C. Constitution and biosynthesis of lignin. Springer-Verlag, Berlin, 1968.

Gottwald, W., Wachter, G. IR-Spektroskopie für Anwender. Gruber, U., Klein W. (Hrsg.). Wiley-VCH Verlag, Weinheim, 1997.

Hergert, H. L. (1971). Infrared spectra. In: Lignins: occurrence, formation, structure and reactions. Sarkanen, K. V., Ludwig, C. H. eds. Wiley Interscience, New York. pp. 267-297.

Holzwirtschaft Schweiz. Lignum, Holz in Bestform. Informationsschrift, Schweizerische Holzwirtschaftskonferenz. Ed. Holzwirtschaft Schweiz. Zürich, 2000.

Horn, O. (2006). Mischung stützt Nadelholz-Klimawandel und Borkenkäfer beeinflussen die Baumartenwahl. Bayerisches landwirtschaftliches Wochenblatt. Deutscher Landwirtschaftsverlag, Hannover.

Johansson, L.-S. Campbell, J.-M. Koljonen, K., Stenius, P. (1999). Evaluation of surface lignin on cellulose fibers with XPS. Applied Surface Science .144-145: 92–95.

Kacuráková, M, Wilson, R. H. (2001). Developments in mid-infrared FT-IR spectroscopy of selected carbohydrates. Carbohydrate Polymers 44 (4): 291-303.

Kharazipour, A., Hüttermann, A. (1998). Biotechnological production of wood composites. In: Bruce, A., Palfreyman, J. W. (1999). Forest products biotechnology. Taylor and Francis, London, UK. pp.141-150.

Kleinschmit, J., Svolba, J. (1979). Die Große Küstentanne (*Abies grandis*) in Deutschland. Allgemeine Forstzeitschrift. 34: 218-220.

Kloeser, L., Kües, U., Schöpper, C., Hosseinkhani, H., Schütze, S., Dantz1, S., Malik, I., Vos, H., Bartholme, M., Müller, C., Polle, A., Kharazipour, A. (2008). Panel boards and conventional adhesives. In: Kües, U. ed. Wood production, wood technology and bio-technological impacts. Universitätsverlag, Göttingen. pp. 297-346

Körner, S., Niemz, P., Wienhaus, O., Henke, R. (1992). Orientierende Untersuchungen zum Nachweis des Klebstoffanteils auf Holzpartikeln mit Hilfe der FTIR- Spektroskopie, Holz Roh - und Werkstoff. 50: 67-72.

Kües, U., Bohn, C., Euring, M., Müller, C., Polle, A., Kharazipour, A. (2008). Enzymatically modified wood in panel board production. In: Kües, U. ed. Wood production, wood technology and bio-technological impacts. Universitätsverlag, Göttingen. Universitätsverlag, Göttingen. pp. 433-467.

Makas, M. (2006). Eigenbindevermögen bei Faserwerkstoffen. In: Institut für Holzbiologie und Holztechnologie (Hrsg.) Tagungsband der 3. Fachtagung Umweltschutz in der Holzwerkstoffindustrie", Mai 18-19, 2006, Göttingen. Cuvillier Verlag, Göttingen. pp. 97-107

Mantau, U., Wierling, R., Weimar, H. (2003). Holzwerkstoffindustrie in Deutschland. Unfassende Studie der Universität zu regionaler Produktionskapazität und Rohstoffeinsatz. Holz-Zentralblatt. 15: 231-234.

Marutzky, R. (2004) Biomassen auf Basis von Holz als Brennstoffe in Österreich, der Schweiz und Deutschland. Nutzungssituation - Theoretische und reale Potentiale - Qualitäten - Wettbewerbssituation - Preistendenzen. Selbstverlag. 26 pp.

Mohtashamipur, E., Norpoth, K., Lühmann, F. (1989). Cancer epidemiology of woodworking. Journal of Cancer Research and Clinical Oncology. 115(6):503-515.

Moser, J., Treml, E., Gütler. H. (2003). Warenkunde für Holzkaufleute. 3. überarbeitete Auflage. Wirtschaftskammer Österreich. http://portal.wko.at/wk/format_detail.wk?angid=1&stid=164059&dstid=6670&openna vid=0 (21.12.2007)

Müller, K. (1935). *Abies grandis* und ihre Klimarassen. In: Mitteilungen der Deutschen Dendrologischen Gesellschaft. 47: 54-123.

Müller, C. (2005). Mechanisch - enzymatischer Aufschluss von Kartoffelpülpe als Bindemittel zur Herstellung von Holzwerkstoffen. Dissertation. Universität Göttingen, Göttingen.

Müller, C., Kües, U., Schöpper, C. Kharazipour, A. (2008) Natural binders. In: Kües, U. ed. Wood production, wood technology and bio-technological impacts. Universitätsverlag, Göttingen. pp. 347-381.

Naaralla, J., Kasanen, J. P., Pasanen, P., Pasanen, A. L., Liimatainen, A., Pennanen, S., Liesivuori, J. (2003). The effects of wood dusts on the redox status and cell death in mouse macrophages (RAW 264.7) and human leukocytes *in vitro*. Journal of Toxicology and Environmental Health. 66: 1221-1235.

Naumann A., Navarro-Gonzalez M., Peddireddi S., Kües. U., Polle A. (2005). Fourier transform infrared microscopy and imaging: Detection of fungi in wood. Fungal Genetics and Biology. 42: 829-835.

Naumann, A., Polle, A. (2006). FTIR imaging as a new tool for cell wall analysis of wood. New Zealand Journal of Forestry Science. 36: 54-59.

Naumann A, Peddireddi S, Kües U, Polle A (2008) Fourier transform infrared microscopy in wood analysis. In: Kües, U. ed. Wood production, wood technology and bio-technological impacts. Universitätsverlag, Göttingen. pp. 179-196.

Nelson, E., Zhou, Z. C., Carmichael, P.L., Norpoth, K., Fu, J. L. (1993). Genotoxic effects of subacute treatments with wood dust extracts on the nasal epithelium of rats - assessment by the micronucleus and P32 postlabeling. Archives of Toxicology. 67: 586-589.

Nörr, R. (2004). Vom Exoten zur Wirtschaftsbaumart: 175 Jahre Douglasienanbau in Deutschland. LWF aktuell. 45: 7-9.

Parker, F. S. Application of infrared, Raman and Resonance Raman spectroscopy in biochemistry. Plenum Press, New York, 1983.

Pandey, K. K. (1999). A study of chemical structure of soft and hardwood and wood polymers by FTIR spectroscopy. Journal of Applied Polymer Science. 71: 1969-1975.

Pandey, K. K., Pitman, A. J. (2003). FTIR-ATR studies of the changes in wood chemistry following decay by brown-rot and white-rot fungi. Intern. Biodeterior. Biodegr. 52: 151-160.

Pandey, K. K., Nagveni, H. C. (2007). Rapid characterisation of brown and white rot degraded chir pine and rubberwood by FTIR spectroscopy. Holz als Roh- und Werkstoff. 65: 477-481.

Pizzi, A. (2006). Recent developments in eco-efficient bio-based adhesives for wood bonding: opportunities and issues. Journal of Adhesion Science and Technology. 20: 829-846.

Reich, I. (2008). Das Holz wird knapp und teuer. Handelsblatt, 11.01.2008. Verlagsgruppe Handelsblatt, Düsseldorf.

Rennenberg, H., Seiler, W., Matyssek, R., Gessler, A., Kreuzwieser, J. (2004). Die Buche (*Fagus sylvatica* L.) - ein Waldbaum ohne Zukunft im südlichen Mitteleuropa? Allgemeine Forst- und Jagdzeitung. 175: 210-224.

Riebel, H. (1994). Über einige Holzeigenschaften der großen Küstentanne (*Abies grandis* [Douglas] Lindley) aus süddeutschen Anbauten. Mitteilung der forstlichen Versuchsanstalt Baden Württemberg, Heft 177.

Roloff, A. (1996). Die Buche und ihre Gefährdung durch anthropogene Umwelteinflüsse. In: ABS C. (Hrsg.) Stiftung Wald in Not (Band 8) Buchenwälder - Ihr Schutz und ihre Nutzung, Bonn.

Röhrig, E. Neuere Grundlagen für den Anbau von *Abies grandis*. Schriften aus der Forstlichen Fakultät der Universität Göttingen und der Niedersächsischen Forstlichen Versuchsanstalt, Band 71. Sauerländer Verlag, Frankfurt am Main, 1981.

Rowell, R. (1984). The chemistry of solid wood. American Chemical Society, Washington, D.C. 614 pp.

Salzer, R., Steiner, G., Mantsch, H. H., Mansfield, J., Lewis, E. N. (2000). Infrared and Raman-imaging of biological and biomimetic samples. Fresenius J. Analytical Chemistry. 366: 712-726.

Schober, R. (1972). Die Rotbuche 1971. Schriftenreihe der Forstlichen Fakultät der Universität Göttingen und Mitteilungen der Niedersächsischen Forstlichen Versuchsanstalt, 43-44, Sauerländer Verlag, Frankfurt.

Schwab, E., Stratmann, J. (1983). Holzeigenschaften norddeutscher Küstentannen. Forst und Holz, 38: 252-256.

Sedlbauer, K. (2004). Dämmstoffe aus nachwachsenden Rohstoffen und Schimmelpilze - ein Junktim? Internationale Fachmesse und Kongress für regenerative Energien und energieeffizientes Bauen und Sanieren. Messe Augsburg (23 October 2004).

Sjöström, E., Alen, R. (1998). Analytical methods in wood chemistry, pulping and papermaking. Springer Verlag, Berlin.

Smok, B. (1999). Ein Einfall für den Abfall: Pulp Science statt Pulp Funktion. In: Kern, H. (Hrsg.). Spektrum - Informationen aus Forschung und Lehre. Universität Göttingen. pp. 16-17.

Sonderegger, W., Niemz, P. (2006). Investigation of swelling and thermal expansion of fiberboard, particleboard and plywood. Holz als Roh- und Werkstoff. 64: 11-20.

Spellmann, H., Kehr, I. (2008). The wood supply in the world, Europe, Germany, and Lower Saxony. In: Kües, U. ed. Wood production, wood technology and bio-technological impacts. Universitätsverlag, Göttingen. pp. 43-55.

Stratmann, J. (1988). Ausländeranbau in Niedersachsen und angrenzenden Gebieten. Schriften aus der Forstlichen Fakultät der Universität Göttingen und der Niedersächsischen Forstlichen Versuchsanstalt, 91, Sauerländer Verlag, Frankfurt.

Teeri, T. T., Brumer, H., Daniel G., Gatenholm, P. (2007). Biomimetic engineering of cellulose-based materials. Trends in Biotechnology. 25: 299-306.

Thoemen, H., Humphrey, P. E. (2003). Modeling the continuous pressing process for wood-based composites. Wood and Fiber Science. 35: 456-468.

Thole, V. (2006). OSB aus Buche. In: Fraunhofer-Institut für Holzforschung - WKI Braunschweig (Hrsg.) Wilhelm Klauditz Forum 9.

Usmanov, Kh. U., Yulchibaev, A. A., Dordzhin, G. S., Valiev, A. (1972). IR spectroscopic analysis of graft co-polymers of cellulose and its derivatives with vinyl fluoride. Fiber Chemistry. 3: 292-295.

Wagenführ, R. (2000). Anatomie des Holzes. DRW-Verlag, Leinfelden-Echterdingen. 188 pp.

Wolf, M. (2005). Freihandel und Umwelt: Außenpolitische Jahrestagung der Böll-Stiftung, 03.06.2005, Berlin.

Youngquist, J. A., Krzysik, A. M., Chow, P., Menimban, R. (1997). Properties of composite panels. In: Rowell, R. M., Young, R. A., Rowell, J. K. eds. Paper and composites from agro-based resources. CRC/Lewis Publishers, Boca Raton, FL. pp. 301-336.

Zanetti, M. Rials, T. G., Rammer, D. (2005). NIR monitoring of in-service wood structures. Proceedings of the 2005 Structures Congress and the 2005 Forensic Engineering Symposium. April 20-24, 2005, New York, NY.

CHAPTER II

2   FTIR spectroscopy in combination with cluster analysis as tool for analysis and control of wood properties and production processes

2.1 Abstract

Grand fir (*Abies grandis* (Douglas ex D. Don) Lindl.) is an introduced species in Germany, which is of interest for wood product industries because of its fast growth. To characterize wood and composed wood products of this species, FTIR-ATR spectra were recorded and the chemical constituents of the wood samples were analyzed. By cluster analysis of the collected FTIR-ATR spectra it was possible to distinguish between different types of cellulose and lignin.

2.2   Introduction

Wood products and derived timber products are used for interior constructions, furniture production, as packing or building materials and are mainly made of coniferous wood (Marutzky and Thole 2003). The properties of the intermediate and final wood products depend on the raw materials as well as on the production processes. For technical wood use, profound knowledge of the structure and chemical composition of wood and its products is of great importance. This holds especially, if novel tree species, for which little experience exists, were introduced into production processes. Such new wood products are e.g. composed timber products of Grand fir (*Abies grandis*).

Grand fir is a fast-growing tree species, which has only recently been introduced in Germany. The natural distribution of this coniferous tree is British Columbia, Washington, Oregon, California and the Pacific Northwest of North America at a sea level of 900-1800 m altitude (Kleinschmit and Svolba 1979). Grand fir is one of the most important introduced tree species in Central Europe, especially in the Atlantic climate area and has a high potential for forestry. The species can develop annual shoots of 1 m per year. Compared to other coniferous trees, volume accumulation of the stem occurs more rapidly (Schuhmacher 1967).

Wood is primarily composed of cellulose, lignin, hemicelluloses and minor amounts of extractives (Sjöström 1998). Cellulose $(C_6H_{10}O_5)_n$, the major component, is a linear polymer consisting of (1-4) ß-linked glucose monomers. The cellulose molecules are arranged into fibrils, which are organized into elements that make up the cell wall of wood fibers. Most of the cell wall cellulose is crystalline (Fengel and Wegener 2003).

Lignin is accumulated particularly in the middle lamellae of tracheids and vessels. It is entangled with cellulose, hemicelluloses and pectin and generates high stability. It is a three-dimensional phenylpropanoid polymer and makes up about one-quarter to one-third of the dry mass of wood (Sjöström 1998, Fengel and Wegener 2003). Gymnosperm lignin consists almost entirely of coniferyl alcohol. Dicotyledonous lignin is a mixture of coniferyl and sinapyl alcohol.

To utilize wood most efficiently, an understanding of product properties requiring laboratory analysis of the anatomy and chemical components is required. A main problem of many established standard methods is that they are labor and time intensive and not appropriate for large-scale fast screening of the material involved (Böttcher 1993).

In contrast to wet chemical methods, FTIR spectroscopy offers a large potential for screening of wood properties, because it is a fast and quite simple method for determination of the chemical composition of complex samples (Naumann et al. 2005; Naumann et al. 2007). The FTIR spectra of wood and wood products are determined by biochemical and physical properties of the material.

The aim of our work was to evaluate the potential of FTIR spectroscopy, and to identify lignin and cellulose of *Abies grandis*. As a basis for these analyses different types of lignin and cellulose were investigated by FTIR.

2.3 Material and methods

2.3.1 Wood samples

Samples of *Abies grandis* were taken in 2006 from three trees grown in the city forest of Höxter (North Rhine-Westphalia). The forest stand has north-east exposition at an altitude of 240-268 m and is located on a weak slope. The soil is deep and contains silty brick earth, has fresh to high moistness and good nutrient supply. The age of the trees was 43 years; the average height 30 m. The breast height diameter was 49 cm in average.

2.3.2 Sample preparation

Two bole disks were excised from each tree, one at the stem base and one below the crown. For FTIR-ATR analysis fine wood powder of two woodblocks per disk (juvenile wood, wood near bark) was prepared. The blocks had a dimension of 1 cm^2 from the radial area and 2 cm in height and were hackled with a gripper to small pieces. The wood parts were milled

(Retsch, MM 2000) for 5 min at 50 u/min The frequency was raised slowly for the next 5 min up to 90 u/min The whole milling process took 10 min for each sample.

2.3.3   Lignin analysis

Wood powder of Grand fir was used for the determination of acid-insoluble Klason lignin after Dence (1992). 500 mg milled powder was weighed into a centrifuge tube (W1), (W2 = W1 + weight of powder and tube). 40 ml 0.5 M KPP-buffer (KH_2PO_4/ $K_2 HPO_4$, pH 7. 8; 0.5 % Triton-X100) were added and the slurry was stirred for 30 min. Afterwards the slurry was centrifuged for 10 min (5000 g, 4 ℃, Rotanta 96R, Hettrich, Tuttlingen). The supernatant was discarded. The sample was resuspended and washed in KPP-buffer. Subsequently, the pellet was washed 4 times (30 min) in 100 % MeOH. Afterwards, 40 ml ethanol (96%)/ cyclohexan mixture (v:v = 1:2) were added and the sample was incubated for 6 h at 50 ℃ (Rettberg, Göttingen). Then the sample was centrifuged for 10 min as above; the supernatant was discarded. The sample was washed again with the ethanol / cyclohexan mixture (40 ml) and centrifuged. The supernatant was discarded. Twenty ml acetone were added, centrifuged, and the supernatant was discarded. Afterwards, the remaining pellet was dried overnight under the hood. The dry sample was weighed (W3 = W1 + pellet weight). 8 ml of 72 % H_2SO_4 were added, mixed and incubated for 60 min at room temperature. Then 200 ml distilled H_2O were added and the sample was shaken for several minutes. Afterwards, the sample was incubated for 1 h at 121 ℃ and 1 bar pressure (HST 666, Zirbus, Bad Grund) and cooled down to room temperature afterwards. Filter paper (Nr: 589/1, Schleicher & Schnüll) with a diameter of 90 mm was weighed (W4) and the fluid with the residue was poured over the filter and washed with H_2O. Filter and sample were dried in an oven for 48 h at 60 ℃ (Rettberg, Göttingen), then cooled down in an exsiccator and weighed (W5). Klason lignin was calculated according to the following equation:

$$Klason\ lignin\ (\%) = \frac{(W5 - W4)}{(W2 - W1)} * 100$$

For FTIR analysis, isolated Klason lignin from Grand fir, ammonium ligninsulfonate (Otto-Dille, Hamburg), accumulating as a by-product during paper manufacture and Kraft lignin of Norway spruce (Aldrich Chemical Company, Munich) were used. In addition, different cellulose samples were analyzed, which were obtained as industrial cellulose powder of Norway spruce (Fluka Chemie AG, Buchs), cotton linters (Buckeye, Memphis) and

chemical pulp of *Tsuga canadensis* (Lenzing AG, Lenzing, Austria). The cellulose samples were pressed. Nine measurements were conducted to get representative means.

2.3.4   FTIR spectroscopy

Innovative measuring devices, such as the ATR-unit (Attenuated Total Reflectance), have been developed recently for FTIR spectroscopy and replaced the necessity to employ KBr-pellets for sample analysis. The measuring technique has been described recently (Naumann et al. 2006). Spectroscopic measurements are possible without any pre-treatment of a sample. It is possible to measure e.g. wood blocks with plane surface and wood powder to determine different wood components like lignin and cellulose. The technique allows determining the structure of substances by the interpretation of the frequencies of functional groups and is convenient to detect the chemical modifications of raw material and mixtures. With a deuterium-triglycinesulfate-detector, measurements of spectra within a frequency range from 6500-600 cm^{-1} are possible.

FTIR-ATR spectra were recorded with an Equinox 55 spectrometer (Bruker Optics, Ettlingen, Germany) with an attached ATR-unit. The unit has a plunger on the top side which is pressed on the sample with constant pressure. FTIR-ATR measurements were conducted with a resolution of 4 cm^{-1} and a number of 32 scans per sample. Three replicates of lignin were analyzed.

The heterogeneity of FTIR spectra can be analyzed by cluster analysis. According to their heterogeneity, spectra are classified into clusters or classes in dendrograms. The first derivative and vector normalization (9 smoothing points) were utilized as pre-treatment methods of the spectra, applying the standard method for creating the distance matrix. For calculating the spectral distances the Ward's Algorithm was applied. The analyzed wavenumber area was 1800-600 cm^{-1}.

2.4   Results

2.4.1   FTIR spectroscopy of lignin and cellulose

To obtain reference spectra for lignin and cellulose analyses in wood, typical FTIR spectra of different isolates of lignin and cellulose were determined (Fig. 1). Lignin spectra, obtained by different isolation procedures from different species, showed pronounced differences (Fig. 1 a), whereas this was not the case for cellulose (Fig. 1 b). The highest number of bands was found in Kraft lignin. These bands were numbered and used to compare the three lignin

types. The numeration was continued for cellulose. The numeration and the tentative assignments of the bands to chemical structures are summarized in table 1.

Klason lignin, isolated from Grand fir and ligninsulfonate, showed a lower number of bands and lower absorption than Kraft lignin. Band 1 (C=O in lignin) and 6 (syringyl ring breathing) were not apparent in the spectrum of Klason lignin (Fig. 1 a). Furthermore, band 2 and 3 (aromatic vibration in lignin), 9 (C-H in plane deformation of syringyl rings) and 11 (C-H out of plane) were slightly displaced, which is caused by inductive effects of the substituents (e.g. H_3CO) in the aromatic ring system of lignin (Pastusiak 2003). Band 2 shows an absorption at 1640 cm^{-1} which is regarded as typically for C=O stretch vibration. However, water is oscillating at the same wavenumber range, too. Hence an influence of water on band 2 is conceivable. Klason lignin showed a lower absorbance at band 2 and a higher one at band 8 (C-O in G ring) and 11 (C-H out of plane) than Kraft lignin. Furthermore band 4 (C-H deformation in lignin) was not as distinct as the one of Kraft lignin. In ligninsulfonate band 10 (C-H in G lignin, C-O deformation in primary alcohols) was evidently higher than that of Klason and Kraft lignin.

The FTIR spectra of cotton linters, industrial cellulose and chemical pulp were very similar (Fig. 1b) and did not show such variations as the lignin spectra. All single spectra showed the same oscillation bands and no displacement. The absorbance rates were also very similar. Thus, it is obvious that the particular isolation method had no influence on the spectra as detected for lignin and suggested similar degrees of purity for the different cellulose types. Spectra for chemical pulp and industrial cellulose were largely identical. For band 21 (C-O vibration in cellulose and hemicelluloses), the absorbance of industrial cellulose was little higher. Cotton linters showed a slightly higher absorbance than chemical pulp and industrial cellulose for CH_2 in cellulose (band 14), C-H vibration in cellulose (band 16) and C-H vibration in cellulose (band 21). In the wavenumber range for polysaccharides (1060- 980 cm^{-1}), the absorbance of linters was a little lower than that of the other cellulose types. Because of the higher bands for cellulose and lower bands for hemicelluloses, it can be derived that cellulose prepared from cotton linters was slightly purer than that in the other samples.

Tab.1: Wavenumber characterization for lignin and cellulose in the fingerprint area (Faix, 1991, Fengel and Wegener 2003, Usmanov et al. 1972). Numbers in the table refer to the numbers assigned to the peaks in figure 1a and b.

Wavenumber (cm⁻¹)	Compound	Peak number from figure 2					
		Klason	Kraft	Lignin-sulfonate	Linters	Industrial cellulose	Chemical pulp
1670-1640	C=O in lignin	-	1	-	-	-	-
1645	symmetric deformational oscillation of water molecules absorbed on the cellulose	-	-	-	13	13	13
1625-1570	aromatic vibration in lignin	2	2	2	-	-	-
1525-1490	aromatic vibration in lignin	3	3	3	-	-	-
1465-1443	C-H deformation in lignin and carbohydrates	4	4	4	-	-	-
1435-1405	C-H deformation in lignin and carbohydrates	5	5	5	-	-	-
1426	scissor oscillation of CH₂ groups characteristic for rotational isomers in cellulose	-	-	-	14	14	14
1385-1355	C-H deformation in cellulose and hemicelluloses	-	-	-	15	15	15
1330-1325	Syringyl ring breathing	-	6	-			
1324-1308	C-H vibration in cellulose	-	-	-	16	16	16
1265+/-5	C-O-C asymmetric stretching vibration of aryl ether linkages	7	7	7	-	-	-
1253-1224	C-O in O=C-O groups (Carbohydrates)	-	-	-	17	17	17
1214	C-O in G ring	8	8	-	-	-	-
1170-1142	C-O-C vibration in cellulose and hemicelluloses	-	-	-	18	18	18
1128	C-H in plane deformation of syringyl rings	9	9	9	-	-	-
1120-1075	O-H in cellulose and hemicelluloses	-	-	-	19	19	19
1070-1040	C-O in cellulose and hemicelluloses	-	-	-	20	20	20
1038-1013	C-O vibration in cellulose and hemicelluloses	-	-	-	21	21	21
1026	C-H in G lignin, C-O deformation in prim. alcohols	10	10	10	-	-	-
910-885	C-H deformation in cellulose	-	-	-	-	-	-
866	C-H out of plane	11	11	11	-	-	-
818	C-H out of plane	12	12	12	-	-	-
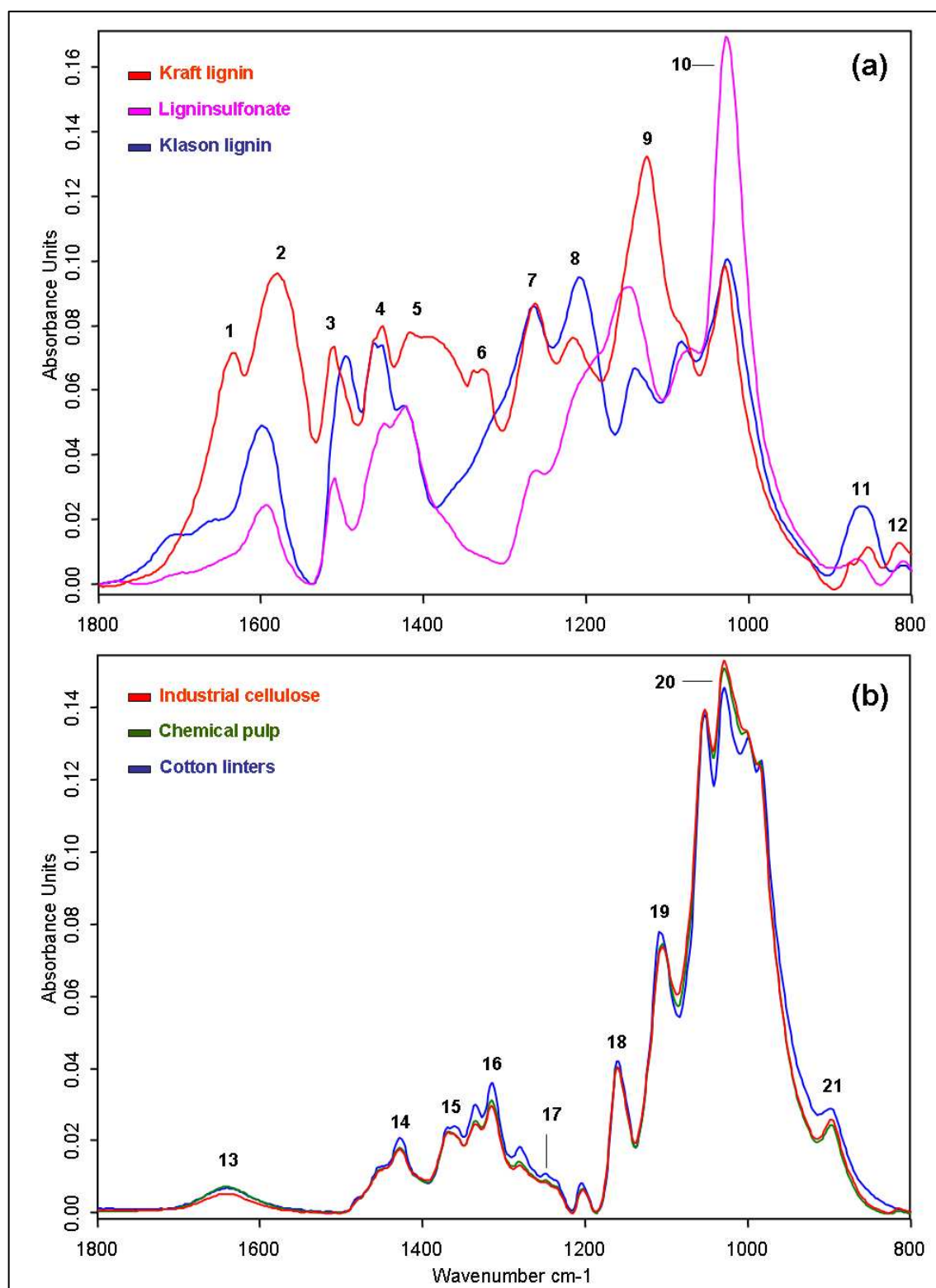
Fig. 1: FTIR-ATR average spectra of three different lignin (a) and cellulose preparations (b) for a wavenumber range from 1800-800 cm^{-1}. Three replicates were measured for lignin and 8 for cellulose with a resolution of 4 cm^{-1} and 32 scans in a wavenumber range from 1800-800 cm^{-1}. The spectra have been baseline corrected and vector normalized. All bands of Kraft lignin and cellulose were numbered for the comparison of the spectra.

2.4.2 Cluster analysis

Cluster analysis was conducted to investigate the similarity of lignin and cellulose spectra, respectively (Fig. 2). FTIR-ATR spectra for lignin revealed two main clusters (Fig. 2 a). One cluster represents technical lignins (Kraft lignin, ligninsulfonate), the other is formed by Klason lignin. The cluster for technical lignin is furthermore split into two further subclusters in which ligninsulfonate and Kraft lignin are assigned separately. The heterogeneity between Klason and technical lignin is twice as high as the one between ligninsulfonate and Kraft lignin. This heterogeneity is likely to be caused by the isolation method, although a species-related influence on lignin composition can not be excluded.

The evaluation of the recorded FTIR-ATR spectra of chemical pulp, cotton linters and industrial cellulose with cluster analysis resulted in two main clusters (Fig 2 b). One cluster was formed by cotton linters, the other by industrial cellulose and chemical pulp. Compared to the cluster analysis of lignin, the heterogeneity, separating the two cellulose clusters, is much lower. This is caused by the high similarity of the samples. Cotton linters formed their own sub cluster. This was probably caused by their lower content of hemicelluloses and higher content of pure cellulose, although this difference was hardly detectable in the spectra.

2.5 Discussion

The interpretation of lignin FTIR spectra to distinguish different lignin types must be undertaken very carefully in general, because there are several uncertainties in the spectra (Fengel and Wegener 2003). Our analyses showed that spectra of Kraft lignin and ligninsulfonate are more similar to each other than spectra obtained for Klason lignin. Fengel and Wegener (2003) also detected differences in absorbance and band position in transmission spectra of technical lignin like ligninsulfonate, milled wood lignin and sulfate lignin of spruce. They assigned these differences to condensation reactions during lignin preparation. In our case Klason lignin was obtained from Grand fir and not from spruce, which might also have contributed to the differences observed. However, since conifer lignin is mainly (<98%) composed of guaiacyl-units, truly pure lignin should show only minor differences in FTIR spectra. It is known that variations in the lignin structure and composition, depending on the origin of the sample and the special isolation procedure, affect FTIR spectra (Fengel and Wegener 2003). Contaminating compounds are e.g. sulphur, NH_3, amino acids and polysaccharides. Generally the sulfur and polysaccharide content of ligninsulfonate is much higher than that of Kraft lignin (Fengel and Wegener 2003). Isosaccharin acids, aliphatic acids, resin, fatty acid, NaOH and NaCl have been determined in

Kraft lignin (Gruber 2007). Thus, different isolation methods result in traces of different residues in lignin preparations. Kraft lignin was isolated with the sulphate method, ligninsulfonate with the sulphite method and Klason lignin of Grand fir under acidic conditions. The strong differences found for spectra of the different preparation indicate that the different residues had an influence on the spectral bands of each lignin type.
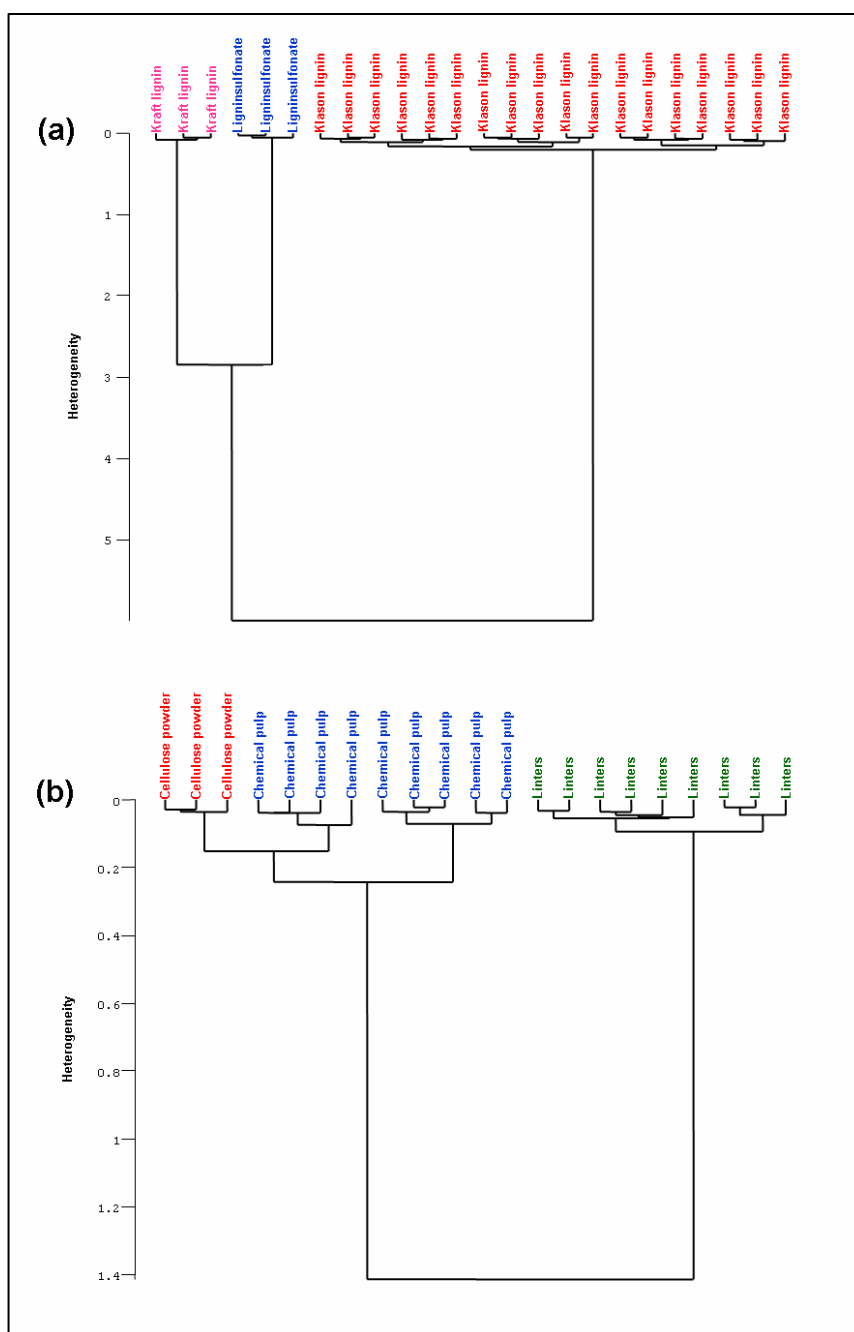

Fig. 2: Dendrogram for the FTIR-ATR spectra recorded of different types of lignin (a) and cellulose (b). The analyzed wavenumber area is 1800-600 cm^{-1}. The spectra have been pre-treated with the first derivation and vector normalization.

The ATR spectra of cellulose obtained here were compared with FTIR spectra, recorded by Hofstetter et al. (2006), who coupled dynamic mechanical analysis with step-scan FTIR to detect the moisture uptake in native cellulose. The spectra were very similar to the ATR spectra of linters, chemical pulp and industrial cellulose. However, in the spectra recorded by Hofstetter et al. (2006) the absorbance ratios for band 14, 15 and 16 were almost identical, whereas in our ATR spectra bands 14 and 15 showed a lower absorbance than band 16. Although the utilized samples differed in their particular origin and chemical pulping, the ATR spectra were very similar. Even though there were nearly no differences detectable between the analyzed cellulose types, it was possible to distinguish their spectra by cluster analysis. The reason is probably the lower content of hemicelluloses/ polysaccharides (e.g. 1075-960 cm^{-1}) and the higher content of cellulose in cotton linters. This is visible in the higher absorbance rate at 910-985 cm^{-1} (C-H deformation in cellulose), 1324-1308 cm^{-1} (C-H vibration in cellulose), 1430 cm^{-1} (scissor oscillation of CH_2 groups in cellulose). This was also noted by Fengel and Wegener (2003), who compared FTIR transmission spectra of cotton linters and chemical pulp. They detected a superior molecular organization of cellulose in cotton linters than in pulp, which implies that the cellulose preparation from cotton linters is purer cellulose than that from chemical pulp.

References

Anonymous. 1995. Benutzerhandbuch. Infrarot-Fourier-Spektrometer IFS 28/ IFS 55 Equinox. Bruker Analytische Messtechnik GmbH.

Bergmann K. 1998. Enzymatische Aktivierung der holzeigenen Bindekräfte zur Herstellung einer bindemittelfreien mitteldichten Faserplatte. Dissertation, Edition Wissenschaft, Reihe Biologie, 151, Tectum Verlag, Marburg, pp. 30-31.

Böttcher J. H. 1993. Quantitative Analyse von Holz und Holzkomponenten mittels FTIR-Spektroskopie unter Anwendung multivariater statistischer Verfahren. Dissertation, Fachbereich Biologie der Universität Hamburg.

Chen L., Carpita N. C., Reiter W., Wilson R., Jeffries C., McCann M. 1998. A rapid method to screen for cell-wall mutants using discriminant analyses of Fourier transform infrared spectra. The Plant Journal, 16, pp. 385-392.

Dence C. W. 1992. Methods in lignin chemistry. Springer-Verlag, Berlin, pp. 33-61.

Faix O. 1991. Classification of lignins from different botanical origins by FT-IR spectroscopy. Holzforschung, 45, pp. 21-27.

Fengel D., Wegener G. 2003. Wood, chemistry - ultrastructure reactions, Kessel Verlag, Remagen.

Gruber E. 2007. Das Kraft-Verfahren. Skript zur chemischen Technologie des Zellstoffs und Papiers. Institut für Makromolekulare Chemie, Fachgebiet Nachwachsende Rohstoffe, TU Darmstadt. Eigenverlag.

Gottwald W., Wachter, G. 1997. IR-Spektroskopie für Anwender. Hrsg. Gruber, U., Klein W. Wiley-VCH Verlag, Weinheim.

Hofstetter K., Hinterstoisser B., Salme L. 2006. Moisture uptake in native cellulose-the roles of different hydrogen bonds: A dynamic FTIR study using deuterium exchange. Cellulose, 13, pp. 131-145, Springer Verlag Berlin.

Kleinschmit J. Svolba, J. 1979. Die Große Küstentanne (*Abies grandis*) in Deutschland. Allgemeine Forstzeitschrift, 34, pp. 218-220.

Kümmerle M., Scherer S., Seiler H. 1998. Rapid and reliable identification of food-borne yeasts by Fourier transform infrared spectroscopy. Applied and Environmental Microbiology, 64, pp. 2207-2214.

Marutzky R., Thole, V. 2003. Eminente Bedeutung - Stand der Technik und aktuelle Entwicklung bei Holzwerkstoffen. HK Holz und Kunststoffverarbeitung, 38, pp. 34-36.

Naumann A., Navarro-Gonzalez M., Peddireddi S., Kües. U., Polle A. 2005. Fourier transform infrared microscopy and imaging: Detection of fungi in wood. Fungal Genetics and Biology, 42, pp. 829-835.

Naumann A., Polle A. 2006. FTIR imaging as a new tool for cell wall analysis of wood. New Zealand Journal of Forestry Science, 36. pp. 54-59.

Naumann, A., Peddireddi, S., Kües, U., Polle A. 2007. New biological methods for the evaluation of wood. Chapter 7, FTIR microscopy. In: Wood production, wood technology and bio-technological impacts, U. Kües (Ed.) Universitätsverlag Göttingen.

Pastusiak R. 2003. Charakterisierung von Zellstoffkomponenten - Analytik, Spektroskopie, Reaktionskinetik und Modellierung. Dissertation, Fakultät für Chemie der Technischen Universität München.

Salzer R., Steiner G., Mantsch H. H., Mansfield J., Lewis E. N. 2000. Infrared and Raman imaging of biological and biomimetic samples. Fresenius J. Analytical Chemistry, 366, pp. 712-726.

Schindel K. 1998. Die Röntgenmikroanalyse von Lignin als Untersuchungsmethode für Holz und Holzwerkstoffe. Dissertation, Fakultät für Forstwissenschaften und Waldökologie der Georg-August-Universität Göttingen..

Schuhmacher W. (Hrsg.) 1967. Der Stofftransport der Pflanze. In: Handbuch der Pflanzenphysiologie, Springer Verlag Berlin, pp. 204-376.

Setz P. 2005. Infrarot Spektroskopie mit modernen FTIR Spektrometern. Praktikumsskript, Physikalische und Analytische Chemie, ETH Zürich. Eigenverlag

Sjöström E. (Hrsg.), Alen R. (Hrsg.) 1998. Analytical methods in wood chemistry, pulping and papermaking. Springer Verlag, Berlin.

Usmanov K.U., Yulchibaev A.A., Dordzhin G.S. and Valiev A.1972. IR spectroscopic analysis of graft co-polymers of cellulose and its derivatives with vinyl fluoride. Fiber Chemistry, 3, pp. 292-295.

Windeisen, E., Strobel, C., Wegener 2003. Chemische Charakterisierung von thermisch belastetem Holz, Bestimmung des Acetylgruppengehalts und FTIR-Spektroskopie. Holz als Roh und Werkstoff, 61, pp. 471-472. http://www.zellstoff-stendal.de/index.php?section=glossar&s_id=&u_id=&value=E (14.06.06)

CHAPTER III

3 FTIR-ATR spectroscopic analysis of changes in wood properties during particle- and fiberboard production of hard- and softwood trees

3.1 Abstract

Fourier transform infrared attenuated total reflectance (FTIR-ATR) spectroscopy was combined with multivariate data analysis to investigate the chemical changes in wood properties during particle- and middle dense fiberboard (MDF) production of Grand fir (*Abies grandis* (Douglas ex D. Don) Lindl.) and beech (*Fagus sylvatica* L.). The mechanical and technological properties of the novel particle and fiber boards from beech or Grand fir wood were similar to those of conventional panels from pine and spruce. This indicates that these timbers can be used as resources for wood panel production. Principle component analysis of FTIR spectra differentiated wood, fibers, particles, MDF and particleboards of both species in the whole production process. Modifications in the spectra of fibers and particles suggested that cellulose properties of wood were changed during mechanical pulping and that these changes were largely reversible upon pressing. Binders and hydrophobic additives were clearly traceable in wood composites. Samples from the same production step were clustered together, indicating high homogeneity of the raw material, the intermediate and final products. This suggests that FTIR spectroscopy in combination with cluster analysis is a useful tool to assess product quality and can be further developed to control and optimize production processes for innovative wood-based panels.

3.2 Introduction

Economic changes in developing countries and globalization are causing increasing costs for fossil fuels, thereby, affecting the demand on wood as bioresource for energy (Wolf 2005; Reich 2008). This leads to shortage of timber for wood processing industries; in Germany, the present stock of timber will be insufficient to meet the needs in the next decades (Behrendt and Rupp 2006). Pöyry Forest Industry Consulting (2006) estimated that the European demand on raw material for panel board production will keep on increasing from 26 million tons absolutely dry wood in 2005 to 37 million tons in 2015. This trend holds particularly for Germany, being the most important panel board producer in Europe (Alteheld 2007).

To ensure long-term supply of wood processing industries, various measures have been suggested, e.g., enlargement of plantations with fast growing tree species in short rotation cycles, the utilization of wood from deciduous tree species or fibers from annual plants, the mobilization of roundwood potential in privately owned forests and the extension of silviculture with fast growing conifers such as Douglas fir and Grand fir (Behrendt et al. 2007; Dohrenbusch and Bolte 2008; Spellmann and Kehr 2008). The latter species have been introduced into Germany from North America and are considered being of high potential for domestic forestry (Röhrig 1981; Nörr 2004). Grand fir seems to be particularly well suited because of its drought tolerance and ecological compatibility (Röhrig 1981). Notwithstanding future needs, most present silvicultural programs in Germany have intensified beech cultivation, because this species is the potentially natural dominant tree in many Central European forests (Ellenberg 1996). This species is at risk under the expected climate change (Rennenberg et al. 2004). Furthermore, it is not used in panel industries because of its high raw density (Wagenführ 2000) and the risk of allergies and cancer, due to its hazardous dust, generated during particle and fiber production (Kloeser et al. 2008). Therefore, knowledge on product properties from wood of beech or of introduced tree species is limited.

In general, low quality woody parts of harvested trees, small or young trees and fast growing species are being used for wood-based panels (Deppe and Ernst 2000; Ambrozy and Giertlova 2005). Wood as a naturally grown resource shows high variability in its chemical, biological and physical properties (Wagenführ 2000; Fengel and Wegener 2003). Therefore, a large-lot production of massive timber products with unaltered material properties is very difficult to achieve and expensive (Holzwirtschaft Schweiz 2007). To overcome this limitation, wood is chipped and processed to fibers and particles to provide intermediate products for medium dense fiber (MDF) and particleboard production (Kloeser et al. 2008). The intermediate wood products are glued by adhesives, usually urea-formaldehyde (UF)-resin with additives (Youngquist et al. 1997; Kharazipour 2004), under pressure at high temperatures to wood-based panels. To date, spruce and pine are the main resources for derived timber products (Wagenführ 2000). Since the conventional resources for wood panels are becoming limited, there is a need to introduce novel materials into these processes. Whether the properties of beech and Grand fir wood are suitable for the use in these production processes and how these processes affect the chemical features of wood of these species is currently unknown.

The aim of this work was to test the usability of wood from beech and Grand fir for fiber and particleboard production and to investigate the chemical changes occurring during

wood processing. To this end, we produced MDF and particleboards from Grand fir and beech and compared their technological properties with those of reference plates from spruce-pine based industrial processes. Beech wood was also used as intermediate layer in the so-called hybrid particleboards. This novel type of wood-composite consists of three layers, whereby Grand fir was used for the overlay, enclosing the particles of beech. To characterize the influence of the production process on the chemical composition of the materials involved, Fourier transform infrared-attenuated total reflectance (FTIR-ATR) spectroscopy was applied. FTIR spectroscopy method has been used in wood analysis for a long time, because it provides a chemical finger-print of the main organic constituents (Fengel and Wegener 2003). It is suitable for the analysis of bonds between wood, wood components and glues (Fabo 2004). We employed FTIR-ATR in combination with unsupervised multivariate statistical methods to investigate the homogeneity of product properties by cluster analysis and to identify small spectral changes by principle component analysis (PCA).

3.3 Material and methods

3.3.1   Wood material

Ten beech (*Fagus sylvatica* L.*)* and ten Grand fir (*Abies grandis* (Douglas ex D. Don) Lindl.) trees, each 56 years old, were harvested in 2006 in the city forest of Schmallenberg (North Rhine-Westphalia, 51° 14' 29'' N, 8° 23' 50'' E). The forest stand has west to northwest exposition at an altitude of 600 m and is located on a steep slope. The soil is brown earth with limited nutrient supply. The forest stand was established by planting. At harvest, the mean height and breast height diameter of beech were 16 m and 18 cm, respectively. Grand fir had an average height and breast height diameter of 29 m and 45 cm, respectively. The wood was used to produce particles and fibers (see below) after cutting two disks from each tree, one at the stem base and one below the crown. From these disks, small blocks (2 per disk) were excised (length: 1 cm, width: 1 cm, height: 2 cm), hackled with a gripper to small pieces, and milled to a fine powder (MM 2000, Retsch, Haan, Germany) for 5 min at 50 u/min. The frequency was raised slowly during the next 5 minutes to 90 u/min. The whole milling process took 10 min for each sample.

3.3.2   Production of fibers and MDF plates of Grand fir and beech

The stems of Grand fir and beech were debarked manually and cleaved afterwards. The wood pieces were processed to wood chips in a drum chipper (Klöckner Trommelhacker KTH

120 x 400 H2WT, Klöckner Wood Technology GmbH, Hirtscheid, Germany). For pulping, the chips were weighed and put into a pressurized laboratory refiner (Laboratory Refiner Type 12, Andritz AG, Graz, Austria). Without any further pre-treatment, the chips were pulped for 5 min under thermal and mechanical conditions (thermo mechanical pulp, TMP) at a temperature of 150 °C and a pressure of 4.8 bar. Afterwards, the fibers were dried in a gas flame heated drying pipe at 125 °C for 3 seconds, to receive the target moisture of 8%.

Ten samples of fibers were taken randomly from different locations of the fiber packages. Fine powder of the dried fibers was prepared for FTIR-ATR analysis as described above. To prepare fibers for MDF production, Melamine-urea-formaldehyde (MUF)-resin (K 413, BASF AG, Ludwigshafen, Germany) with a solids content of 68 % (w/v), containing of < 5 % (w/v) melamine, was utilized. The concentration of the binder was 12 % (solid resin/dry fiber mass (w/w)). Paraffin (HydroWax® 730, Sasol, Hamburg, Germany) with a solids content of 60 % (w/v) and a concentration of 1 % (dry paraffin/dry fiber mass (w/w)) was mixed with the UF-resin before spraying the glue mixture onto the fibers.

The sprayed fibers were scattered and pressed in a hot-press to boards of a thickness of 10 mm. The pressing process took 3 min (18 s/mm) at 200 °C and 220 bar. MDF boards of beech were produced with raw densities of 500, 600, 700 and 800 kg/m^3, respectively, and MDF boards of Grand fir with densities of 500, 600 and 700 kg/m^3, respectively. The board densities resulted from the specific net weight of absolutely dry fibers. For each density, two boards were investigated, of which 10 samples were taken.

3.3.3 Particleboard manufacturing of Grand fir and beech

3.3.3.1 Particle production

Logs of beech and Grand fir were processed to wood chips in a drum chipper (Klöckner Trommelhacker KTH 120 x 400 H2WT, Klöckner Wood Technology GmbH, Hirtscheid, Germany). The wood chips were converted into particles in a knife ring flaker (Condux HS 350, Condux Maschinenbau GmbH. and. Co. KG, Hanau, Germany) with a knife overhang of 0.45 mm and dried at 100 °C in a drum drier (ecoDry, SC Technology GmbH, Hendschiken, Switzerland) for 25 min. With a tumbler screening machine (TSM 1200/4, Allgaier Werke GmbH, Uhingen, Germany), the particles were separated in five fractions. Four sieves with a mesh size of 5.0 mm, 3.15 mm, 1.25 mm und 0.6 mm were utilized. 6 fractions of particles with different dimensions were received, including particles > 5.0 mm and < 0.6 mm. In dependency of the particular type of particleboard, different ratios of the particular fractions were utilized. 10 random samples were collected from particle packages consisting of

particles of all dimensions. Fine powder of dried particles of beech and Grand fir wood was prepared for FTIR-ATR analyses as described above.

3.3.3.2 Three-ply particleboard of Grand fir

To produce particleboards, Urea-formaldehyde (UF)-resin (K 350, BASF AG, Ludwigshafen, Germany) with a solids content of 68 % (w/v) was utilized. The concentration of the binder was 8 % (solid resin/dry fiber mass (w/w)) for the intermediate layer and 10 % (solid resin/dry particle mass (w/w)) for the overlay. Paraffin (HydroWax® 138, Sasol, Hamburg, Germany) with a solids content of 60 % (w/v) and a concentration of 2 % (dry paraffin/dry particle mass (w/w)) for the intermediate layer and 1 % (dry paraffin/dry particle mass (w/w)) for the overlay was utilized. As hardener, ammonium sulphate (AppliChem GmbH, Darmstadt, Germany) with a solids content of 33 % (w/v) and a concentration of 2 % (dry hardener/ solid resin (w/w)) for the intermediate layer and 1 % (dry hardener/ solid resin (w/w)) for the overlay was applied. Paraffin and hardener were admixed to the UF-resin before spraying the glue mix onto the particles and pressing the boards. The overlay of the three-ply particleboard consisted of 50 % particles of a dimension of 1.25 mm and 50 % particles of 0.6 mm. The intermediate layer was composed of 20 % particles of a dimension of > 5.0 mm, 60 % of 3.15 mm and 20 % of 1.25 mm. Grand fir particles with 10 % moisture for the overlay and 8.5 % for the intermediate layer were sprayed with the binder (see above) and paraffin, scattered and pressed in a hot-press to three-ply particleboards with a thickness of 20 mm. The weight ratios (%) of the overlays to intermediate layer were 20 : 60 : 20 of absolutely dry particle mass. The boards were pressed for 4 min (12 s/mm) at 200 °C and 220 bar. Board densities of Grand fir of 500, 600 and 700 kg/m^3, respectively, were produced. The board density resulted from the specific net weight of absolutely dry particles. Two boards were investigated per density, of which 10 samples were taken.

3.3.3.3 Monolayer particleboard of beech

For particleboards from beech UF-resin (K 350, BASF AG, Ludwigshafen, Germany) with a solids content of 68 % (w/v) was utilized. The concentration of the binder for the monolayer boards was 8 % (solid resin/dry fiber mass (w/w)). Paraffin (HydroWax® 138, Sasol, Hamburg, Germany) with a solids content of 60 % (w/v) and a concentration of 2 % (dry paraffin/dry particle mass (w/w)) was utilized. As hardener, ammonium sulphate (AppliChem GmbH, Darmstadt, Germany) with solids content of 33 % (w/v) and a concentration of 2 % (dry hardener/ solid resin (w/w)) was applied. Paraffin and hardener were admixed to

UF-resin before spraying the glue mix onto the particles and pressing the boards. The monolayer of the particleboard consisted 100 % of particles of all dimensions. The beech particles were sprayed with the composite binder of UF resin K 350, ammonium sulphate and HydroWax® 138, scattered and pressed in a hot-press to monolayer particleboards with a thickness of 20 mm. The pressing process took 4 min (12 s/mm) at 200 °C and 220 bar. The particleboards of beech had a density of 600 and 700 kg/m³. For each density 2 boards were investigated, of which 10 samples were taken.

3.3.3.4 Three-ply particleboard of beech and Grand fir (hybrid board)

Particles of beech and Grand fir were sprayed with composite adhesives used for Grand fir particleboard (see above). Particles of Grand fir were taken for the overlay, particles of beech for the intermediate layer. The overlay of the hybrid board consisted of 30 % particles of a dimension of 1.25 mm, 50 % of 0.6 mm and 20 % particles < 0.6 mm. The intermediate layer consisted 100 % of particles of all dimensions. Hybrid boards of densities of 500, 600 and 700 kg/m³, respectively, were produced as described for Grand fir. For each density two boards were investigated, of which 10 samples were taken.

3.3.4 Production of reference boards
3.3.4.1 MDF boards

Industrial fibers (Steico AG, Feldkirchen, Germany) of *Pinus sylvestris* and *Pinus radiata* (mixing ratio 1 : 1) were utilized. The fibers were produced of wood chips, pulped at a temperature of 160-180 °C and a pressure of 8-12 bar. They were decomposed in a defibrator (L 36, Sunds Defibrator Industries, Solna, Sweden) at a constant pressure of 11 bar. The fibers were sprayed with composite binder and used to prepare boards as described above for MDF plates of beech and Grand fir.

3.3.4.2 Three-ply particleboards

Industrial particles (Pfleiderer Holzwerkstoffe GmbH & CO. KG, Neumarkt, Germany), composed of saw dust (45 %), solid wood (30 %) and wood chips (25 %) were used. The saw dust originated from the sawmill industry, the chips were produced of pulp- and recycling wood, which contained spruce and pine as major fractions and small amounts of beech. The production was the same as that used to prepare three-ply particleboards of Grand fir.

3.3.5 FTIR-ATR spectroscopy and multivariate data analysis

FTIR-spectroscopy is a powerful technique for determination of molecular structures, identification of compounds in biological samples and investigation of complex polymers (Arndt et al. 1999; Kacuráková and Wilson 2001). The ATR (attenuated total reflection) technique as a universal sampling accessory to FTIR provides reproducible qualitative and quantitative analysis of samples with little to no sample preparation (Bukowski and Monti 2007). The principles and limitations of FTIR-ATR spectroscopy have been reviewed recently (Naumann et al. 2008). FTIR-ATR spectra were recorded in the wave number range from 4500-600 cm^{-1} with an Equinox 55 spectrometer (Bruker Optics, Ettlingen, Germany) including a deuterium-triglycinesulfate-detector and an attached ATR-unit (DuraSamplIR, SensIR Europe, Warrington, England). A resolution of 4 cm^{-1} and a number of 32 scans per sample was used. The samples of solid wood, fibers and particles were powdered. Specimen of MDF (length: 5 cm, width: 1 cm, height: 1 cm) and particleboards (length: 5cm, width: 1 cm, height: 2cm) were investigated. 12 (wood) or 10 (fibers, particles, board) replicates were analyzed and averaged, whereby 5 measurements were respectively accomplished for the outer- and the inner layer of each board specimen. If not indicated otherwise, 10 individual samples were analyzed per experimental variable, thus, yielding 100 to 120 spectra. Because of the high spectral homogeneity of liquid UF-resin and HydroWax$^{®}$, 3 FTIR-ATR measurements were performed on each sample.

The heterogeneity of the recorded FTIR-ATR spectra was investigated by cluster analysis. According to their spectral heterogeneity, spectra were classified into clusters or classes in dendrograms. The first derivative and vector normalization (9 smoothing points) was utilized as pre-treatment method of the spectra, applying the standard method for creating the distance matrix with the OPUS 6.5 software (Bruker Optics, Ettlingen, Germany). For calculating the spectral distances the Ward's Algorithm was applied. The analyzed wavenumber range was 4500-600 cm^{-1}.

PCA was applied to classify the principal components in the spectra of different samples. The first derivative and vector normalization (9 smoothing points) was utilized as pre-treatment of the spectra, applying the factorization as algorithm for calculating the spectral distances. Three factors were used for spectra evaluation with the OPUS 6.5 software (Bruker Optics, Ettlingen, Germany). The analyzed wavenumber range was 4500-600 cm^{-1}.

3.3.6   Mechanical and technological properties of MDF and particleboards

Technological properties were determined according to EU standards. Tensile strength (EN 319), bending strength (EN 310), and surface soundness for particleboards only (EN 311) were measured with a universal testing machine (T1-FR010TH.A50, Zwick/Roell, Ulm, Germany) with maximum test load of 10 kN. The raw density of the boards (EN 323) was analyzed with a density measuring system (DA-X, GreCon, Alfeld, Germany). Additional board properties, such as moisture content (EN 322) and thickness swelling after 24 h water storage (EN 317) were investigated. For each type of board two panels were analyzed. Sampling and cutting of the boards was accomplished as described in EN 326-1. The dimensions of the specimens were determined as described in EN 325.

3.4 Results

3.4.1   Mechanical and technological properties of panel boards

Novel MDF, particle, and hybrid particleboards composed of beech and Grand fir consistently showed higher tensile strength, bending strength, and surface soundness than reference boards (Table 1). Only MDF boards of beech displayed a lower bending strength than the reference. The swelling factors of all panels were almost identical to those of their respective reference (Table 1). This indicates that spruce or pine-based production processes for MDF and particleboards can also be applied to beech and Grand fir wood.

Table 1: Mechanical and technological properties of novel and conventional panel boards.

Tree species	Type of Panel board	Thickness	Raw density	Tensile strength	Bending strength	Surface soundness	Swelling/ 24h
		mm	kg/m³	N/mm²	N/mm²	N/mm²	%
Reference (Pine)	MDF	9	600	0.43	30.25	-	15.4
Grand fir	MDF	9	600	0.65	34.52	-	15.3
Beech	MDF	9	600	0.81	22.38	-	15.6
Reference (Spruce, Pine, Beech)	Particleboard	19	600	0.45	14.10	0.89	13.9
Grand fir	Particleboard	19	600	1.27	18.13	1.72	12.6
Grand fir + Beech	Hybrid particleboard	19	600	0.86	16.38	1.42	14.1

3.4.2   Beech and Grand fir solid wood

To investigate chemical differences in wood of the two species and changes occurring during the production processes, beech and Grand fir wood were characterized by FTIR spectroscopy (Fig. 1). All major bands were numbered and the components, to which these peaks were attributable, are shown in table 2.

Table 2: *Wavenumber characterization (Usmanov et al. 1972; Parker 1983; Faix 1991; Faix 1992; Fengel and Wegener 2003; Pandey and Pitman 2003). Numbers in the table refer to the numbers assigned to the bands in figures 1, 2, 3, 4 and 5.*

Wavenumber cm^{-1}	Compound	Band numbers
3336	O-H stretch	1
2938	CH- stretch in methyl- and methylene groups	2
2882	CH- stretch in methyl- and methylene groups	3
2103	Absorption caused by the ATR crystal	4
1990	Absorption caused by the ATR crystal	5
1738	C=O stretch in unconjugated ketones, carbonyls and in ester groups (frequently of carbohydrate origin)	6
1649	Absorbed O-H and conjugated C-O	7
1593	Aromatic skeletal vibration plus C=O stretch	8
1549	Secondary amides (-CO-NH-)	9
1505	Aromatic skeletal vibration plus C=O stretch	10
1460	CH- deformation; asymmetric in –CH$_2$- and -CH$_3$-	11
1424	Aromatic skeletal vibration combined with CH in plane deformation	12
1372	CH deformation in cellulose and hemicelluloses	13
1328	S ring plus G ring condensed	14
1318	C-H vibration in cellulose and C-O vibration in syringyl derivates	15
1267	Guaiacyl ring breathing, C-O stretch in lignin; C-O linkage in guaiacyl aromatic methoxy groups	16
1235	Syringyl ring and C= stretch in lignin and xylans	17
1157	C-O-C vibration in cellulose and hemicelluloses	18
1032	Aromatic C-H in plane deformation, guaiacyl type and C-O deformation; primary alcohol	19
897	C-H deformation in cellulose	20

In the wavenumber range from 4000-1800 cm^{-1} wood from both species showed strong spectral similarities (Fig. 1). Bands 4 and 5 are caused by the ATR unit. Differences between the two species occurred mainly in the fingerprint region (1800-850 cm^{-1}).
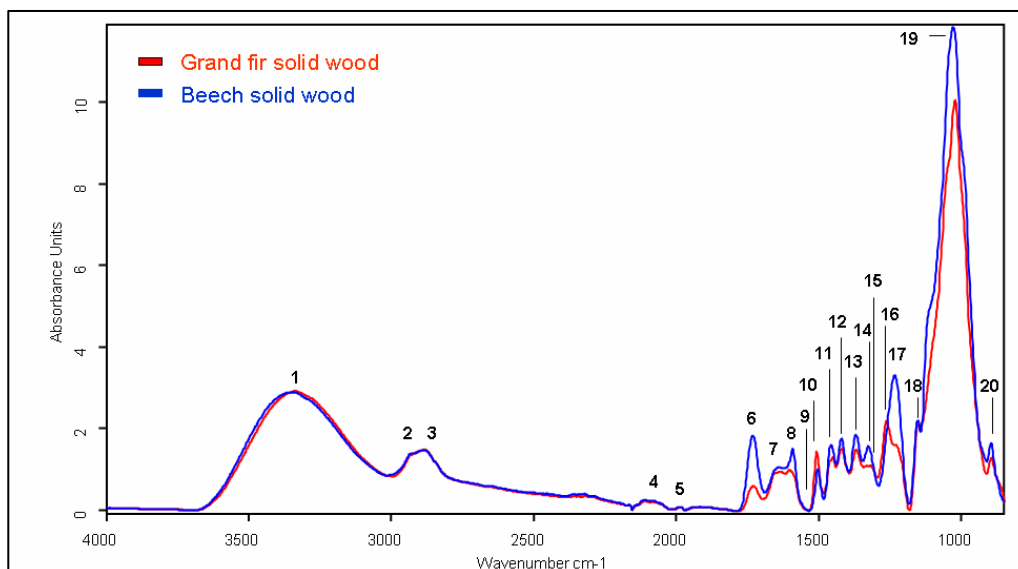

Fig. 1: FTIR-ATR mean spectra of beech and Grand fir solid wood powder in the wavenumber range from 4000-850 cm^{-1}. The spectra were baseline corrected and vector normalized, the band assignments are shown in table 2.

We observed higher absorbance for beech wood in bands 6, 8, 11, 12, 13, 19 and 20, typical of holocellulose, suggesting a higher amount of holocellulose in beech than in Grand fir (Fig. 1). Pronounced differences occurred also at bands 14, 16 and 17, typical for lignin. These differences were expected, because conifers contain mainly guaiacyl (G) lignin, whereas angiosperm lignin is composed of G and syringyl (S) units (Pandey 1999; Fengel and Wegener 2003). Band 14 represents a mixture of G- and S units. In the spectrum of Grand fir at position 14 only a shoulder appeared (Fig. 1), whereas a clear peak was present in beech wood (Fig. 1). Band 16, typically for G units, showed a shoulder in beech and a peak in Grand fir (Fig. 1). Beech displayed a broad band 17, typical for S-lignin, which covered the G-units (band 16) to some extent. Overall these analyses illustrate that major differences between beech and Grand fir wood existed with respect to lignin composition and holocellulose content.

3.4.3 Particleboards from beech and Grand fir

We identified a clear influence of the production process on wood properties (Fig. 2). Particles displayed higher absorbance in band 1, 6, 7, and 19 than wood, suggesting an increase in free OH-groups. These increases were found in both, particles from Grand fir and beech (Fig. 2 a, b), suggesting that the same chemical bonds were released during particle production of both species.
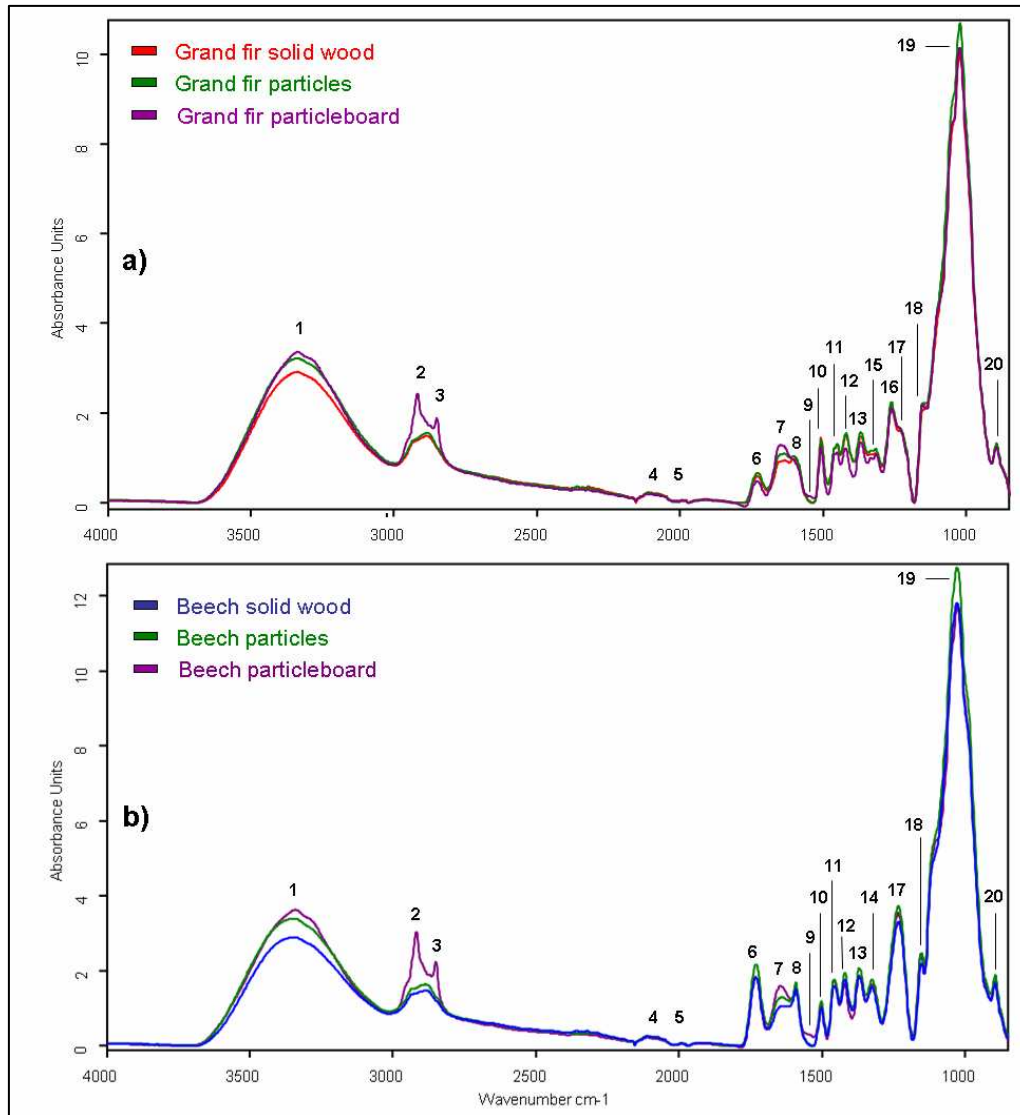

Fig. 2: FTIR-ATR mean spectra of particles and particleboards of Grand fir (a) and beech (b). Spectra were acquired in the wavenumber range from 4000-850 cm^{-1} (n = 10 per sample) and the mean was calculated. Spectra of solid wood powder from fig. 1 are shown for comparison. Particleboards of ρ= 600 kg/m^{3} are shown. The spectra were baseline corrected and vector normalized; the band assignments refer to table 2.

From the intermediate (particles) to the final product (particleboard) further changes occurred, which were characteristic for wood from both species, but additionally, some alterations specific for particleboards were found. Band 1 increased further, when particles were pressed to boards, whereas bands 6 and 19 decreased. Bands 2 and 3 as well as band 9 appeared only in the final products and band 7, which was only present as a shoulder in wood or particles, was increased to a pronounced peak (Fig. 2 a, b).

Since the particleboards contain UF-resin as binder and additives to prevent swelling (HydroWax®), these compounds were also analyzed. Comparative analyses of the UF-resin and of HydroWax® spectra showed that band 2 and 3 were characteristic of HydroWax® (Fig. 3). Band 9 is close to the position where UF-resin showed the highest peak (Fig. 3). This peak might have been caused by amides (Table 2). However, in boards the maximum was shifted compared with binder (Fig. 3).
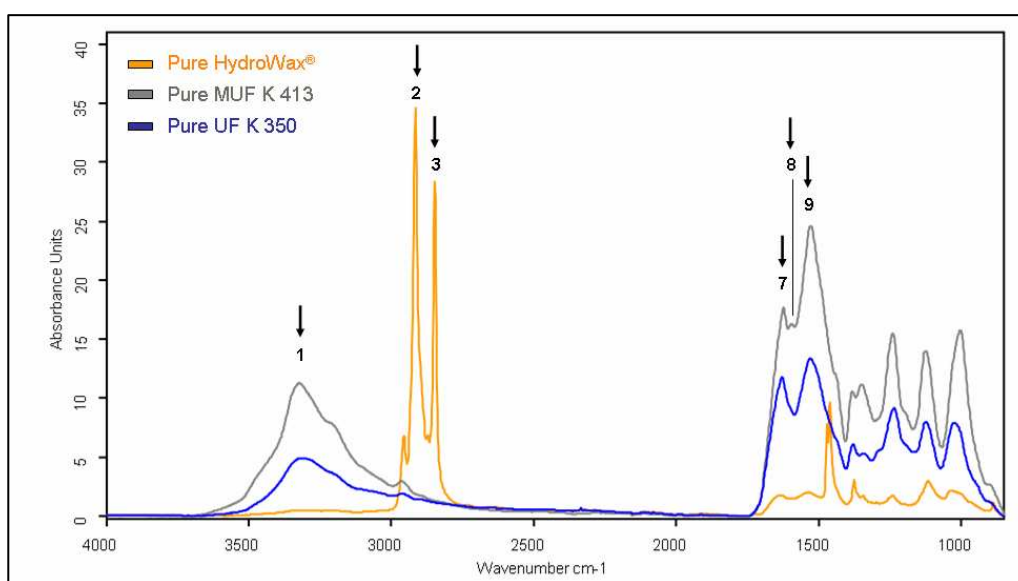

Fig. 3: FTIR-ATR averaged spectra of MUF K 413, UF K 350 and Hydrowax® in the wavenumber range from 4000-850 cm⁻¹. The spectra were baseline corrected and vector normalized. The bands showing the most significant influences in the spectra of the final products were marked. Band assignments are shown in table 2.

The presence UF-resin furthermore affected the shape of peak 1 in particleboards (Fig. 2), where a shoulder appeared due to the strong peak at position of 3324 cm⁻¹ of UF-resin (Fig. 3). UF-resin also showed some absorbance at the position of peak 7 (Fig. 2, 3). However, not all bands increased. The intensities of bands 12, 13 and 19, indicative for

holocellulose, decreased in boards compared to particles. In Grand fir materials, these decreases were stronger than in those of beech.

Particleboards of different densities were also analyzed. However, board density had no effect on the resulting FTIR spectra (see appendix I and Fig. 1).

3.4.4   MDF boards from beech and Grand fir

To investigate the influence of the production process of MDF boards on wood properties, FTIR spectra of wood, fibers and boards were compared (Fig. 4). Wood and fibers displayed only small differences, which were most pronounced in the carbohydrate range and for aromatic compounds (band 18 and 19) as observed also for particles (see above, Fig. 2). This was true for both species.
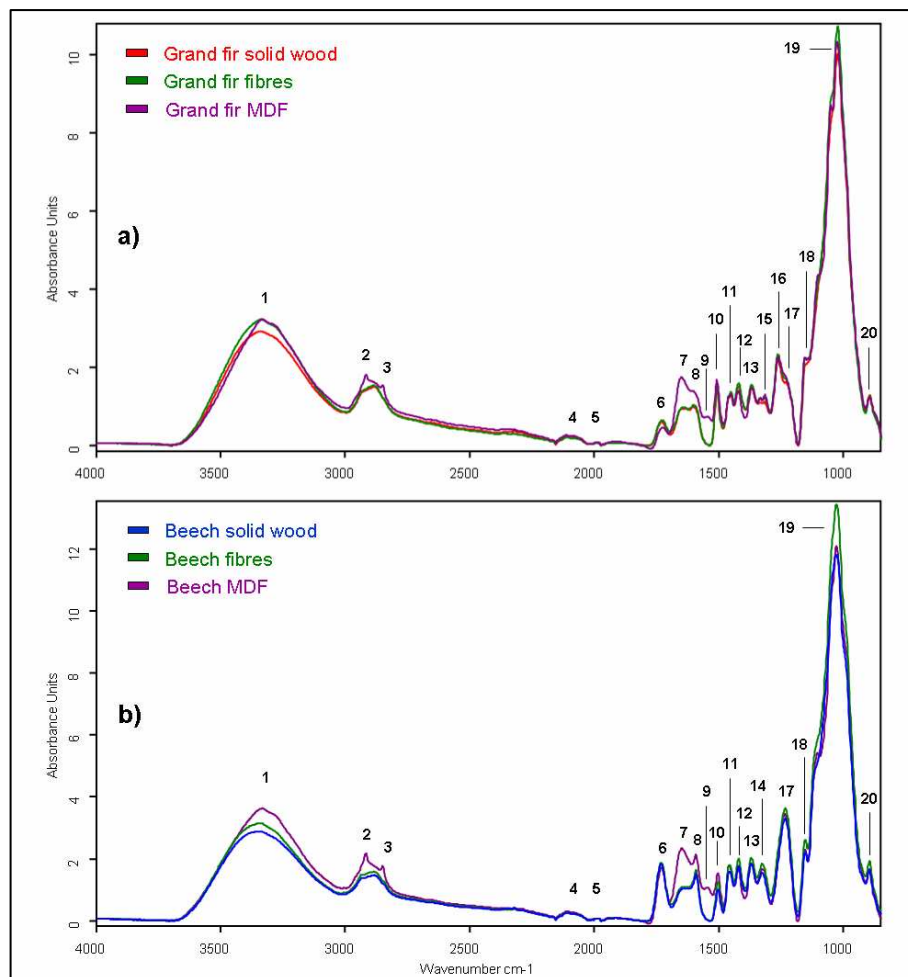

Fig. 4: FTIR-ATR mean spectra of fibers and MDF boards of Grand fir (a) and beech (b). Spectra were acquired in the wavenumber range from 4000-850 cm^{-1} (n = 10 per sample) and the mean was calculated. Spectra of solid wood powder from fig. 1 are shown for comparison. MDF boards of ρ= 600 kg/m^3 are shown. The spectra were baseline corrected and vector normalized; the band assignments refer to table 2.

FTIR spectra of MDF plates showed characteristic deviations from wood or particle spectra. Peaks 2 and 3, indicative for the addition of HydroWax®, were present (Fig. 4). Furthermore, peaks 7 and 9, the latter probably characteristic of amides in UF-binder, increased strongly (Fig. 4) as observed also in particleboards (Fig. 2). Peak 7 present as a shoulder in fibers was strongly increased in MDF boards of both species (Fig. 4 a, b). Peak 8 also showed increases, which suggests increased aromatic vibrations or C=O stretch (Fig. 4). Since this increase was found in MDF boards of both, Grand fir and beech, but not in particleboards, it must be regarded to present specific changes due to MDF processing. Peak 8 might have been caused by use of different UF-resin formulations for particleboards (UF-resin with a valley at position 8) and particleboards (MUF with a peak at position 8). MDF boards of different densities were also analyzed. However, board density had no effect on the resulting FTIR spectra (see appendix I and Fig. 2).

3.4.5 Three-ply hybrid particleboard with an outer layer made of Grand fir particles and an inner layer of beech particles

For a better overview solid wood, particles and the corresponding layer in the hybrid board were illustrated separately, depending on the particular tree species (Fig. 5).

Spectral differences between intermediate- and final product were visible in band 2, 3, 7, and 9, illustrating an obvious increase of the absorbance units in the spectrum of the hybrid boards. This held for overlay and intermediate layer, whereas in band 7 and 9 the increase was more obvious for the overlay. In contrast to this result, the absorbance unit in band 19 showed a decrease, which was more apparent in the spectrum of the intermediate layer. Other spectral differences were hardly notable. Additionally, we detected higher absorbance units in bands 7 and 9 of the outer layer, compared to the particleboard of Grand fir, whereas the inner layer did not show significant spectral differences compared to the particleboard of beech.
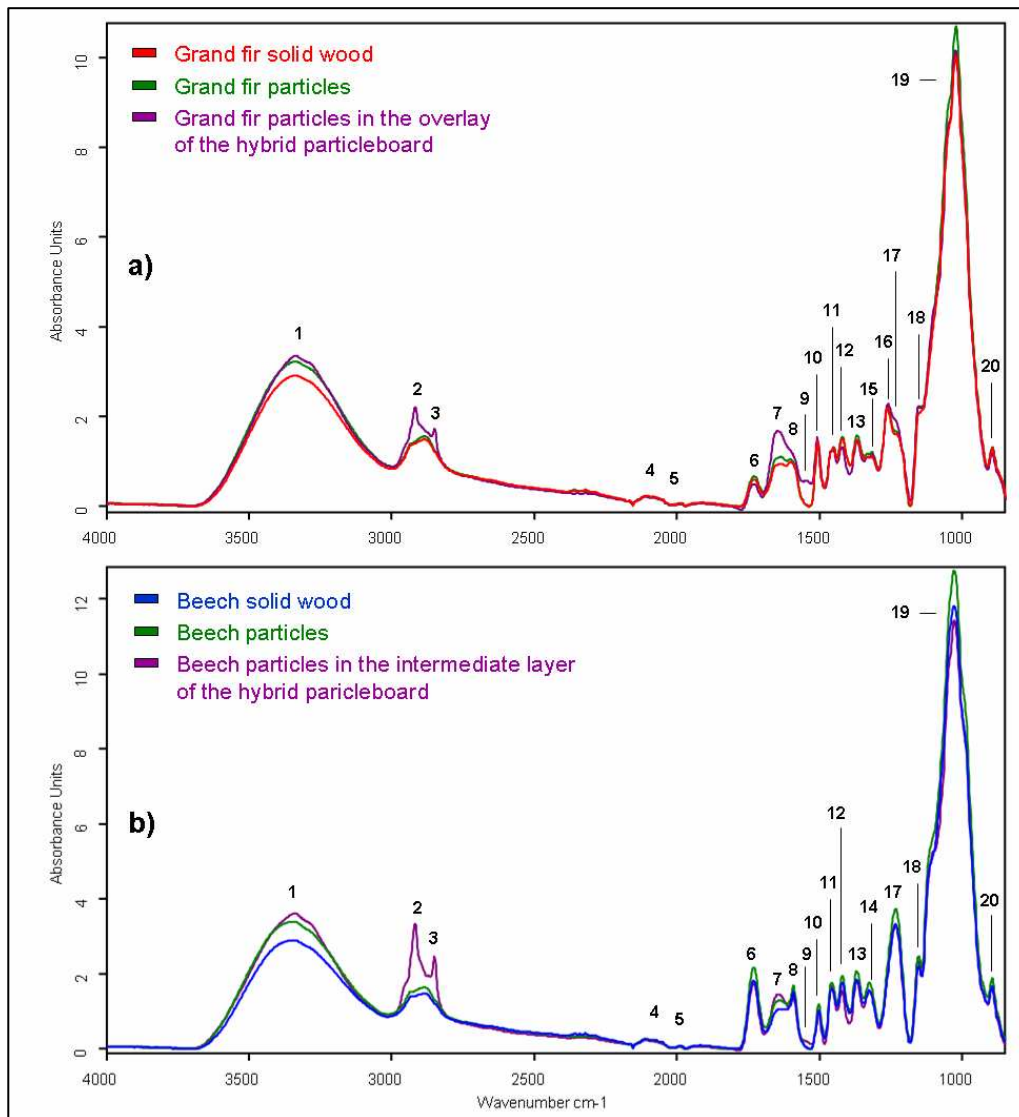
Fig. 5: FTIR-ATR averaged spectra of the production process of hybrid boards (ρ= 600 kg/m³) in the wavenumber range from 4000-850 cm⁻¹. The overlay with particles of Grand fir (a) and the intermediate layer with particles of beech (b) were illustrated separately. The spectra were baseline corrected and vector normalized, the particular bands numbered in reference to table 2.

3.4.6   Multivariate analysis of FTIR spectra to elucidate product quality and properties

PCA analysis was conducted to find out if the different samples could be grouped according to species and sample processing. Using normalized first derivatives of the original spectra across the whole wave number range, we obtained four PCAs, which contributed 92.97, 5.76, 0.97 and 0.19 % to the total variation, respectively. Since PC1 resembled strongly the original spectrum, it was not considered further.

A 3-dimensional scatter plot showed that the 10 different sample types (2 tree species with the following products: wood, fibers, particles, MDF and particleboards) grouped according to PC2, PC3, and PC4 (Fig. 6). PC2 was mainly responsible for the separation of the two species: Grand fir products (wood, fibers, particles, MDF and particleboards) scored positive, whereas the corresponding beech products had negative scores for PC2 (Fig. 6). PC3 separated final products of both species (MDF and particleboards, negative scores) from raw and intermediate materials of both species (wood, fibers and particles, positive scores). PC4 was mainly responsible for the separation of fibers, particles, and wood with fibers, showing more negative scores than particles and particles more negative than wood (Fig. 6). Fibers, particles and wood showed some overlap, but the gross groups were still discernable.
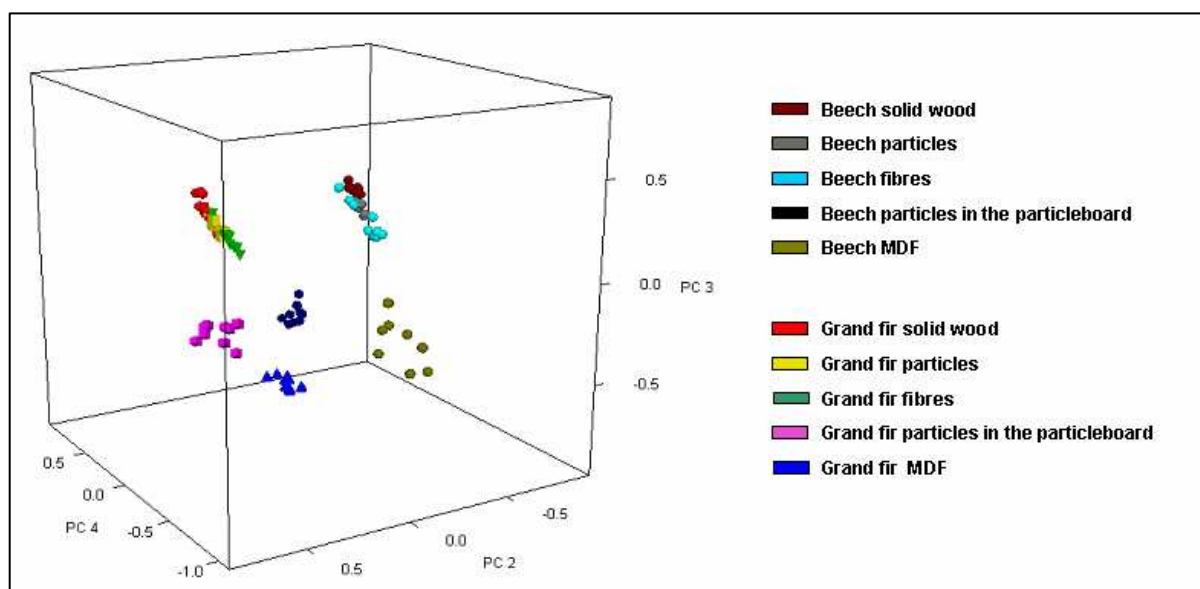

Fig. 6: Principle component analysis (PCA) for the FTIR-ATR spectra of the different production steps of beech and Grand fir wood. Spectra were used in the wavenumber range from 4500-600 cm^{-1}. First derivation and vector normalization have been used as pre-treatment of the spectra. For the factorization 9 smoothing points and 3 factors have been chosen.

To elucidate which spectral differences were mainly responsible for the separation of the groups, the factor loadings were analyzed (Fig. 7). Since the factor loadings are based on the first derivatives, we determined the zero-points between the 10 most pronounced valleys and hills, representing the 10 main peaks and assigned their tentative chemical origin, using published data (Fig. 7, Table 3).
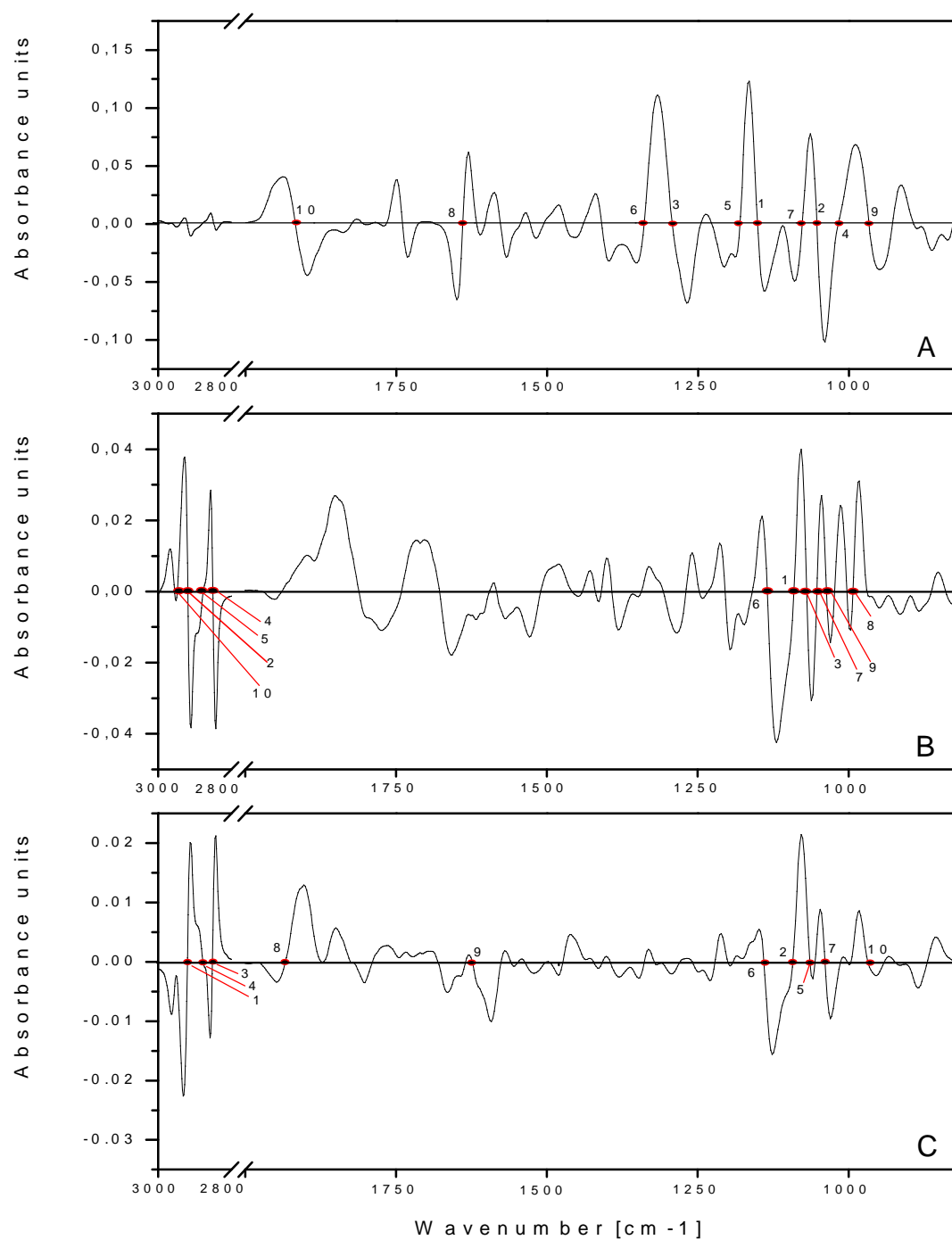
Fig. 7: Factor loadings of the second (A), third (B), and fourth (C) factor obtained by PCA, respectively. The zero-points between the 10 most pronounced valleys and hills, representing the 10 main peaks, were numbered. The different numbers in B, C and D refer to wave number assignments in Table 3. The numbers in parenthesis indicate the position according to height.

It is immediately apparent that compounds representing lignin (e.g. position 1, 3, 5, 6, 8 among them syringyl ring breathing at position 3, Table 3) played a major role in PC2, which separated predominately the two species (Fig. 7). In PC3, wave numbers indicative of lipophilic compounds (wax) as well as for N-containing compounds were dominant as reasons for the separation of boards from raw and intermediate products (Fig. 7, Table 3). In PC4 similar wave numbers were dominant as in PC3, though in slightly different order. In addition, position 9 and 10 indicated the contribution of C=C aromatic bonds to this factor (Fig. 7, Table 3).

Table 3: *Wavenumber characterization (according to Usmanov et al. 1972; Parker 1983; Faix 1991; Naumann et al. 1991; Fengel and Wegener 2003; Pandey and Pitman 2003) of the second (PC2), third (PC3) and fourth (PC4) factor loadings obtained by PCA. The zero-points between the 10 most pronounced valleys and hills, representing the 10 main peaks, were tentatively assigned to their chemical origin. The numbers in parenthesis indicate the position in figure 7.*

Wave number (cm^{-1})			Compound
2nd factor	3rd factor	4th factor	
1122 (1)			Aromatic skeletal and C-O stretch
1042 (2)			C-O stretch
1235 (3)			Syringyl ring, C-O stretch in lignin and xylans
1016 (4)			C-OH in alcohols
1143 (5)			C-H in plane deformation of guaiacyl ring, O-H in lignin
1272 (6)			Guaiacyl ring breathing
1061 (7)			C-C, C-O, C=O stretching in cellulose and hemicelluloses
1513 (8)			Aromatic skeletal vibration in lignin
974 (9)			-HC = CH- out-of-plane deformation
1733 (10)			C=O stretch in COOH, C=O stretch in unconjugated ketones, carbonyls and in ester groups (frequently of carbohydrate origin)
	1074 (1)		C-H, C-O deformation
	2920 (2)		Methylene and methine group
	1055 (3)		C-O stretch in cellulose and hemicelluloses
	2850 (4)		C-H stretch in CH$_3$ and CH$_2$ groups, N-H
	2878 (5)		C-H stretch in CH$_3$ and CH$_2$ groups, N-H
	1680 (6)		C=O stretch in conjugated ketones and secondary amides
	1108 (7)		C-O-C, C-O dominated by ring vibration of carbohydrates
	992 (8)		-HC = CH- out-of-plane deformation
	1030 (9)		Aromatic C-H in plane deformation, guaiacyl type and C-O deformation; primary alcohol
	2947 (10)		O-H vibration
		2920 (1)	Methylene and methine group
		1074 (2)	C-H, C-O deformation
		2852 (3)	C-H stretch in CH$_3$ and CH$_2$ groups, N-H
		2878 (4)	C-H stretch in CH$_3$ and CH$_2$ groups, N-H
		1050 (5)	C-O stretch in polysaccharides
		1114 (6)	O-H association band in cellulose and hemicelluloses
		1032 (7)	Aromatic C-H in plane deformation, C-O in prim. Alcohols, C=O stretch
		1747 (8)	C=O stretch
		1500 (9)	Aromatic C=C
		974 (10)	-HC = CH- out-of-plane deformation

PCA for hybrid particleboards resulted in 6 single scatter-plots, which illustrated the principal components of the FTIR-ATR spectra (Fig. 8). The scatter plots of beech solid wood and particles in the intermediate layer were easy to distinguish from Grand fir solid wood and particles in the overlay. Additionally, the principle components of the overlay and the intermediate layer were distinguishable from each other.
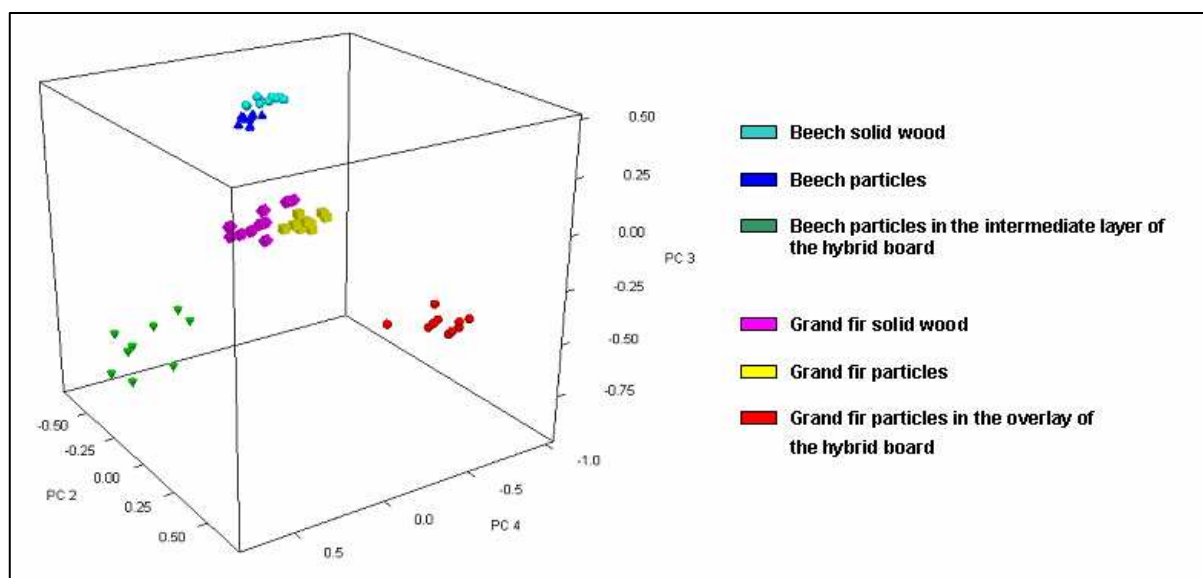

Fig. 8: PCA for the FTIR-ATR averaged spectra of the hybrid boards production process in the wavenumber range from 4500-600 cm^{-1}. First derivation and vector normalization have been used as pre-treatment of the spectra. For the factorization 9 smoothing points and 3 factors have been chosen.

While PCA is a data reduction technique that maps the main components of the spectra in scatter-plots and, thus, allows identifying the spectral origin leading to the formation of groups (McCann et al. 1997), cluster analysis classifies the intrinsic interrelationship between structure and property of samples (Everitt 1993). Cluster analysis is useful to assess the similarity or dissimilarity between samples and therefore, is useful to assess the quality of production processes. We subjected the spectral data of all samples to cluster analysis and calculated their heterogeneity. We tested different calculation methods (nearest neighbor, furthest neighbor, centroid, median, Ward's) and obtained the best results using Ward's method for calculation of the distance matrix, based on Euclidean distance. Using this approach, we received two main sub-clusters, separating both tree species, beech and Grand fir, respectively (Fig. 9).
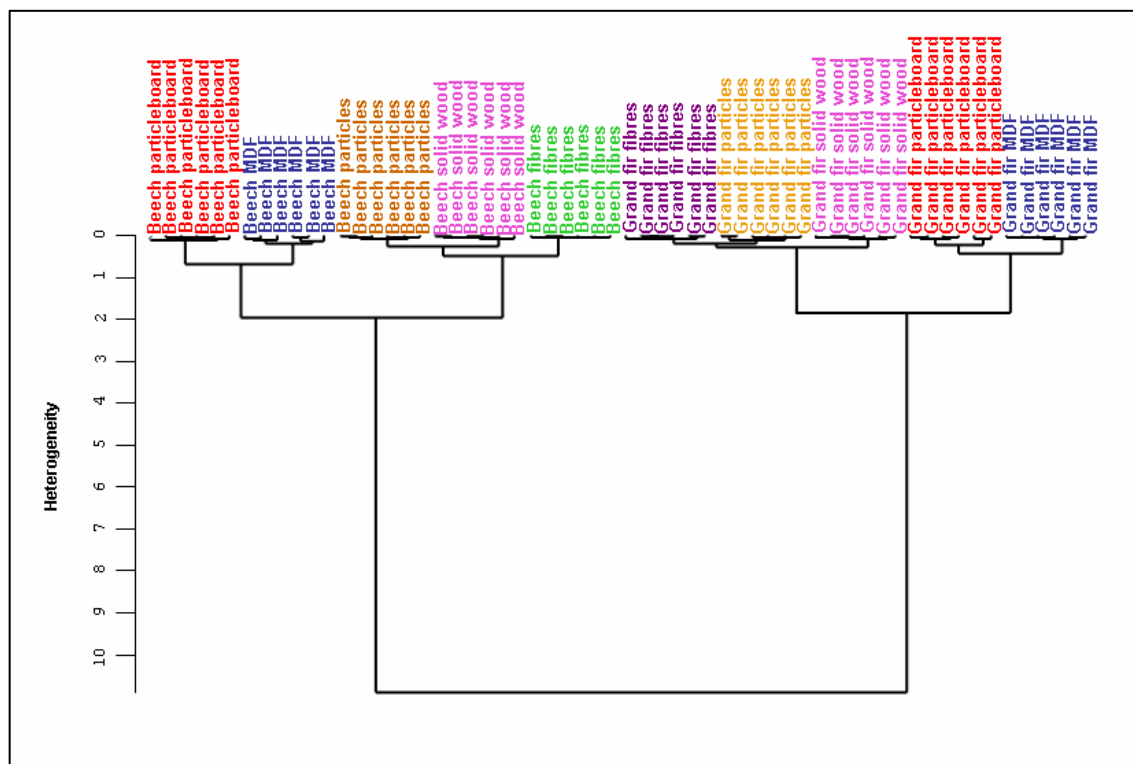
Fig. 9: Cluster analysis of FTIR-ATR spectra of samples of solid wood, fibers, particles, particleboards and MDF plates of beech and Grand fir. Spectral data were used in the wavenumber range from 2968-841 cm^{-1} and classified into classes according to their spectral heterogeneity. The first derivation and vector normalization was utilized as pre-treatment of the spectra. For clarity only 6 of 10 spectra have been shown for each production step. Spectra, which have not been shown, clustered in their respective groups. The different production steps have been indicated in different colors.

These clusters were split in two further 2nd order sub-clusters. Each of these 2nd order sub-clusters separated raw material and intermediate products in one 3rd order sub-cluster and the final products in the other 3rd order sub-cluster.

This shows the low spectral heterogeneity among raw material and intermediate wood products. Still, there were sufficiently large spectral differences between raw material, intermediate and final products, to yield 4th order sub-cluster. The same was true for the end products, MDF and particleboards, respectively. The heterogeneity between the 4th order sub-clusters of raw and intermediate products was much lower than that observed for final products.

Cluster analysis of the hybrid particleboards resulted in two main clusters, separating both species (Fig. 10). The spectra of beech solid wood, particles and intermediate layer of the hybrid boards, composed of beech particles, were combined into one cluster. The spectra of Grand fir solid wood, particles and overlay of the hybrid board in the other one. Thus, it was

possible to retrace the composition of the particular layer to the tree species used for the particles. In addition, for both species, the main clusters were separated in two sub clusters with solid wood and particles on the one hand and the particular layer of the final product on the other hand. This showed the low spectral heterogeneity among raw material and intermediate wood products and spectral differences in the final product.
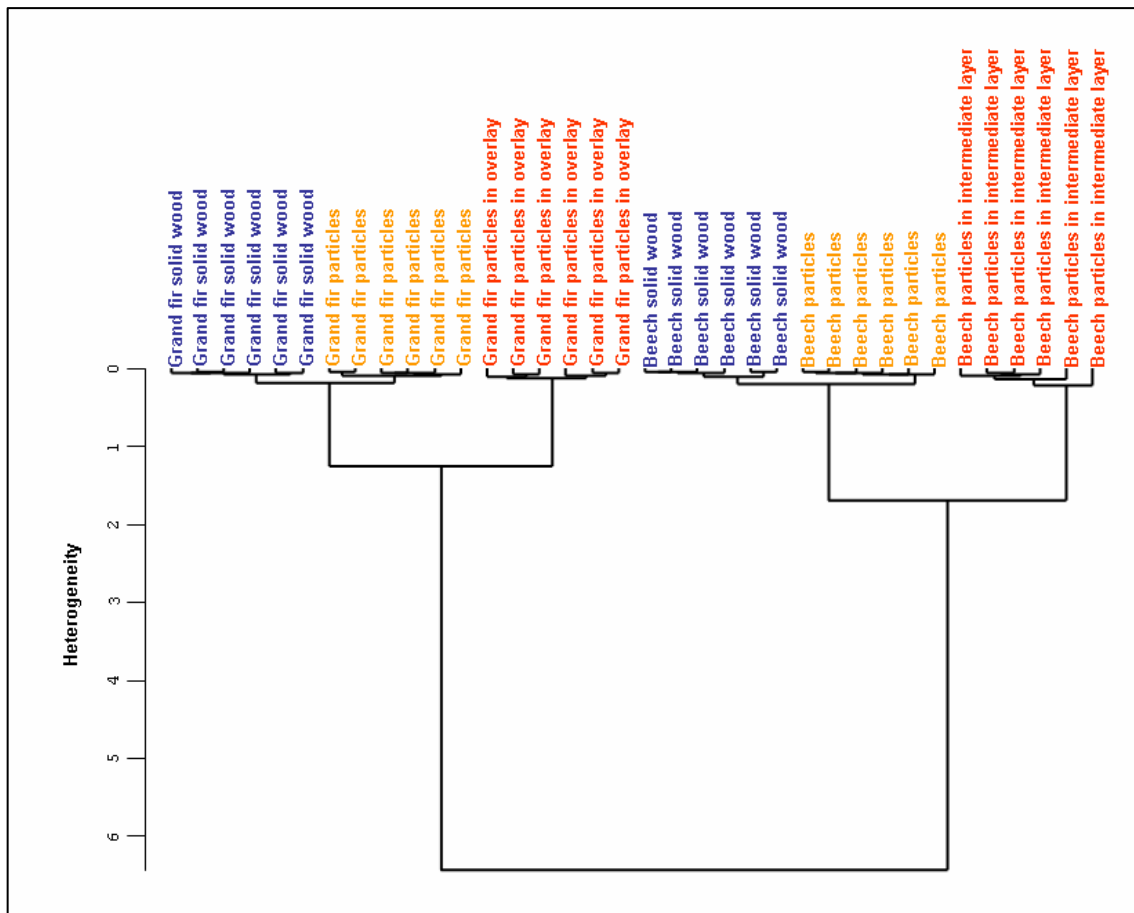

Fig. 10: Cluster analysis for the manufacture of hybrid boards composed of particles of beech in the intermediate layer and Grand fir in the overlay. The spectra were analyzed in the wavenumber range from 4500-600 cm^{-1}. For the sake of clarity 6 of 10 average spectra have been selected randomly from each production step. The particular production steps were mapped in different colors.

3.5 Discussion

In this study we demonstrated the potential of FTIR spectroscopy to characterize the whole production of wood fiber and particleboards starting with the raw material harvested in the forest. Currently, there is little experience with the production processes of panels based on beech and Grand fir, because conventional boards are produced mainly from pine and spruce. Since beech silviculture is expanding in Germany, the amount of inferior beech wood will

increase (Borchert and Kölling 2004; Horn 2006) and added-value products from these resources are needed. Previous studies with beech have already shown that the bending strength of particleboards was strongly affected by particle size, surface layer compactness and the coverage ratio of the particle surface with adhesive (Medved and Resnik 2004). Here, we document that these novel boards comply with the requirements of European standards.

In addition to beech, Grand fir wood was tested, because this species is growing fast, is probably well adapted to the expected climate change (Hamann and Wang 2006) and forms non-resinous wood (Wagenführ 2000). Composite boards of Grand fir revealed excellent strength values, most likely due to the homogenous wood texture (Alden 1997), resulting in low piled density of the particles and fibers, leading to higher contact with the composite binder. Our study did not reveal any major technical obstacles for the production of wood composite boards from European beech or Grand fir.

A main question of our investigations was, if FTIR-spectroscopy combined with multivariate data analysis has the potential to characterize the production processes of the novel boards, to identify the influence of additives on the chemical composition and to distinguish between different raw materials. Clear spectral deviations were found between beech and Grand fir (Fig. 1). This was expected since wood of soft- and hardwood species can easily be separated by FTIR spectroscopy because of their different contents of phenylpropanoids and holocellulose (Faix 1991, Pandey 1999; Pandey and Pitman 2003, 2004; Kubo and Kadla 2005; Fackler et. al 2007). Our study shows that these differences were maintained throughout all productions steps, affording very clear separation of particle or MDF boards made of beech or Grand fir wood (Fig. 6). Based on the results of PCA and factor loadings we conclude that the production process has no major influence on the chemical constituents that distinguish soft- and hardwoods.

Interestingly, it was possible to differentiate FTIR spectra obtained for wood, fibers and particles. Since all measurements were done on milled powder, differences in light scattering due to different particle dimensions can be excluded. It has been reported that polyoses can depolymerize at temperatures below 180 °C (Sivonen et al. 2002; Garrote et al. 2001). The slight deviations in the spectra of particles (Fig. 2) and fibers (Fig. 4) might have been caused by a modification and decomposition of the holocellulose fraction. This would be expected to increase the number of O-H and C-H and thus, lead to the observed increases in absorbance at position 1032 cm^{-1} (Fig. 2, 4). Hennecke and Roffael (2006) also found a decomposition of hemicelluloses to lower molecular weight sugars during the pulping of fibers under thermal-mechanical conditions. The distinct decline of the absorbance units at 1738 cm^{-1} and

1032 cm^{-1} (bands 6 and 19) of the spectra of all final products, compared with fibers and particles, was a further indication for modifications of the holocellulose fraction during panel board processing (Fig. 2, 4, 5). During the pressing process the overlay of the boards can reach temperatures of 200 °C (Deppe and Ernst 2000; Ohlmeyer 2002), which might have led to a decomposition of C=O and an opening of the C-O bonds of polyose residues (Kollmann and Fengel 1965; Bourgois and Guyonnet 1988). This may have generated opportunities for additional cross-linking, thereby leading to losses of absorbance at bands 6 and 19, compared with these bands in fibers or particles. The significant differentiation of the principle components of the overlay and intermediate layer of the hybrid particleboards (Fig. 8) might have been caused by the general spectral discrepancy of beech and Grand fir (Fig. 1) and the different amount of composite binder, used for the particular layer (Fig. 3). Overall, these changes suggest that some of the modification in the FTIR spectra were caused by differences in cross-linking.

Using FTIR-spectroscopy, clear effects of the binders and additives on the spectral properties of the final products were identified (Fig. 2, 4, 5). The most obvious deviations were detected in the wave number range from 3500-2500 cm^{-1}, where lipophilic compounds are found (bands 2 and 3, Fig. 2, 4, 5). Therefore, paraffin-based additions to make the boards water-repellent can easily be identified.

The presence of UF-binders was also immediately apparent from the FTIR spectra of MDF and particleboards. This was previously reported by Körner et al. (1992), investigating industrial-processed particleboards with FTIR spectroscopy. They detected significant bands of pure UF-resin in the same wavenumber range as in our study with a pronounced peak at 3363 cm^{-1} (band 1 in Fig 3), which they assigned tentatively to O-H and N-H vibrations (Körner et al. 1992). Körner et al. (1992) found a further band at 1704 cm^{-1} in the spectrum of pure UF-resin which was assigned to formaldehyde. In our study, this band was missing in the spectra of pure K 350 and K 413 as well as in those of the boards.

Band 9 at wave number 1549 cm^{-1} was only detectable in the final products (Fig. 2, 4, 5). According to Körner et al. (1992) this band was caused by secondary amides (-CO-NH-), resulting from a modification of pure urea (-CO(NH$_2$)$_2$) as a component of UF-resin. In our study band 9 was higher in the spectra of MDF than in those of particleboards (Fig. 2, Fig. 4). This was probably caused by differences in the content and composition of the applied binder. This held true for the overlay of the hybrid particleboards, showing an increased absorbance unit in this band, caused by the higher concentration of composite binder (Fig. 5). Correlations between the coverage of fibers with adhesives and the portion of resin in MDF

boards of spruce and aspen have been reported (Pakdel et al. 2008). Our study furthermore shows that the absorbance increases at positions 9 and 7 were much higher in MDF than in particleboard spectra (Fig. 2, 4). This was probably related to the utilization of two types of UF-resin: K 413 used for MDF production comprised a higher fraction of urea than K 350 and contained melamine ($C_3H_6N_6$) as further additive. Spectroscopic investigations of both binders revealed consistently higher absorbance units for K 413 than for K350 (Fig. 3). FTIR spectra of MDF boards were distinguished from those of particleboards by an additional increase in absorbance at 1596 cm^{-1} (position 8), which was most likely caused by the typical amine band of K 413 at this position (Fig. 3). These analyses show that adhesives and other additions can be traced in the in the resulting products.

Compared to the spectrum of the particleboards of Grand fir, higher absorbance units were particularly detectable in bands 7 and 9 of the outer layer of the hybrid boards (Fig. 5 a). However, the inner layer did not show such significant differences (Fig. 5 b). Since binder and pressing parameters were the same for particle- and hybrid particleboards, an increased modification of urea due to the temperature might have been possible. Furthermore, the moisture content of the particles during gluing might have influenced the admixed binder percentage. A varying moisture content of fibers and particles leads to an over- and underdose of resin (Körner et al. 1992). If the humidity of the intermediate products is higher than the target moisture, this leads to an overdose of resin (Körner et al. 1992).

In conclusion, we show that each production step introduced specific modifications that affected FTIR spectra in a specific manner. Therefore, spectroscopic changes in the infrared can be used to identify changes of the chemical constituents during panel board manufacturing, especially when combined with PCA. For quality control cluster analysis is promising. We showed that different samples from the same production step were clustered together, suggesting a high homogeneity of the raw materials as well as of the resulting intermediate and final products. This indicates that FTIR spectroscopy in combination with cluster analysis is a tool to control product quality if standards are available. Since the beech and Grand fir boards produced in this study showed mechanical and technological properties similar to those from conventional production processes, standardization and application of this novel methodology is promising and should be further developed.

References

Alden, H.A. (1997) Softwood of America. US Department of Agriculture, Forest Service, Forest Products Laboratory. Madison, Wisconsin. Gen. Tech. Rep.-102

Alteheld, R. (2007) Veränderte Stoffströme bei Sägeresthölzern: Auswirkungen auf den Holzmarkt. Kongress „Rohholzmanagement in Deutschland", 22.-23. März 2007, Hannover

Ambrozy, H.G., Giertlova, Z. Planungshandbuch Holzwerkstoffe: Technologie-Konstruktion-Anwendung. Springer Verlag, Wien, 2005

Arndt, K.F., Richter, A., Ludwig, S., Zimmermann, J., Kressler, J., Kuckling, D., Adler, H.J. (1999) Poly(vinyl alcohol)/poly(acrylic acid)hydrogels: FT-IR spectroscopic characterization of crosslinking reaction and work at transition point. Acta Polymerica. 50 (11-12):383-390

Behrendt, S., Rupp, J. Perspektiven der Holzmobilisierung zur Stärkung nachhaltiger Zukunftsmärkte der Forst- und Holzwirtschaft. Hrsg. Institut für Zukunftsstudien und Technologiebewertung. Eigenverlag, Berlin, 2006

Behrendt, S., Henseling, C., Erdmann, L., Knoll, M., Rupp, J. Trendreport: Zukunftstrends für das Bauen mit Holz. Hrsg. Institut für Zukunftsstudien und Technologiebewertung. Eigenverlag, Berlin, 2007

Borchert, H., Kölling, C. (2004) Waldbauliche Anpassung der Wälder an den Klimawandel jetzt beginnen. LWF aktuell. 43:28-30

Bourgois, J., Guyonnet, R. (1988) Characterization and analysis of torrefied wood. Wood Science and Technology. 22 (2):143-155

Bukowski, E.J., Monti, J.A. (2007) FTIR-ATR spectroscopy for identification of illicit drugs seized from clandestine laboratories. American Laboratory. 39 (20):16-19

Deppe, H.-J., Ernst, K. Taschenbuch der Spanplattentechnik. DRW Verlag, Leinfelden-Echterdingen, 2000

Dohrenbusch, A., Bolte, A. (2008) Forest plantations. In: Wood production, wood technology and bio-technological impacts. Ed. Kües, U. Universitätsverlag, Göttingen. pp. 73-83

Ellenberg, H. Vegetation Mitteleuropas mit den Alpen in ökologischer Sicht. Eugen Ulmer Verlag, Stuttgart, 1996

European standard EN 310 (1993) Wood-based panels; determination of modulus of elasticity in bending and of bending strength. European Committee for Standardization, Brussels, Belgium

European standard EN 311 (2002) Wood-based panels - surface soundness - test method. European Committee for Standardization, Brussels, Belgium

European standard EN 317 (1993) Particleboard and fiberboards; determination of swelling in thickness after immersion in water. European Committee for Standardization, Brussels, Belgium

European standard EN 319 (1993) Particleboard and fiberboards; determination of tensile strength perpendicular to the plane of the board. European Committee for Standardization, Brussels, Belgium

European standard EN 322 (1993) Wood-based panels; determination of moisture content. European Committee for Standardization, Brussels, Belgium

European standard EN 323 (1993) Wood-based panels; determination of density. European Committee for Standardization, Brussels, Belgium

European standard EN 325 (1993) Wood-based panels; determination of dimensions of test pieces. European Committee for Standardization, Brussels, Belgium

European standard EN 326-1 (1994) Wood-based panels; sampling, cutting and inspection; Part 1: Sampling and cutting of test pieces and expression of test results. European Committee for Standardization, Brussels, Belgium

Everitt, B.S. Cluster analysis. John Wiley, Toronto, 1993

Fabo, A. (2004) Untersuchungen zur Wechselwirkung von Polyethylenimin (PEI) mit Holzkomponenten. Dissertation. Universität Hamburg, Hamburg, Germany

Fackler, K., Schwanninger, M., Gradinger, C., Srebotnik, E., Hinterstoisser, B., Messner, K. (2007) Fungal decay of spruce and beech wood assessed by near-infrared spectroscopy in combination with uni- and multivariate data analysis. Holzforschung. 61:680-687

Faix, O. (1991) Classification of lignins from different botanical origins by FT-IR spectroscopy. Holzforschung. 45:21-27

Faix, O. (1992) Fourier transform infrared spectroscopy. In: Methods in lignin chemistry. Eds. Lin, S.Y., Dence, C.W. Springer, Berlin. pp. 83-109

Fengel, D., Wegener, G. Wood - chemistry, ultrastructure reactions. Kessel Verlag, Remagen, 2003

Garrote, G., Dominguez, H., Parajo, J.C. (2001) Study on the deacetylation of hemicelluloses during the hydrothermal processing of Eucalyptus wood. Holz als Roh- und Werkstoff. 59 (1-2):53-59

Hamann, A., Wang, T. (2006) Potential effects of climate change on ecosystem and tree species distribution in British Columbia. Ecology. 87 (11):2773-2786

Hennecke, U., Roffael, E. (2005) Charakterisierung einiger auswaschbarer Stoffe in thermomechanisch gewonnenen Holzstoffen der Buche. Holz als Roh- und Werkstoff 63 (6):408-413

Hennecke, U., Roffael, E. (2006) Veränderungen der chemischen Eigenschaften von Fasern und MDF durch Waschen der aufgeschlossenen Fasern. Holz als Roh- und Werkstoff. 64 (4):305-311

Holzwirtschaft Schweiz. Holz in Bestform. Hrsg. HWS-Holzwerkstoffe Schweiz. Kalt-Zehnder, Zug, 2007

Horn, O. (2006) Mischung stützt Nadelholz-Klimawandel und Borkenkäfer beeinflussen die Baumartenwahl. Bayerisches landwirtschaftliches Wochenblatt 43. Deutscher Landwirtschaftsverlag, Hannover

Kacuráková, M., Wilson, R.H. (2001) Developments in mid-infrared FT-IR spectroscopy of selected carbohydrates. Carbohydrate Polymers. 44 (4):291-303

Kharazipour, A. (2004) Holz als Werkstoff. In: Jahrbuch 2004/2005. Nachwachsende Rohstoffe, Wirtschaftsfaktor Biomasse. Hrsg. C.A.R.M.E.N. e.V., Straubing. pp. 325-337

Kloeser, L., Kües, U., Schöpper, C., Hosseinkhani, H., Schütze, S., Dantz1, S., Malik, I., Vos, H., Bartholme, M.., Müller, C., Polle, A., Kharazipour, A. (2008) Panel boards and conventional adhesives. In: Wood production, wood technology and bio-technological impacts. Ed. Kües, U. Universitätsverlag, Göttingen. pp. 297-346

Kollmann, F., Fengel, D. (1965) Änderung der chemischen Zusammensetzung von Holz durch thermische Behandlung. Holz als Roh- und Werkstoff. 12:461-468

Körner, S., Niemz, P., Wienhaus, O., Henke, R. (1992) Orientierende Untersuchungen zum Nachweis des Klebstoffanteils auf Holzpartikeln mit Hilfe der FTIR-Spektroskopie. Holz als Roh- und Werkstoff. 50:67-72

Kubo, S. Kadla, J.-F. (2005) Hydrogen bonding in lignin: A Fourier transform infrared model compound study. Biomacromolecules. 6: 2815-2821

McCann, M.C., Chen, L., Roberts, K., Kemsley, E.K., Sene, C., Carpita, N.C., Stacey, N.J., Wilson, R.H. (1997) Infrared microspectroscopy: Sampling heterogeneity in plant cell wall composition and architecture. Physiol. Plant. 100 (3):729-738

Medved, S., Resnik, J. (2004) Influence of particle size on the surface covered with adhesive at particles from beech wood. Wood Research (Bratislava). 49 (1):33-40

Naumann, D., Labischinski, H., Giesbrecht, P. (1991) The characterization of microorganisms by Fourier transform infrared spectroscopy (FT/IR). In: Modern techniques for rapid microbial analysis. Ed. Nelson, W.H. VCH, New York. pp. 43-96

Naumann, A., Peddireddi, S., Kües, U., Polle, A. (2008) Fourier transform microscopy in wood analysis. In: Wood production, wood technology and bio-technological impacts. Ed. Kües, U. Universitätsverlag, Göttingen. pp. 179-196

Nörr, R. (2004) Vom Exoten zur Wirtschaftsbaumart: 175 Jahre Douglasienanbau in Deutschland. LWF aktuell. 45:7-9

Ohlmeyer, M. (2002) Untersuchung über die Eigenschaftsentwicklung von Holzwerkstoffplatten nach dem Heißpressen. Dissertation. Universität Hamburg, Hamburg, Germany

Pakdel, H., Cyr, P.-L., Riedl, B., Deng, J. (2008) Quantification of urea formaldehyde resin in wood fibers using X-ray photoelectron spectroscopy and confocal laser scanning microscopy. Wood Science and Technology. 42 (2):133-148

Pandey, K.K. (1999) A study of chemical structure of soft and hardwood and wood polymers by FTIR spectroscopy. Journal of Applied Polymer Science. 71 (12):1969-1975

Pandey, K.K., Pitman, A.J. (2003) FTIR-ATR studies of the changes in wood chemistry following decay by brown-rot and white-rot fungi. Intern. Biodeterior. Biodegr. 52 (3):151-160

Pandey, K.K., Pitman, A.J. (2004) Examination of lignin content in a softwood and a hardwood decayed by a brown-rot fungus with acetyl bromide method and Fourier transform infrared spectroscopy. J. Polym. Sci. A: Polym. Chem. 42: 2340-2346

Parker, F.S. Application of infrared, Raman and resonance Raman spectroscopy in biochemistry. Plenum Press, New York, 1983

Pöyry Forest Industry Consulting (2006) Wood-based panels. JP Viewpoint-Europe

Reich, I. (2008) Das Holz wird knapp und teuer. Handelsblatt, 11.01.2008. Verlagsgruppe Handelsblatt, Düsseldorf

Rennenberg, H., Seiler, W., Matyssek, R., Gessler, A., Kreuzwieser, J. (2004) Die Buche (*Fagus sylvatica* L.) - ein Waldbaum ohne Zukunft im südlichen Mitteleuropa? Allgemeine Forst- und Jagdzeitung. 175:210-224

Röhrig, E. Neuere Grundlagen für den Anbau von *Abies grandis*. Schriften aus der Forstlichen Fakultät der Universität Göttingen und der Niedersächsischen Forstlichen Versuchsanstalt. Sauerländer Verlag, Frankfurt am Main, 1981

Sivonen, H., Maunu, S.L., Sundholm, F., Jämsä, S., Viitaniemi, P. (2002) Magnetic resonance studies of thermally modified wood. Holzforschung. 56:648-654

Spellmann, H., Kehr, I. (2008) The wood supply in the world, Europe, Germany, and Lower Saxony. In: Wood production, wood technology and bio-technological impacts. Ed. Kües, U. Universitätsverlag, Göttingen. pp. 43-55

Usmanov, Kh. U., Yulchibaev, A.A., Dordzhin, G.S., Valiev, A. (1972) IR spectroscopic analysis of graft co-polymers of cellulose and its derivatives with vinyl fluoride. Fiber Chemistry. 3 (3):292-295

Wagenführ, R. Anatomie des Holzes. DRW-Verlag, Leinfelden-Echterdingen, 2000

Wolf, M. (2005) Freihandel und Umwelt: Außenpolitische Jahrestagung der Böll-Stiftung, 03.06.2005, Berlin

Youngquist, J.A., Krzysik, A.M., Chow, P., Menimban, R. (1997) Properties of composite panels. In: Paper and composites from agro-based resources. Eds. Rowell, R.M., Young, R.A., Rowell, J.K. CRC/Lewis Publishers, Boca Raton. pp. 301-336

Appendix I
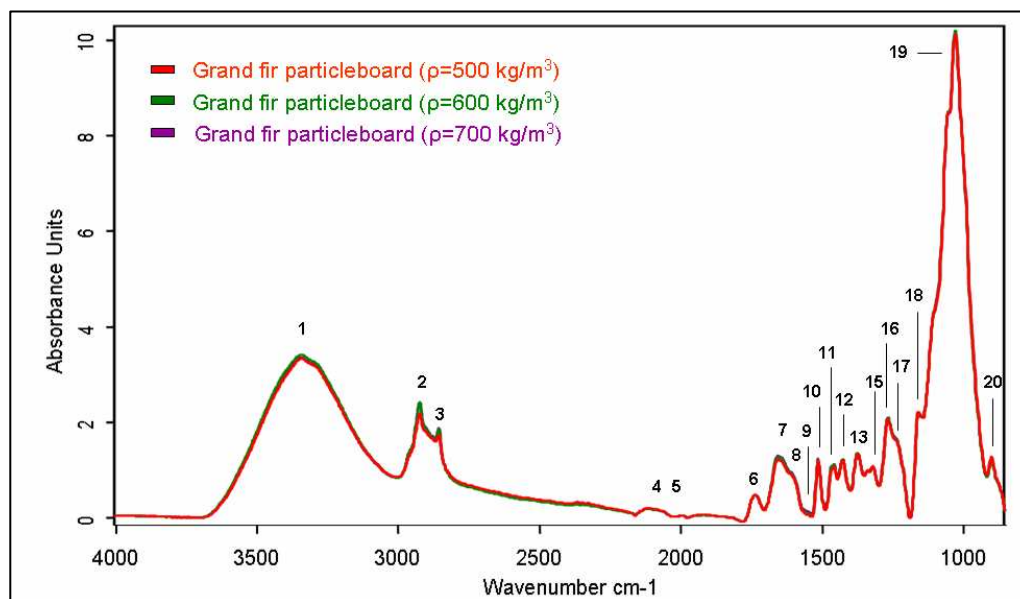
Fig. 1: FTIR-ATR mean spectra of Grand fir particleboards ($\rho=$ 500, 600, 700 kg/m^3). Spectra were acquired in the wavenumber range from 4000-850 cm^{-1} (n = 10 per sample) and the mean was calculated. The spectra were baseline corrected and vector normalized; the band assignments refer to table 2.
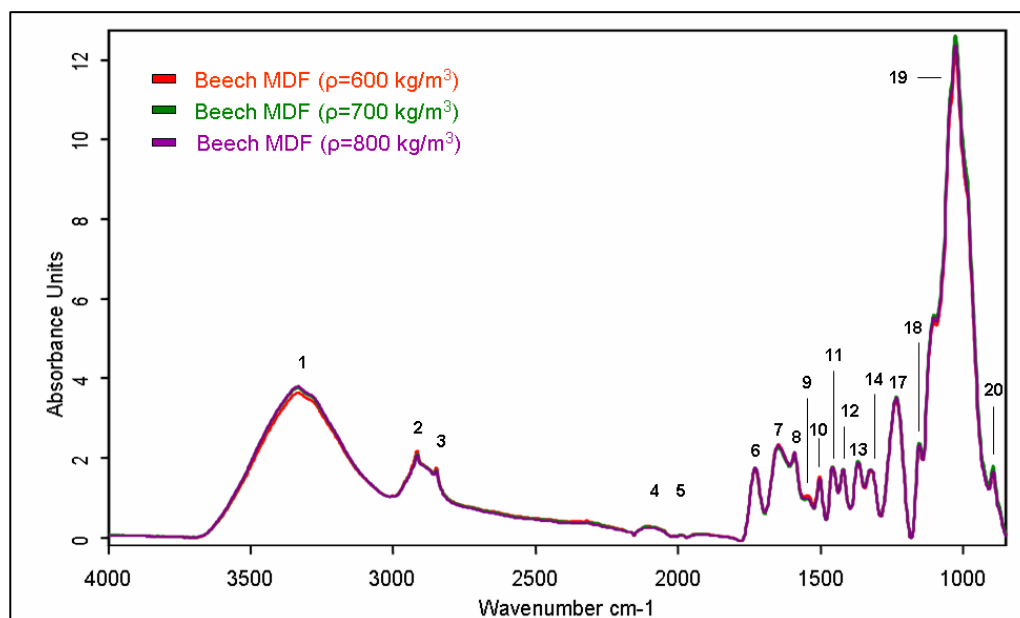

Fig. 2: FTIR-ATR mean spectra of beech MDF boards ($\rho=$ 600, 700, 800 kg/m^3). Spectra were acquired in the wavenumber range from 4000-850 cm^{-1} (n = 10 per sample) and the mean was calculated. The spectra were baseline corrected and vector normalized; the band assignments refer to table 2.

CHAPTER IV

4 FTIR-ATR spectroscopic analysis of changes in fiber properties during insulating fiberboard manufacture of beech wood

4.1 Abstract

Fourier transform infrared – attenuated total reflectance (FTIR-ATR) spectroscopy was applied to trace changes in chemical fiber properties during the production process of insulating fiber mats. In combination with cluster analysis FTIR spectra were used to control the homogeneity of the products. Beech wood (*Fagus sylvatica* L.) was used as novel sustainable material for fiberboards production. The insulating softboards were either processed without any adhesives or with potato pulp or potato starch as renewable binders and dried in a dryer or by microwaves. FTIR spectral analyses revealed chemical modifications at the -O-H association band of carbohydrates that distinguished the two different drying methods. Additions of plant-based renewable adhesives diminished the absorbance of the resulting products at characteristic wavenumbers in the infrared. These decreases were strictly correlated with the amount of added binder and, thus, have the potential to quantify adhesive additions to the fiberboards. Cluster analysis grouped FTIR spectra of samples from different production steps or processes correctly and, thus, is an appealing, simple technique for quality control of insulating fiberboards from renewable resources.

4.2 Introduction

Innovative insulants based on renewable resources are still niche products (Sedlbauer 2004). To date, some insulation materials based on plant products, such as wood and palm fibers, bark, rice straw and husk have been tested (Mishra et al. 1986; Richter 1993; Han-Seung et al. 2002; Scheiding 2000; Scheiding 2002; Al-Sulaiman 2003; Naundorf et al. 2004). But overall, there is only limited experience with the chemical, mechanical, and technological characteristics of these insulants (Sedlbauer 2004).

Wood fibers are strong, lightweight, nonabrasive, abundant and cost effective (Clemons 2002). Processed to insulating wood fiberboards, they are suitable for internal and external use as thermal and acoustic insulation on floors, walls and ceilings (Moser et al. 2003). Compared to conventional insulants, mostly based on polystyrene and polyurethane produced of mineral oil (Kleinhempel 2005), softboards of wood fibers have advantages through exceptional thermal insulating and favorable hygroscopic properties (Sedlbauer 2004). The

bio-degradability of these materials, desired for ecological reasons, limits, however, the field of application (Sedlbauer 2004).

Insulating wood fiberboards can be produced in wet- or dry-processes (Moser et al. 2003; Chapman 2006). The dry-process requires an admixture of adhesives (Moser et al. 2003). Applying the wet-process, adhesives can be added, but depending on fiber length they may not be essential since cross linking occurs due to the plastification of lignin and formation of hydrogen bonds (Makas 2006). To avoid the use of adhesive formulations based on the use of petro-chemical products, binders from renewable resources, such as potato pulp or potato starch can be used. These bio-based binders afford the degradability of the final products (Smok 1999; Müller 2005). To date, there is no information, how these binders influence chemical product properties.

One of the most important steps in wood processing is drying (Leiker and Adamska 2004). The most common industrial method for drying fiber mats is in belt dryers at 160-220 °C (Kutschera and Winter 2006). However, drying by microwave energy is much faster without deteriorating the quality of the dried products (Hansson and Antti 2003).

To date, spruce and pine are the main resources for derived timber products (Wagenführ 2000). Since the conventional resources for wood panels are becoming limited, there is a need to introduce materials from other tree species into these production processes. Novel wood products are currently being developed using European beech (*Fagus sylvatica* L.). Beech cultivation is currently increasing in Germany, because this species plays a major role in all nature-orientated silvicultural concepts as the potentially dominant species in most forests of middle Europe (Ellenberg 1986). Thus, it is expected that this resource of wood will increase in the next years. To generate added-value products from low quality wood, the utilization of beech fibers for novel commodities is currently being investigated. Beech has not been used in wood processing industries before because of its high raw density of wood (Wagenführ 2000) and furthermore the risk of allergies and cancer, due to potentially hazardous dusts, generated during particle- and fiber production (Kloeser et al. 2008). However, wet production processes may circumvent the latter problem because dust formation is avoided.

The aim of this work was to investigate changes in beech fiber properties during processing to insulating wood fiberboards. To characterize the influence of fiber processing on the chemical composition of the fibers, Fourier transform infrared-attenuated total reflectance (FTIR-ATR) spectroscopy was applied. FTIR spectroscopy has been used for determination of molecular structures, identification of compounds in biological samples and investigation of complex polymers (Arndt et al. 1999; Kacuráková and Wilson 2001) and is,

therefore, a powerful tool for wood analysis (Fengel and Wegener 2003). In combination with ATR, FTIR analysis permits reproducible qualitative and quantitative analysis of samples with little or no sample preparation (Bukowski and Monti 2007, Naumann et al. 2008). We employed FTIR-ATR to trace the changes in fiber properties during the production process of insulating fiber mats of beech wood. We tested, whether the observed changes could be used to classify the spectra into clusters according to their spectral heterogeneity and to identify chemical alterations, caused by the addition of different binders or drying methods.

4.3 Material and methods

4.3.1   Wood material

Ten 56-year-old beech (*Fagus sylvatica* L.*)* trees were harvested in 2006 in the city forest of Schmallenberg (North Rhine-Westphalia, 51° 14' 29'' N, 8° 23' 50'' E), compartment 238 a. The forest stand, established by planting and representing a mixture of *Fagus sylvatica* (40 %), *Abies grandis* (50 %) and *Pseudotsuga menziesii* (10 %), has west to northwest exposition at an altitude of 600 m and is located on a steep slope. The soil is brown earth with limited nutrient supply. At harvest, the mean height and breast height diameter of beech were 16 m and 18 cm, respectively. The wood was used to produce fibers.

4.3.2   Production of fibers and softboards of beech

The stems of beech were debarked manually with a drawing knife and cleaved afterwards. The wood pieces were processed to wood chips in a drum chipper (Klöckner Trommelhacker KTH 120 x 400 H2WT, Klöckner Wood Technology GmbH, Hirtscheid, Germany). For pulping the chips were weighed and put into a pressurized laboratory refiner (Laboratory Refiner Type 12, Andritz AG, Graz, Austria). Without any further pre-treatment, the chips were pulped for 5 minutes at a temperature of 150 °C and a pressure of 4.8 bar, yielding thermo mechanical pulp (TMP). Afterwards, the fibers were dried in a gas flame heated drying pipe at 125 °C for 3 seconds to a target moisture of 8 %. Ten samples of fibers were taken randomly from different locations of the fiber packages. The fibers were milled to a fine powder (MM 2000, Retsch, Haan, Germany) for 5 minutes at 50 u/min. The frequency was raised slowly during the next 5 min to 90 u/min. The whole milling process took 10 min for each sample.

Three types of softboards were produced in a wet-process. One type was completely free of any adhesive; both other types were glued with increasing amounts of binder, yielding

10, 20 and 30 % of potato starch (Avebe Kartoffelstärke nativ, Prignitz/Wendland GmbH, Dallmin, Germany) or potato pulp (KF 200 dehydralisiert, Emsland-Stärke GmbH, Emlichheim, Germany), respectively. The latter contained 30 % (w/w) starch. The shortness of beech fibers necessitates an admixture of adhesives to improve the bonds among the fibers and to increase the strength values of the fiber mat.

A suspension of 500g fibers in 15 l of water was produced. Depending on the type of board, 1 l of water was mixed with 50, 100 or 150g (10-30 % (w/w)) potato pulp or 50, 100 or 150g (10-30 % (w/w)) potato starch and admixed to the water-fiber suspension. It was stirred for 1 h for soaking the fibers. Afterwards, the suspension was poured on a sieve in a self-constructed casting mold (length: 50 cm, width: 30 cm, height: 60cm). The effluent was discarded leading to pancaking of the fibers, generating the fiber mat. The mat was dehydrated in a cold press for 2 minutes at 100 bar. Subsequently, mats with different binder percentages and a target thickness of 20 mm and a moisture content of 100-120 % were dried either for 7 min by microwave (MWDA 6x1.1kW, Fricke und Mallah Microwave Technology GmbH, Peine, Germany) at 6600W or for 2 h in a dryer (UNE 800, Memmert GmbH & Co. KG, Schwabach, Germany) at 170°C. The board densities (Tab. 1) resulted from the particular type of binder, the binder percentage and the moisture content of the mats before drying. For each binder percentage and particular type of drying two boards were taken, of which 10 specimen were analyzed.

Table 1: *Raw densities of the insulating wood fiberboards of beech in dependency on the type and amount of binder.*

Type of binder	Binder [%]	Raw density of the softboard [kg/m^3]
Potato starch	10	181
Potato starch	20	198
Potato starch	30	213
Potato pulp	10	173
Potato pulp	20	196
Potato pulp	30	226
No binder	0	163

4.3.3   FTIR-ATR spectroscopy and cluster analysis

FTIR-ATR spectra were recorded in the wave number range from 4500-600 cm^{-1} with an Equinox 55 spectrometer (Bruker Optics, Ettlingen, Germany) including a deuterium-triglycinesulfate-detector and an attached ATR-unit (DuraSamplIR, SensIR Europe, Warrington, England). A resolution of 4 cm^{-1} and a number of 32 scans per sample was used. Specimen of all fiberboards as described above (length: 5cm, width: 3 cm, height: 2cm) were investigated. If not indicated otherwise, 10 individual samples were analyzed per experimental variable, thus, yielding 100 spectra. Because of the high spectral homogeneity of potato starch and potato pulp, 3 FTIR-ATR measurements were performed on each of these samples. Cluster analysis as unsupervised method was used to investigate intrinsic relationship between sample properties. According to the spectral heterogeneity, spectra were classified into clusters or classes in dendrograms. The first derivative and vector normalization (9 smoothing points) was utilized as pre-treatment method of the spectra, applying the standard method for creating the distance matrix with the OPUS 6.5 software (Bruker Optics, Ettlingen, Germany). For calculating the spectral distances the Ward's Algorithm was applied. The analyzed wavenumber range was 1800- 600 cm^{-1}.

4.4 Results

4.4.1   FTIR spectra distinguish beech fibers, binders and softboards

To investigate the influence of fiber processing on fiber properties, FTIR spectra of fibers, pure binders, and softboards produced without binder or with pulp or starch as binders were analyzed in the fingerprint-region from 1800-850 cm^{-1} (Fig. 1). Major spectral changes (bands 1 to 16 in Fig. 1) were assigned to chemical bonds using published data (Table 2).

Table 2: *Wavenumber characteristic (after Usmanov et al. 1972; Faix 1991; Faix 1992; Pandey and Theagarjan 1997; Fengel and Wegener 2003; Pandey and Pitman 2003). Numbers in the table refer to the numbers assigned to the bands in figure 1.*

Wavenumber [cm^{-1}]	Compound	Band numbers
1732	C=O stretch in unconjugated ketones, carbonyls and in ester groups (frequently of carbohydrate origin); C=O in xylans (hemicelluloses)	1
1649	Absorbed O-H and conjugated C-O	2
1593	Aromatic skeletal vibration plus C=O stretch	3
1505	Aromatic skeletal vibration plus C=O stretch	4
1460	C-H- deformation; asymmetric in -CH$_3$- and -CH$_2$-	5
1424	Aromatic skeletal vibration combined with C-H in plane deformation	6
1372	C-H deformation in cellulose and hemicelluloses	7
1328	S ring plus G ring condensed	8
1235	Syringyl ring and C= stretch in lignin and xylan	9
1157	C-O-C vibration in cellulose and hemicelluloses	10
1109	O-H association band in cellulose and hemicelluloses	11
1076	C-H, C-O deformation	12
1056	C-O stretching in cellulose and hemicelluloses	13
1031	Aromatic C-H in plane deformation, guaiacyl type and C-O deformation; primary alcohol	14
998	C-O stretching in cellulose and hemicelluloses	15
897	C-H deformation in cellulose	16

Fiberboards free of adhesives had the highest absorbance of all materials investigated across the whole fingerprint region, especially in the cellulose and hemicelluloses regions (peaks 13-15, Fig. 1). Spectra of fibers and fiberboards glued with pulp were overlapping over large areas and the lowest absorbance was generally found for spectra of starch-glued fiberboards (Fig. 1).

Fibers showed lower absorbance than adhesive-free fiber boards (Fig. 1). The spectral differences indicated modifications of C=O, C-H, C-O and O-H bonds for the entire fingerprint-region. Furthermore, fiberboards without binder showed a distinct band at position 11, whereas fibers had a spectral shoulder at this wavenumber (Fig. 1). Since the boards were free of any adhesives, the distinct band was most likely caused by the drying process, leading to a modification of O-H in cellulose and hemicelluloses.

Fiberboards glued with potato pulp showed absorbance units in bands 5-9, 13 and 15 similar to those of fibers (Fig. 1), whereas spectral deviations were detected in the other

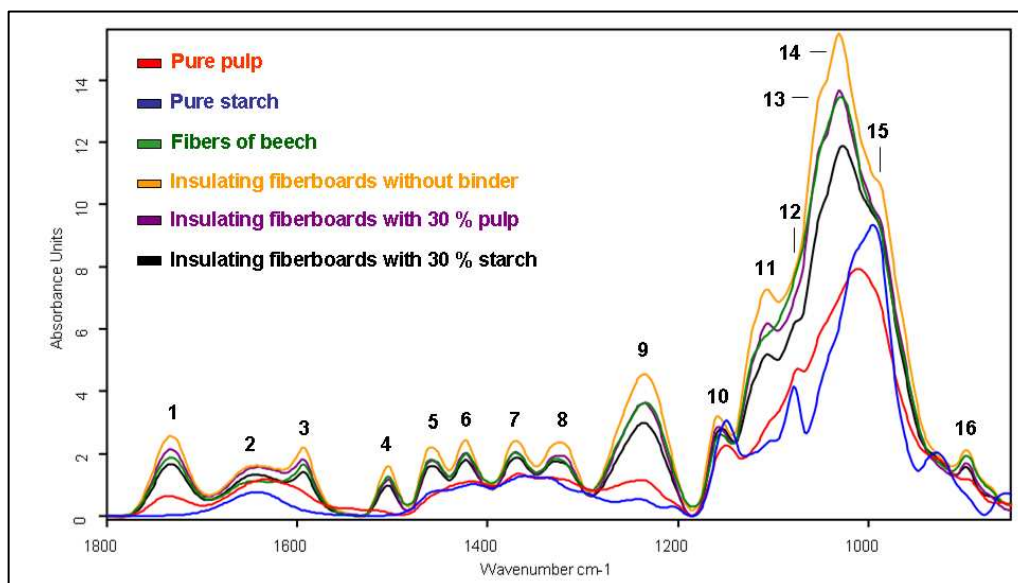bands: increases in bands 1-3, 10, 11 and 14 and decreases in bands 4, 12 and 16, respectively.

Fig. 1: Mean FTIR-ATR spectra of beech fibers, pulp and starch as binder, and different types of insulating fiberboards, dried by microwave. For each spectrum 10 individual samples were averaged. The spectra were baseline corrected and vector normalized; the bands numbers have been assigned to the compounds indicated in table 2.

At position 11 (1109 cm^{-1}) pulp-glued fiberboards showed a spectral deviation that was also present fiberboards without additives and which is most likely attributable to the drying process. Furthermore, in the spectra of pulp-glued boards a new spectral shoulder was identified at position 12. Fibers did not show a comparable band at this wavenumber. However, a significant band was detected at this position in the spectrum of pure pulp. Thus, band 12 in the fiberboards can be ascribed to the influence of the binder. This was the only new band in the spectra of fiberboards with adhesives.

Fiberboards glued with potato starch displayed higher absorbance units at bands 2 and 10 than those of fibers (Fig. 1). All other bands showed lower absorbance across the whole fingerprint-region. The repressions were particularly pronounced at band positions 9 and 14 (Fig. 2). At position 11, the band indicative of the drying process was present (Fig. 1). At position 12, a band appeared, which was not detected for fibers but in the spectrum of pure starch and also in the spectrum of pulp-glued bards (Fig. 1).

Comparing the spectra of potato pulp and potato starch, several differences were apparent (Fig. 1). Pulp, which contains, unlike starch, cell debris with cell fragments, amino acids, etc., showed a richer spectrum than starch. Starch, which is a polymer of α-*D*-glucose,

had two prominent peaks at band 12 and 15, respectively, whereas pulp showed e.g. an additional broad peak at position 1, which is indicative for xylans. Since the bands at position 12 were characteristic for pulp and starch but not for fibers, which consist mainly of cellulose (β-*D*-glucose units), changes at position 12 may represent differences between α and β-glucose polymers.

4.4.2   Increasing binder concentrations affect spectral properties of fiberboards

It was unexpected that spectra of fiberboards glued with pulp or starch showed significant decreases in the absorbance compared to those of fiberboards free of adhesives. This might have been caused by chemical modification due to increased formation of covalent linkages or simply by "dilution" of the original absorbance due to addition of agents with little or no absorbance at the wavenumbers in question. In the latter case we would expect a linear correlation between the decrease in absorbance and the increase in binder. To test this hypothesis, we produced fiberboards with increasing binder amounts from 0 to 30 % (see Table 1).

The FTIR spectra of fiberboards containing increasing binder concentrations showed decreasing absorbance units at most spectral positions (see appendix II and Fig. 1, 2). To analyze these relationships, band 1 at 1732 cm^{-1}, typically for carbohydrates and hemicelluloses, was selected. The decrease of absorbance at this position was significantly correlated with an increase of the binder yielding correlation coefficients of R = 0.991 for pulp and R = 0.984 for starch (Fig. 2).
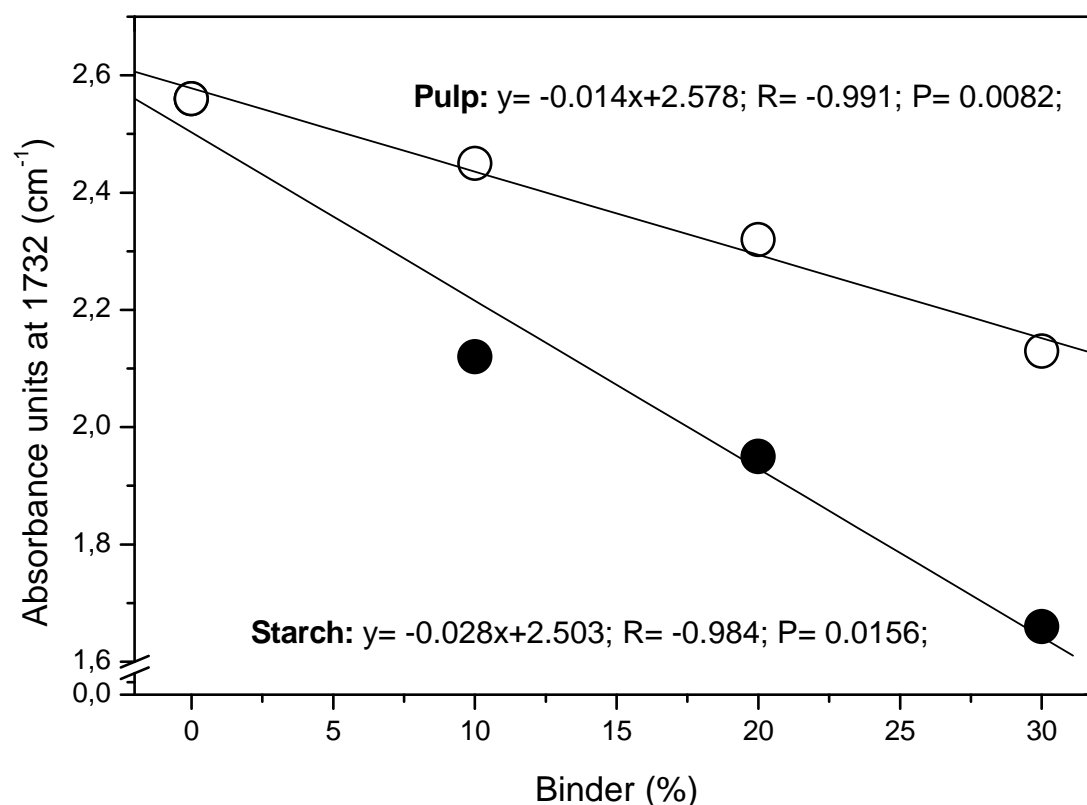
Fig. 2: Correlation of absorbance units and percentage of pulp or starch binder in the insulating fiberboard. The absorbance of band 1 (1732 cm^{-1}, C=O stretch in unconjugated ketones, carbonyls and in ester groups (frequently of carbohydrate origin, C=O in xylans) was plotted with the amount of binder added for fiberboard production. The points were plotted by linear regression analysis.

However, the decrease was about 2-times less pronounced for pulp than for starch (Fig. 2). This was probably caused by the fact that pulp contains a xylan peak at position 1, which was absent in starch. Overall, this analysis indicates that the loss in absorbance was caused by a "dilution" effect of the binder and can be used to quantify binder additions.

4.4.3 FTIR spectroscopy and cluster analysis can be used to characterize different production processes.

4.4.3.1 Fiberboards with different binders.

To ensure high quality products, uniformity of production processes and the resulting products is required. We reasoned that it should be possible to separate raw material and products based on the spectral differences. If the production processes led to uniform products, they should be separable in distinct groups. To test these assumptions, the FTIR

spectra obtained for individual sample were subjected to cluster analysis. By this means, the heterogeneity of the spectra of fibers and boards, glued with different types of binder or without binder was investigated yielding a dendrogram (Fig. 3).

In the dendrogram the different materials clearly formed distinct groups indicating that the heterogeneity within a certain class of materials was much smaller than between different materials.

Two main sub-clusters were obtained separating the spectra of fibers from those of fiberboards (Fig. 3). The spectral heterogeneity between fiberboards and fibers was 2.1, which was twice as high as the heterogeneity within the different fiberboard products. Within the sub-cluster for fiberboards, two 2nd order sub-clusters were obtained, separating boards glued with starch from those free of any adhesives or glued with pulp (Fig. 3). The sub-clusters of the fiberboards showed heterogeneity of 0.9, more than four times as high as that of pure fibers. The heterogeneity between boards free of adhesive and boards glued with pulp was approximately 0.2, twice as high as that of fiberboards, glued with starch.

Boards with increasing binder content were analyzed and form clear groups according to binder content and binder type (see appendix II and Fig. 3).
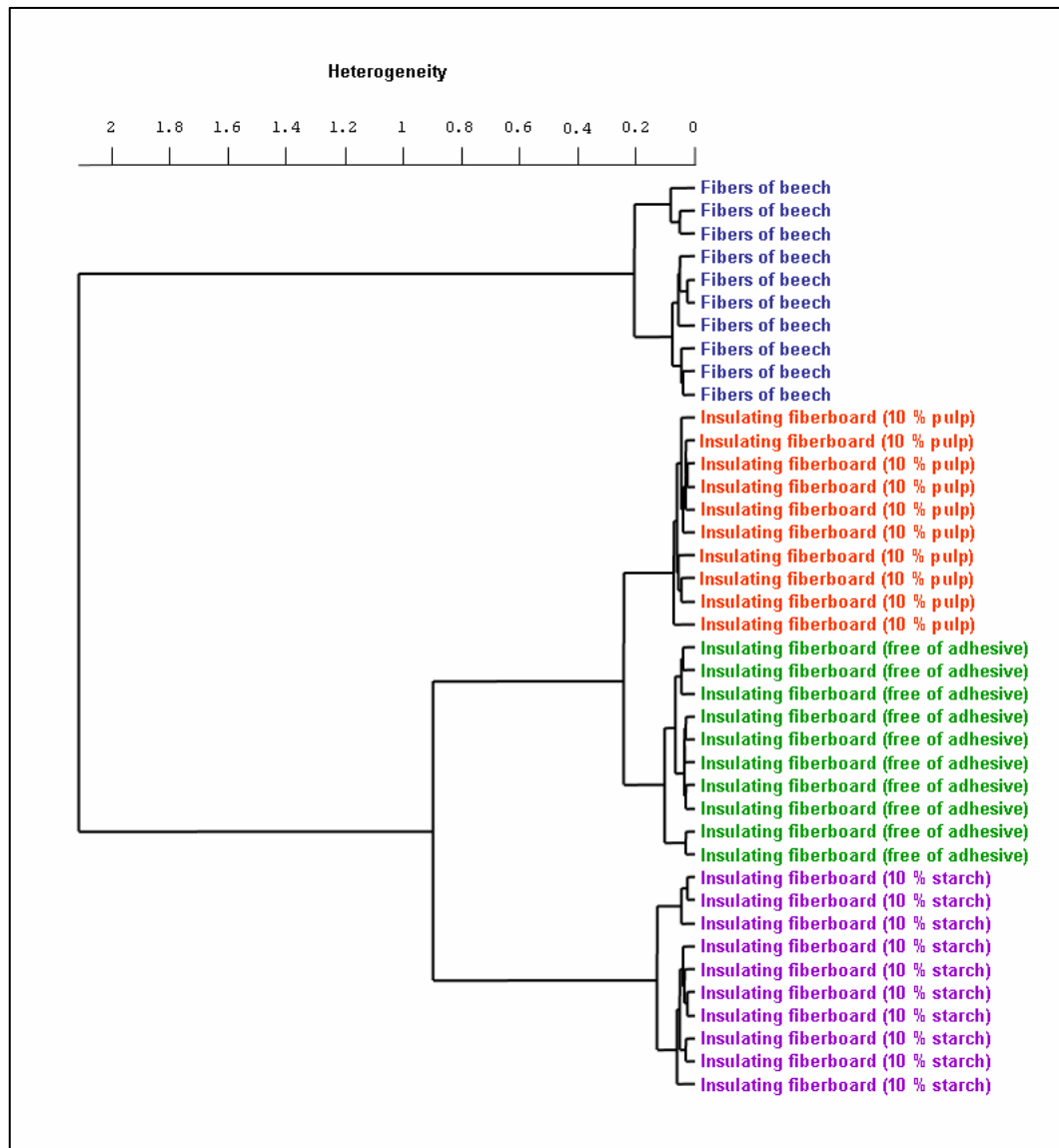
Fig. 3: Cluster analysis for individual spectra of beech fibers, insulating fiberboards glued with 10 % pulp or 10 % starch, and fiberboards free of any binder. All boards have been dried by microwave. Cluster analysis was performed with the spectral data in the wavenumber range from 1800-600 cm^{-1}.

4.4.3.2 Fiberboards dried by microwave or in the dryer.

In addition to microwave drying, fiberboards were also dried conventionally in a drying oven. We measured a maximum temperature of 170 °C in the dryer and temporarily 220 °C in the fiber mats dried by microwave, suggesting differences in thermal modification of the fibers in the boards. Bands 11, 14 and 16, typical for O-H, C-H and C-O in cellulose and hemicelluloses, decreased very subtly in the boards dried by microwave, compared to boards dried in the dryer (see appendix II and Fig. 4). Although the spectra of fiberboards dried by

the different methods were quite similar, cluster analysis was able to distinguish successfully materials from the different drying processes (Fig. 4). We received two main clusters separating fibers and fiberboards without any binder.
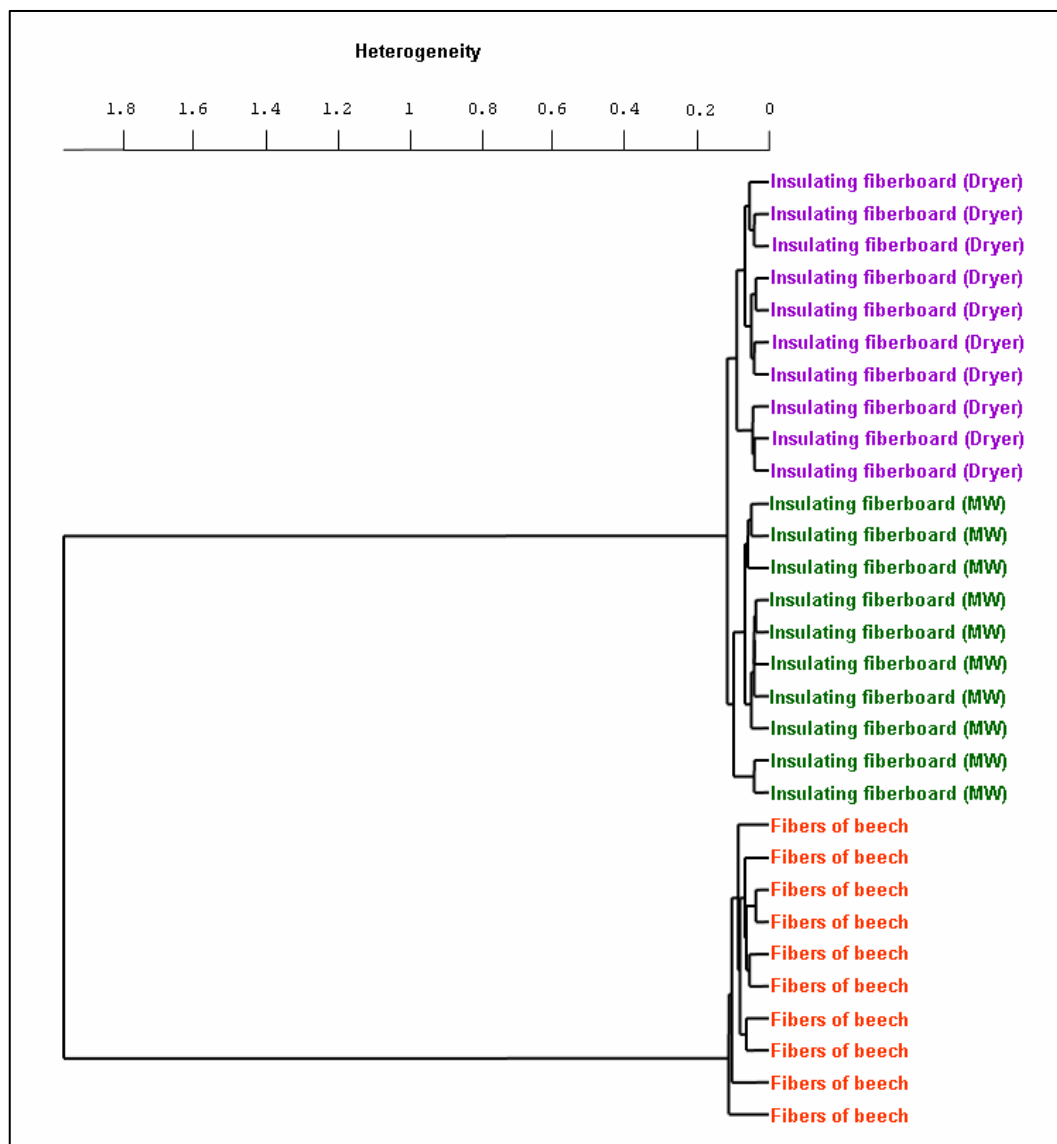
Fig. 4: Cluster analysis for individual spectra of beech fibers and insulating fiberboards, dried by microwave (MW) or in the dryer, respectively. Cluster analysis was performed with the spectral data in the wavenumber range from 1800-600 cm^{-1}.

The latter cluster was split into two further sub-clusters, which contained spectra due to the particular drying technique. Fibers and fiberboards displayed a high spectral heterogeneity of 2.0, more than ten times higher than the heterogeneity within the fibers or within the fiberboards. Still, the heterogeneity among the fiberboards was sufficiently high to separate their spectra due to the particular drying technique. The differences caused by the drying

method between fiberboards were also maintained in boards glued with adhesives (see appendix II and Fig. 5).

4.5 Discussion

To our best knowledge, this is the first study in which changes in the chemical fingerprint of beech fibers have been analyzed during the processing to insulating wood fiberboards. We showed that FTIR-ATR spectroscopy combined with cluster analysis has the potential to characterize spectral deviations between fibers and novel softboards and can be used to identify the influence of adhesives from renewable resources on the chemical composition of the resulting insulants.

We detected a decrease of the absorbance units in the spectra of the fiberboards with increasing binder concentrations (Fig. 2). Initially, we assumed that a possible reason might have been the modification and decomposition of the holocellulose fraction during drying the boards. This might have led to free chemical bonds linking with the adhesive. However, analysis of a series of fiberboards with increasing adhesive clearly revealed strict correlations between the amount of binder and the decrease in absorbance. We, therefore, conclude that the fiberboard composition is diluted by the particular adhesive. A consequence of the observed strict correlations is that this type of spectral analysis can be used to quantify the amount of binder added to the product.

FTIR spectroscopy also enabled us to identify modifications of the chemical constituents during processing. Since polyoses can depolymerize at temperatures below 180 °C (Sivonen et al. 2002; Garrote et al. 2001), the deviations in the spectra of fibers and fiberboards might have been caused by a modification and decomposition of C=O, C-H and C-O bonds of the holocellulose fraction during the drying process (Fig. 1). These deviations were independent of the adhesive or its particular concentration in the board. Furthermore, we determined a significant increase in band 11, typical for O-H in cellulose and hemicelluloses. Since this band appeared in the spectra of all softboards but not in the fibers, the deviation was most likely caused by the drying process. The high temperatures in the dryer and the microwave might have led to a modification of cellulose and hemicelluloses, separating O-H bonds and leading to higher absorbance units at this wavenumber.

FTIR spectroscopy identified a clear spectral influence of pulp and starch binders on band 12 (Fig. 1). This band only occurred in the spectra of fiberboards glued with adhesives and in the spectra of the adhesives themselves, and was most likely due to α-glucose-units.

The differences in the mean spectra identified by direct interpretation were apparently sufficiently high and consistently present in individual samples to enable grouping of the different products by cluster analysis. Spectra of all fiberboards were distinguishable from those of the fibers (Fig. 3). Fiberboards glued with 10 % pulp were more similar to boards free of any adhesives than to boards glued with starch (Fig. 3). This was most likely due to the high spectral similarity, visible in bands 5-9, 13 and 15 (Fig. 1). However, it must be noted that cluster analysis does not give any information on chemical basis of the differences. Still, it is a very useful method to supervise and control production processes since the homogeneity as an inherent feature of product quality can be easily assessed.

The conventional technique for drying fiber mats is still by air circulation (Kutschera and Winter 2006). However, drying by microwave energy is much faster (Hansson and Antti 2003). Therefore, we dried fiber mats conventionally or by microwave and used cluster analysis to investigate influence of the particular drying technique on the chemical composition of the fibers (Fig. 4). The spectra of fibers were separated from spectra of fiberboards, illustrating modification of the chemical components during drying. These were most pronounced at band 11, which indicates changes in O-H associations in cellulose and hemicelluloses (Table 2). The drying technique resulted in further sub-clustering of fiberboard spectra (Fig. 4). It is likely that different temperatures during drying and different principals of drying caused different modifications of the chemical compounds. A dryer warms up the surrounding area of the sample with the highest temperatures prevailing on the surface (Fischer et al. 2007). Microwave drying is based on the so-called volumetric warming which warms up the sample itself and leads to the highest temperatures in the centre of the sample (Fischer et al. 2007). The increased heating rate during microwave drying can cause micro-structural changes (Rhee 2002). Kaasová et al. (2001) described a modification of starch caused by the absorbed microwave energy and temperature of treatment. Due to these effects, a significant modification of the chemical constituents might have taken place, enabling us to separate both drying techniques with cluster analysis.

In conclusion, we showed that FTIR spectroscopy can be used to unravel changes in beech fiber properties during processing to insulating wood fiberboards. Drying results in chemical modifications which can be used to distinguish the applied drying method. Our results also show that additions of plant-based renewable adhesives can be quantified by specific decreases in absorbance of the fiber board spectra. Since cluster analysis is a method to group samples according to similarity, it is suitable for quality control of products. Here, we have shown that cluster analysis of FTIR-ATR spectra can be applied to distinguish fibers

and fiber boards from different production processes. Therefore, these methods can be used to support the optimization of production processes for innovative insulating wood fiberboards or other organic compounds.

References

Al-Sulaiman FA (2003) Date palm fiber reinforced composite as a new insulating material. International Journal of Energy and Research 27:1293-1297.

Chapman KM (2006) Wood-based panels: particleboard, fiberboards and oriented strand board. Pages 427-475 *in* JCF Walker, ed. Primary Wood Processing-Principles and Practice. Springer, Netherlands.

Clemons CM (2002) Wood-plastic composites in the United States: The interfacing of two industries. Forest Prod. J 52 (6):10-18.

Ellenberg H (1986) Vegetation Mitteleuropas mit den Alpen in ökologischer Sicht. Ulmer Verlag, Stuttgart. 1095 pp.

Faix O (1991) Classification of lignins from different botanical origins by FT-IR spectroscopy. Holzforschung 45: 21-27.

Faix O (1992) Fourier transform infrared spectroscopy. Pages 83-109 *in* SY Linand CW Dence, eds. Methods in lignin chemistry. Springer, Berlin.

Fengel D, Wegener G (2003) Wood - chemistry, ultrastructure reactions. Kessel Verlag, Remagen. 613 pp.

Fischer B, Lampke Th, Walter G, Wielage B (2007) Mikrowellenangepasstes Sintern von Ferriten. Mat.-wiss. u. Werkstofftech 38 (10): 808-815.

Garrote G, Dominguez H, Parajo JC (2001) Study on the deacetylation of hemicelluloses during the hydrothermal processing of Eucalyptus wood. Holz als Roh- und Werkstoff 59 (1, 2): 53-59.

Han-Seung Y, Dae-Jun K, Hyun-Joong K (2002) Rice straw-wood particle composite for sound absorbing wooden construction materials. Bioresource Technology 86 (2): 117-121.

Hansson L, Antti AL (2003) Design and performance of an industrial microwave drier for on-line drying of wood components. 8th IUFRO Wood drying conference, Brasov, Romania. http://www.unitbv.ro/il/iufro2003modific/postiufro/ Session4.%20Fast%20drying%20procedures/Hansson%20-%20Antti.pdf. (24-29 August 2003).

Kaasová J, Kadlec P, Bubník Z, Hubáèková B, Pøíhoda J (2002) Physical and chemical changes during microwave drying of rice. Chemical Papers 56 (1): 32-35.

Kacuráková M, Wilson RH (2001) Developments in mid-infrared FT-IR spectroscopy of selected carbohydrates. Carbohydrate Polymers 44 (4): 291-303.

Kleinhempel AK (2005) Innovative Dämmstoffe im Bauwesen: Forschungsstand und Marktübersicht. Bericht des Bremer Energieinstituts. Universität Bremen, Bremen. http://www.energiekonsens.de/Downloads/Aktuelles/Innovative_Daemmstoffe_ Bauwesen.pdf. (12 January 2008).

Kloeser L, Kües U, Schöpper C, Hosseinkhani H, Schütze S, Dantz1 S, Malik I, Vos H, Bartholme M, Müller C, Polle A, Kharazipour A (2008) Panel boards and conventional adhesives. Pages 297-346 *in* U Kües, ed. Wood production, wood technology and bio-technological impacts. Universitätsverlag, Göttingen.

Kutschera U, Winter B (2006) Stand der Technik zur Span- und Faserplattenherstellung: Beschreibung von Anlagen in Österreich und Luxemburg. Umweltbundesamt Wien, Österreich. http://www.umweltbundesamt.at/umweltschutz/industrie/branche/span1/. (12 January 2008).

Leiker M, Adamska MA (2004) Energy efficiency and drying rates during vacuum microwave drying of wood. Holz als Roh- und Werkstoff 62 (3): 203-208.

Makas M (2006) Eigenbindevermögen bei Faserwerkstoffen. Pages 97-107 *in* Institut für Holzbiologie und Holztechnologie (Hrsg.) Tagungsband der 3. Fachtagung Umweltschutz in der Holzwerkstoffindustrie", Mai 18-19, 2006, Göttingen. Cuvillier Verlag, Göttingen.

Mishra P, Chakraverty A, Banerjee HD (1986) Studies on physical and thermal properties of rice husk related to its industrial application. Journal of Material Science 21 (6): 2129-2132.

Moser J, Treml E, Gütler H (2003) Warenkunde für Holzkaufleute. 3. überarbeitete Auflage. Wirtschaftskammer Österreich. http://portal.wko.at/wk/format_detail.wk? angid=1&stid=164059&dstid=6670&opennavid=0 (13 December 2007).

Müller C (2005) Mechanisch-enzymatischer Aufschluss von Kartoffelpülpe als Bindemittel zur Herstellung von Holzwerkstoffen. Doctoral thesis, Universität Göttingen, Göttingen, IN. Pp. 76-77.

Naumann A, Peddireddi S, Kües U, Polle A (2008) Fourier transform infrared microscopy in wood analysis. Pages 179-196 *in* U Kües, ed. Wood production, wood technology, and biotechnological impacts. Universitätsverlag, Göttingen.

Naundorf W, Wollenberg R, Schubert D (2004) Veredlung von Rinden zu körnigen Füll- und Dämmstoffen. Holz als Roh- und Werkstoff 62 (6): 397-404.

Pandey KK, Theagarjan KS (1997) Analysis of wood surface and ground wood by diffuse reflectance (DRIFT) and photoacoustic (PAS) fourier transform infrared spectroscopy. Holz als Roh- und Werkstoff 55 (6): 383-390.

Pandey KK, Pitman AJ (2003) FTIR-ATR studies of the changes in wood chemistry following decay by brown-rot and white-rot fungi. Intern. Biodeterior. Biodegr. 52: 151-160.

Rhee S (2002) Mikrowellenprozesstechnik für keramische Werkstoffe der Mikrosystemtechnik. Doctoral thesis, Universität Freiburg, Freiburg, IN. Pp. 38-39.

Richter C (1993) Neues Verfahren zur Herstellung von Dämmstoffen niedriger Dichte aus Holz und Einjahrespflanzen. Holz als Roh- und Werkstoff 51 (4): 235-239.

Scheiding W (2000) Untersuchungen zur Wärmeleitfähigkeit von Holzfaserstoff. Holz als Roh- Werkstoff 58 (3): 177-181.

Scheiding W (2002) Herstellung und Eigenschaften wasserglasgebundener Holzfaserdämmplatten. Holz als Roh- und Werkstoff 60 (6): 389-393.

Sedlbauer K (2004) Dämmstoffe aus nachwachsenden Rohstoffen und Schimmelpilze-ein Junktim? Internationale Fachmesse und Kongress für regenerative Energien und energieeffizientes Bauen und Sanieren. Messe Augsburg (23 October 2004). http://www.ibp.fhg.de/literatur/konfe/04_Daemmsstoffe-aus-nachw-Rohstoffen-Impulskongress.pdf. (November 2007).

Sivonen H, Maunu SL, Sundholm F, Jämsä S, Viitaniemi P (2002) Magnetic resonance studies of thermally modified wood. Holzforschung 56 (6): 648-654.

Smok B (1999) Ein Einfall für den Abfall: Pulp Science statt Pulp Funktion. Pages 16-17 *in* H Kern (Hrsg.). Spektrum-Informationen aus Forschung und Lehre. Universität Göttingen.

Usmanov KhU, Yulchibaev, AA, Dordzhin, GS, Valiev, A (1972) IR spectroscopic analysis of graft co-polymers of cellulose and its derivatives with vinyl fluoride. Fiber Chemistry 3 (3): 292-295.

Wagenführ R (2000) Anatomie des Holzes. DRW-Verlag, Leinfelden-Echterdingen. 188 pp.
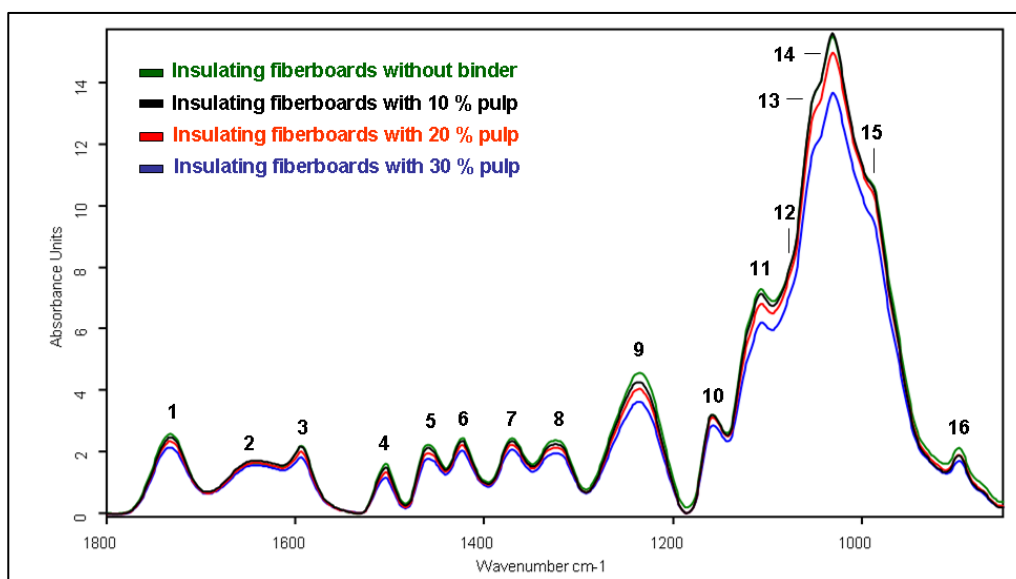
Appendix II

Fig. 1: Mean FTIR-ATR spectra of 4 different types of fiberboards glued with potato pulp. The binder percentage is increasing from 0-30 %. For each spectrum 10 individual samples were averaged. The spectra were baseline corrected and vector normalized; the band assignments refer to table 2.
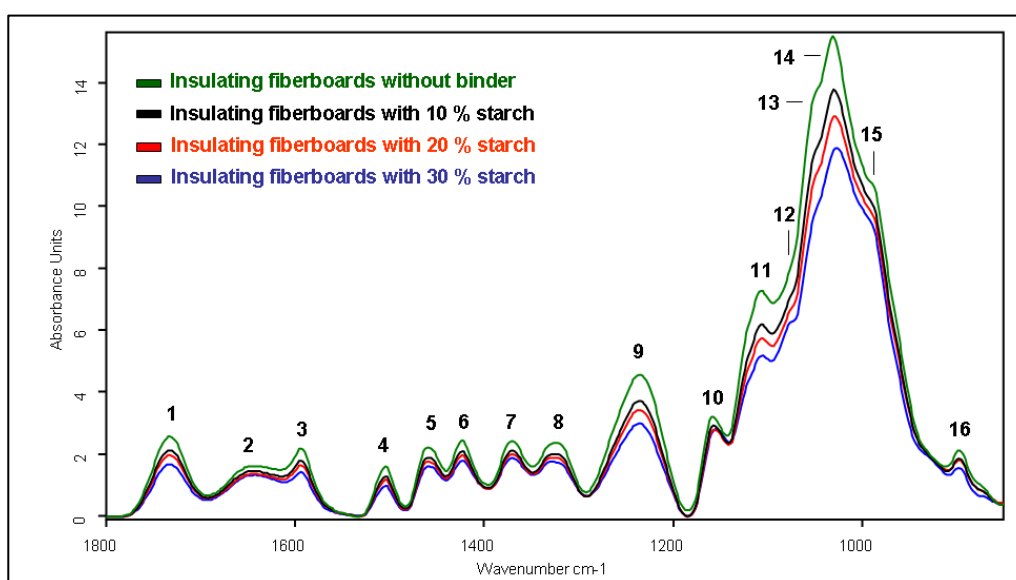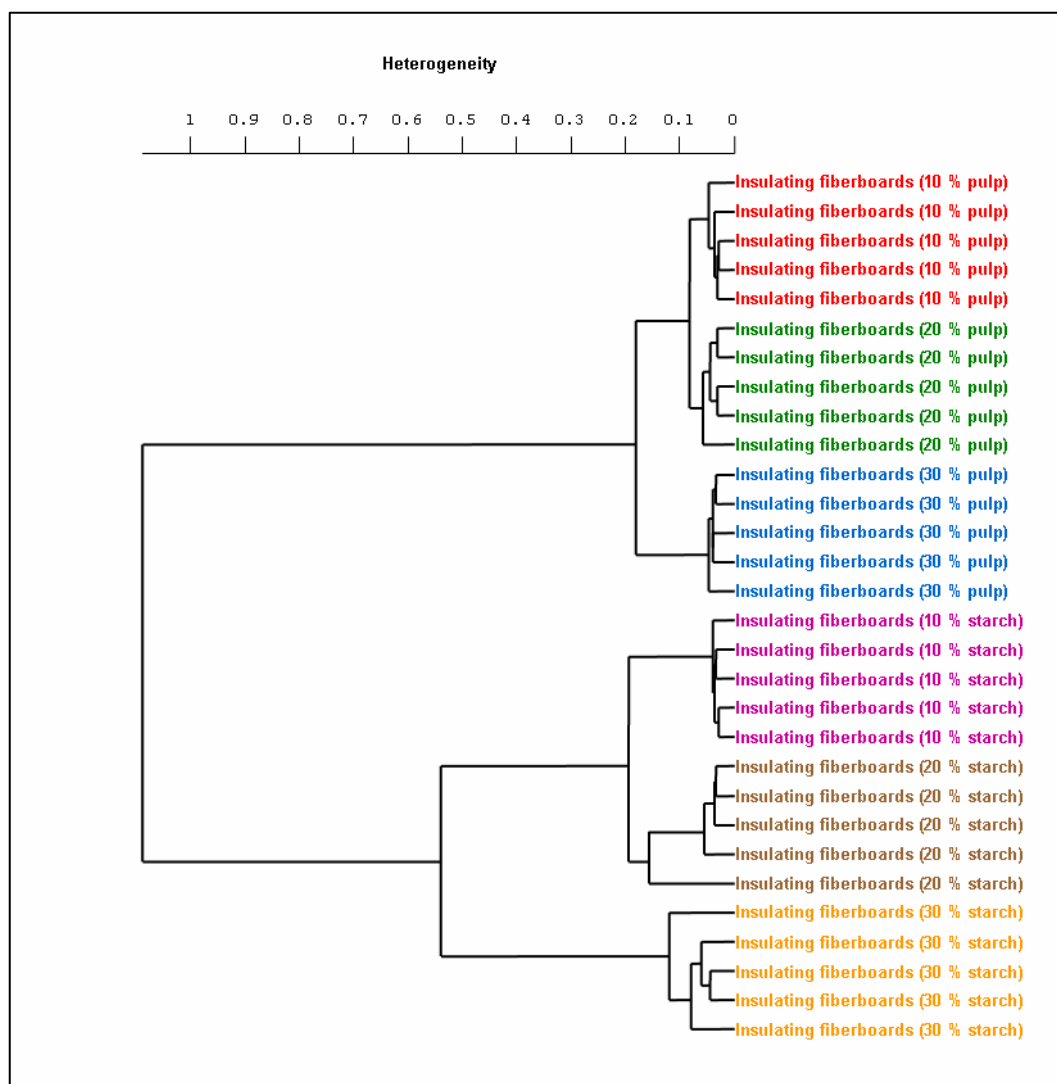

Fig. 2: Mean FTIR-ATR spectra of 4 different types of fiberboards glued with potato starch. The binder percentage is increasing from 0-30 %. For each spectrum 10 individual samples were averaged. The spectra were baseline corrected and vector normalized; the band assignments refer to table 2.

Fig. 3: Cluster analysis for individual spectra of insulating fiberboards, glued with different types and percentages of adhesives. Cluster analysis was performed with the spectral data in the wavenumber range from 3630-830 cm-1. For clarity 5 of 10 average spectra have been selected randomly for each type of board and mapped in different colors.
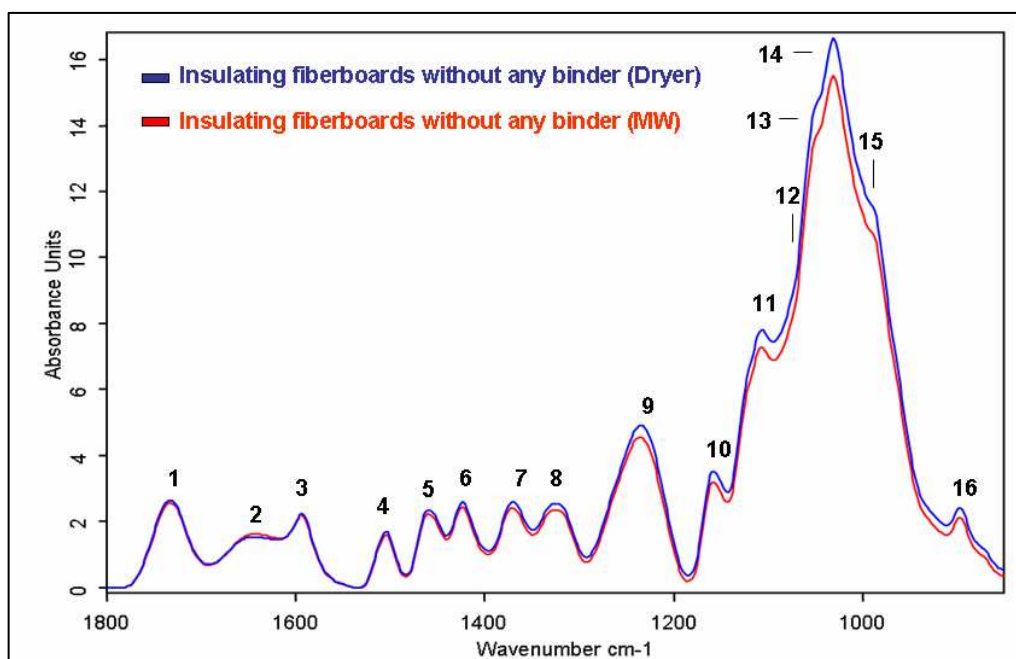
Fig. 4: Mean FTIR-ATR spectra of fiberboards without any binder, dried in the dryer and by microwave. For each spectrum 100 individual samples were averaged. The spectra were baseline corrected and vector normalized; the numbers of the bands have been assigned to the compounds indicated in table 2.
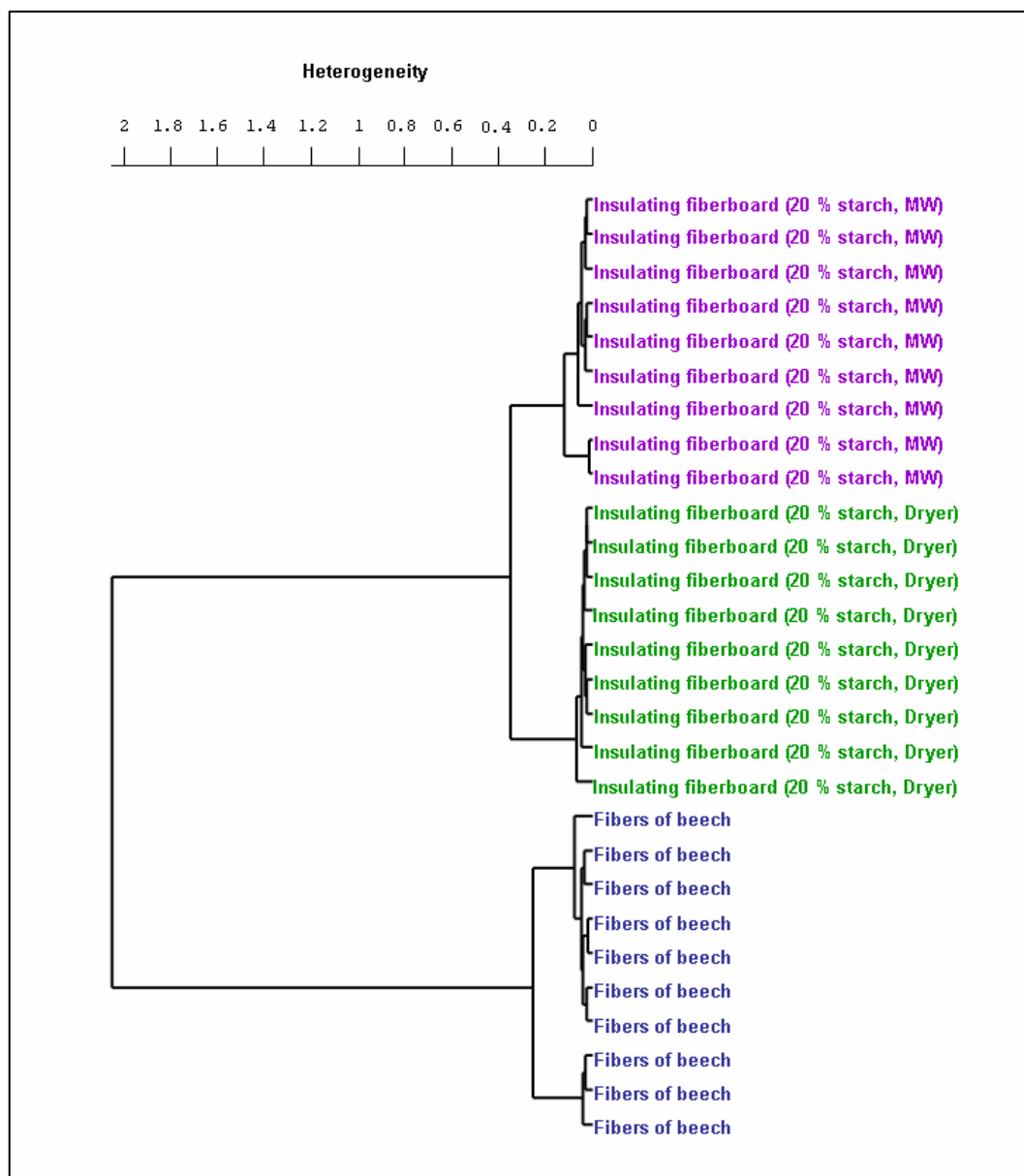
Fig. 5: Cluster analysis for individual spectra of beech fibers and insulating fiberboards, bond with 20 % starch and dried by microwave (MW) or in the dryer, respectively. Cluster analysis was performed with the spectral data in the wavenumber range from 1800-600 cm^{-1}.

CHAPTER V

5   Imaging of lignin and cellulose in soft- and hardwood species using Fourier transform infrared microscopy and Scanning transmission electron microscopy

5.1 Abstract

FTIR microscopy combined with a focal plane array (FPA) detector was used for illustration of the distribution of cellulose and lignin in wood of Grand fir (*Abies grandis* (Douglas ex D. Don) Lindl.) and European beech (*Fagus sylvatica* L.). Two independent visualization methods were applied and compared. The first method evaluated all spectra by integrating the wavenumber range considered as typical for cellulose (1390-1350 cm^{-1}) and lignin (1530-1490 cm^{-1}), respectively, calculating the area below each spectrum. The second method, called trace-computation, correlated all spectra of the FTIR-FPA data set with an averaged FTIR spectrum of cellulose and acid insoluble Klason lignin, respectively, corresponding to the correlation for each spectrum. The results of both methods were illustrated in color coded images and displayed a homogenous distribution of cellulose in wood of Grand fir and beech, respectively. Imaging lignin indicated higher contents in the middle lamellae, the angels of the cells and in the wood rays, using trace-computation and integration, respectively. Since the cells in the section of Grand fir were larger compared to those of beech, they could be illustrated in a better resolution.

Since FTIR microscopy is a relatively new optical method employed in wood science, STEM-EDX was applied to validate the results obtained by FTIR microscopy. Labeling lignin in sections of Grand fir with mercury (Hg) enabled an indirect identification of lignin by detecting and imaging Hg in the sections with STEM-EDX mapping at the sub-cellular level. STEM showed an enrichment of Hg in cell corners, the middle lamellae and in tracheids, compared to other cell wall areas, thus supporting FTIR imaging data. This underlines a high potential of FTIR microscopy in identifying and illustrating chemical constituents of wood samples.

5.2 Introduction

Wood is primarily composed of cellulose, lignin, hemicelluloses and minor amounts of extractives (Sjöström 1998; Fengel and Wegener 2003). Cellulose $(C_6H_{10}O_5)_n$, the major component, is a linear polymer consisting of (1-4) ß-linked glucose monomers. The cellulose

molecules are arranged into fibrils, which are organized into elements that make up the cell wall of wood fibers. Most of the cell wall cellulose is crystalline (Fengel and Wegener 2003). Three types of methods are known to determine cellulose. The first one is based on the separation of the main portions of polyoses and residual lignin from holocellulose. The second method directly isolates cellulose from wood; the third one determines the cellulose content by total hydrolysis of wood, holocellulose or cellulose with subsequent determination of the resulting sugars. However, in any isolation method, cellulose cannot be obtained in pure conditions (Fengel and Wegener 2003). Wright and Wallis (1998) determined the content of cellulose in *Eucalyptus nitens* by gravimetric methods and by high-performance anion-exchange chromatography. Lichtenegger et al. (1999) used position-resolved synchrotron X-ray microdiffraction to image cellulose fibrils in the S2 layer of *Picea abies*. Agarwal et al. (2007) analyzed the anisotropy of cellulose cell wall of black spruce by Raman imaging, revealing differences in the images of the S2 and S1 layer, depending on the orientation of fibrils or the concentration of cellulose.

Lignin is a complex three-dimensional phenolic polymer, derived from three hydroxycinnamyl alcohols: *p*-coumaryl (4-hydroxy-cinnamyl), coniferyl (3-methoxy-4-hydroxy-cinnamyl) and sinapyl alcohol (3,5-dimethoxy-4-hydroxy-cinnamyl), with differing degree of methoxylation (Donaldson 2001; Anterola and Lewis 2002; Boerjan et al. 2003). Conifers contain largely G-lignin, whereas hardwood lignin contains GS-lignin. Lignin makes up approximately one-fourth to one-third of the dry mass of wood (Fengel and Wegener 2003). The values are based on direct determination with wet-chemical methods, by which lignin is obtained as residue, and indirect methods, revealing the lignin content as calculated value after determination of polysaccharides or as result from reactions of lignin with oxidizing chemicals. Furthermore, the lignin content of softwood is determined by spectrophotometric methods (Fengel and Wegener 2003). Lignin is accumulated particularly in the middle lamellae of tracheids and in the secondary cell wall, determined by e.g. microautoradiography, UV absorbance, interference microscopy, fluorescence microscopy and transmission electron microscopy (e.g. Fergus 1969; Saka and Thomas 1982; Donaldson 1985a; Donaldson 2001). Additionally, UV-microspectrophotometry or histochemical staining under acidic conditions with e.g. Wiesner and Mäule reagent are used for localization of lignin in wood tissue (Adler 1948; Jensen 1962; Iiyama and Pant 1988; Möller et al. 2005; Schmitt et al. 2006).

Another method for lignin determination is the labeling of lignin with mercury, firstly used by Freudenberg et al. (1931) for characterizing the lignin structure.

Westermark et al. (1988) described the indirect determination of lignin by detecting Hg in cell walls of spruce by Scanning electron microscopy combined with Energy dispersive X-ray spectroscopy (SEM-EDX). The mercurization reaction is occurring under mild conditions and seems to be less sensitive to the substitution pattern of the aromatic ring. Mercuric acetate reacts under mildly acidic conditions via an electrophilic substitution reaction with the aromatic moiety of lignin, producing a covalent bond between the aromatic ring and the acetoxymercuric group (Westermark et al. 1988). Since mercury is bond with lignin, the results revealed the lignin content and its distribution between middle lamella and cell wall (Westermark et al. 1988). The ratio of lignin in the middle lamellae at the cell comers to the lignin in the secondary wall is given with $2.5 \pm 0.6{:}1$ for late- and earlywood (Westermark et al. 1988). Other investigations have been made by Fromm et al. (2003) using field-emission-Scanning electron microscopy (FE-SEM), combined with a back-scattered electron detector on mercurized specimen. Fromm et al. (2003) determined the distribution of lignin in cell walls of spruce and beech, detecting the highest lignin levels in the compound middle lamella and the cell corners. Schindel (1998) analyzed the distribution of mercurized lignin and its degradation by white- and brown rot fungi in cell walls of beech and pine with TEM-EDX.

Another microscopic technique for detecting the lignin distribution in wood tissue is Scanning transmission electron microscopy (STEM) combined with Energy dispersive X-ray spectroscopy (EDX). It is able to generate mappings of the elemental distribution of fine structure in high resolution but has not been used for lignin analysis (Tsuneta et al. 2002).

A modern method to study the chemical composition of organic compounds is Fourier transform infrared (FTIR) spectroscopy. Infrared radiation is absorbed by molecular bonds in the sample, such as C-H, O-H, N-H, C=O, C-C, resulting in bending, stretching, and twisting of the bonds and leading to characteristic transmittance and reflectance patterns at significant wavenumbers (Günzler and Gremlich 2002). Combined with microscopy and imaging techniques, spatial resolution of the chemical composition is achieved (Salzer et al. 2000; Naumann et al. 2005; Naumann and Polle 2006). Principals and limitations were described recently by Naumann et al. (2008). FTIR microscopy was used e.g. to detect fungi in beech (Naumann et al. 2005) and for evaluation of differences in the chemical composition of transgenic aspens (Labbé et al. 2005).

For FTIR imaging a FPA (Focal Plane Array) -detector is used to obtain chemical images of high resolution from a sample area of tissue sections. The FPA-detector contains 64 x 64 (4096) detector elements generating 4096 independent spectra per scan. The 64 detector elements on each detector side with a size of 4 µm x 4 µm yield a measuring area

of 256 µm x 256 µm. The spatial resolution of the FTIR images is determined by the wavenumber of the radiation and size of the single detector elements (Naumann and Polle 2006). FTIR-FPA images can be evaluated by two methods: The first method integrates the 4096 spectra of the FPA data set for a particular wave number range which is considered as typical for a chemical component in the sample, e.g. lignin or cellulose, generating a particular area below each spectrum. The obtained area values are semiquantitatively illustrated in a color coded image, ranging from blue (no content) to pink (high content).

The second evaluation method requires a FTIR-ATR spectrum of a reference sample of the chemical component of interest, e.g. of lignin or cellulose. The so-called correlation method calculates the correlation of the reference spectrum with each of the 4096 spectra of the FPA data set. The obtained values are illustrated in a color coded image, ranging from blue (no) to pink (high), indicating the strength of correlation.

We selected European beech and Grand fir for our investigations to image lignin and cellulose in both, hard- and softwood, differing e.g. in the dimension of cells and lumina.

The aim of this work was to test the potential of FTIR-FPA microscopy for detecting, quantifying and illustrating lignin and cellulose in wood of Grand fir and beech, using the correlation method as new tool for image evaluation. For this purpose, the correlation method was compared with the integration method. STEM-EDX was utilized as an independent method for validation of the lignin distribution obtained by FTIR microscopy.

5.3 Material and methods

5.3.1   Wood material

Ten beech (*Fagus sylvatica* L.*)* and ten Grand fir (*Abies grandis* (Douglas ex D. Don) Lindl.) trees, each 56 years old, were harvested in 2006 in the city forest of Schmallenberg (North Rhine-Westphalia, 51° 14' 29'' N, 8° 23'50'' E). The forest stand has west to northwest exposition at an altitude of 600 m and is located on a steep slope. The soil is brown earth with limited nutrient supply. The forest stand was established by planting. At harvest, the mean height and breast height diameter of beech were 16 m and 18 cm, respectively. Grand fir had an average height of 29 m and a breast height diameter and 45 cm. Two disks were cut from each tree, one at the stem base and one below the crown, yielding 6 disks for each species. From each disk, one wood block was excised (length: 1 cm, width: 1 cm, height: 2 cm) near the bark, yielding 12 blocks for both species. The wood was used to prepare acid-insoluble Klason lignin for FTIR spectroscopy as well as for wood sections for FTIR and STEM microscopy (see below).

5.3.2   Lignin determination

The 12 blocks were hackled with a gripper to small pieces and milled to a fine powder (MM 2000, Retsch, Haan, Germany) for 5 min at 50 u/min. The frequency was raised slowly during the next 5 min to 90 u/min. The whole milling process took 10 min for each sample. The obtained wood powder was used for preparation of acid-insoluble Klason lignin of each wood block of the upper and the lower discs, according to Dence (1992).

500 mg milled powder was weighed into a centrifuge tube (W1), (W2 = W1 + weight of powder and tube). 40 ml 0.5 M KPP-buffer (KH_2PO_4/ K_2HPO_4, pH 7. 8; 0.5 % Triton-X100) were added and the slurry was stirred for 30 min. Afterwards the slurry was centrifuged for 10 min (5000 g, 4 ℃, Rotanta 96R, Hettrich, Tuttlingen, Germany). The supernatant was discarded. The sample was resuspended and washed in KPP-buffer. Subsequently, the pellet was washed 4 times (30 min) in 100 % MeOH. Afterwards, 40 ml ethanol (96%)/ cyclohexan mixture (v:v = 1:2) were added and the sample was incubated for 6 h at 50 ℃ (Rettberg, Göttingen, Germany). Then the sample was centrifuged for 10 min as above; the supernatant was discarded. The sample was washed again with the ethanol/cyclohexan mixture (40 ml) and centrifuged. The supernatant was discarded. Twenty ml acetones were added centrifuged, and the supernatant was discarded. Afterwards, the remaining pellet was dried overnight under the hood. The dry sample was weighed (W3 = W1 + pellet weight). 8 ml of 72 % H_2SO_4 were added, mixed and incubated for 60 min at room temperature. Then 200 ml distilled H_2O were added and the sample was shaken for several minutes. Afterwards, the sample was incubated for 1 h at 121 ℃ and 1 bar pressure (HST 666, Zirbus, Bad Grund) and cooled down to room temperature afterwards. Filter paper (Nr: 589/1 (black ribbon), Schleicher & Schnüll, Dasell, Germany) with a diameter of 90 mm was weighed (W4) and the fluid with the residue was poured over the filter and washed with H_2O. Filter and sample were dried in an oven for 48 h at 60 ℃ (Rettberg, Göttingen), then cooled down in an exsiccator and weighed (W5). Klason lignin was calculated according to the following equation:

$$Klason\ lignin\ (\%) = \frac{(W5-W4)}{(W2-W1)} * 100$$

The obtained lignin powder of the 6 samples of each species was analyzed by FTIR spectroscopy. Since the powder was inhomogeneous and lumped, it had to be milled again to a finer powder (MM2000, Retsch, Haan, Germany) for 15 minutes.

5.3.3   Determination of nitrogen

To determine nitrogen concentrations in Klason lignin, 0.6-1.0 mg of the dry and fine lignin powder were weighed into 5x9 mm cartouches (Hekatech, Wegberg, Germany) and analyzed by the Elemental Analyzer EA1108 (Carlo Erba Strumentazione, Rodano, Italy). Acetanilide (71.09 % C, 10.36 % N; Carlo Erba Strumentazione, Rodano, Italy) was used as a standard.

5.3.4   FTIR spectroscopy

FTIR-ATR spectra of beech and Grand fir Klason lignin and cellulose were recorded in the wave number range from 4500-600 cm^{-1} with an Equinox 55 spectrometer (Bruker Optics, Ettlingen, Germany) including a deuterium-triglycinesulfate-detector and an attached ATR-unit (DuraSamplIR, SensIR Europe, Warrington, England). A resolution of 4 cm^{-1} and a number of 32 scans per sample was used. The 6 lignin samples of each tree species were powdered. Three replicates per lignin sample were analyzed, yielding 18 spectra averaged to one spectrum with the OPUS 6.5 software (Bruker Optics, Ettlingen, Germany).

In addition, cellulose (Cotton linters, Buckeye, Memphis, USA) was investigated. The cellulose sample was pressed. Nine measurements were conducted to get representative means with the OPUS 6.5 software (Bruker Optics, Ettlingen, Germany).

5.3.5   Specimen preparation for FTIR microscopy

Wood blocks were excised near the bark of Grand fir and beech, consisting of early and latewood. Counted from the bark side, the wood area around the fifth growth ring was chosen. The blocks were sectioned in cross-sectional direction with a sledge-microtome (Reichert-Jung, Heidelberg, Germany). Sections with a thickness of approximately 10 µm were prepared for Grand fir. Due to the thickness of the cell walls of beech, sections of approximately 7 µm had to be prepared for this species. The sections were dried on microscope slides at room temperature, covered with a coverslip and weighted with a lead block to keep the sections flat.

5.3.6   FTIR microscopy

FTIR transmission spectra of 10 µm sections of Grand fir and 7 µm sections of beech were recorded with the FTIR spectrometer Equinox 55 combined with the IR microscope Hyperion 3000 (Bruker Optics, Ettlingen, Germany), including a focal plane array (FPA) detector (Bruker Optics, Ettlingen, Germany), in the wavenumber range from 3900-900 cm^{-1}. The

detector consists of 64 x 64 detector elements, each with a dimension of 4 µm x 4 µm and simultaneously records 4096 spectra without moving the sample, covering a total sample area of 256 µm x 256 µm. A spectral resolution of 8 cm^{-1} and a number of 10 scans per measurement were used. The sections were placed on a round potassium bromide (KBr) window (diameter: 13 mm, height 2 mm) used as a sample holder.

For evaluation of the FTIR-FPA data set, two different methods were applied. The first one integrated in each of the 4096 spectra a band that is considered as typical for the compound under investigation. Using the OPUS 6.5 software (Bruker Optics, Ettlingen, Germany), the borders for spectra integration were set from 1530 cm^{-1} and 1490 cm^{-1} for lignin (Faix 1991) and 1390-1350 cm^{-1} for cellulose (Pandey and Pitman 2003), respectively. A straight baseline was drawn connecting the local band minima at the defined wavenumbers. The area between spectrum and corresponding baseline for each of the 4096 spectra was calculated. Figure 1 (A) shows the principal of this method exemplarily for one spectrum of Grand fir. The scale was automatically adjusted between the lowest and highest peak areas, which were visualized by a color code from blue (no lignin or cellulose) to pink (highest lignin or cellulose content). The distribution of lignin and cellulose was illustrated in color coded images, respectively. The color of each pixel was assigned directly to the calculated area received for each spectrum and, thus, indicated semiquantitatively the respective content in the sample.
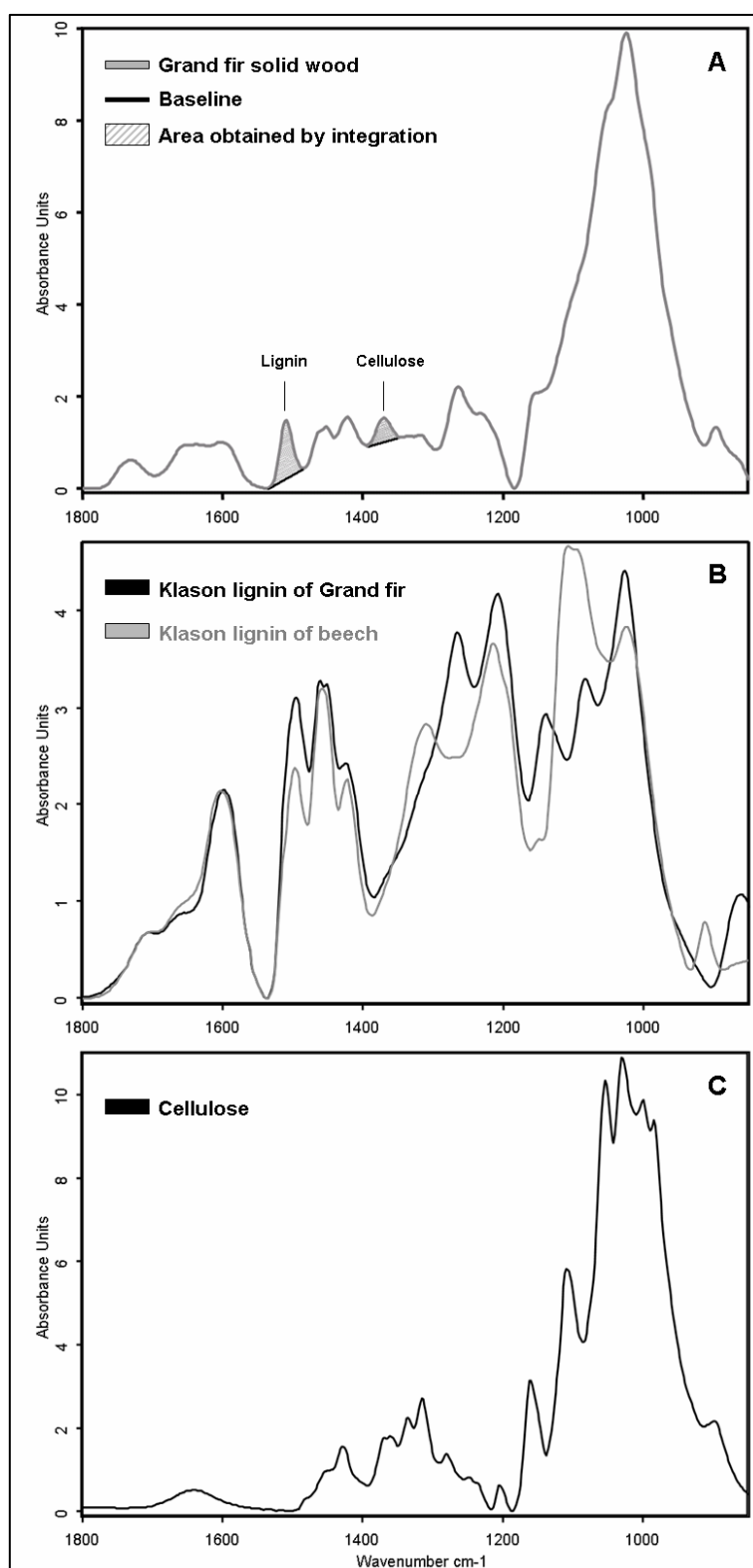
Fig. 1 A-C: Principal of the integration method, exemplarily shown for a FTIR-ATR spectrum of Grand fir (A). The areas below the spectral bands, obtained after integration, are hatched in grey color. For the correlation method the averaged ATR spectra of 18 beech and 18 Grand fir Klason lignin ATR spectra (B) as well as of 9 cellulose spectra (C) were used and correlated with the FPA data set, respectively. The ATR spectra are given in the wavenumber range from 1800-850 cm^{-1}.

The second method used for image evaluation was the so-called correlation method or trace-computation. The averaged ATR spectra of pure Klason lignin powder of beech and Grand fir (see above) and cellulose (Cotton linters, Buckeye, Memphis, USA) were used as reference spectra (Figure 1 B, C). The 4096 spectra of the FPA data set were used for the function "trace-computation" of the OPUS 6.5 software (Bruker Optics, Ettlingen, Germany), calculating the correlation between the particular mean spectrum of Klason lignin, linters and the 4096 spectra of the FPA data set. Figure 2 shows a typical example of an averaged FPA spectrum (n=5), extracted from the cell corner, and averaged ATR spectra of beech (A) and Grand fir (B).
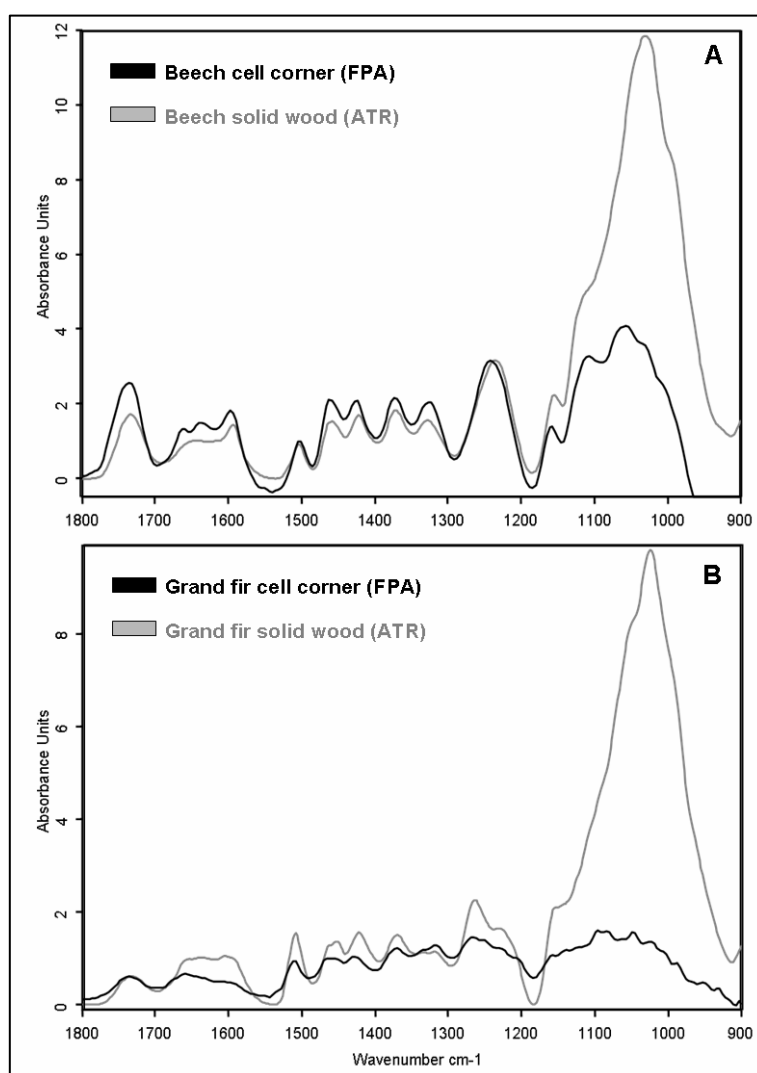
Fig. 2 A, B: (A) FTIR-ATR spectrum of beech solid wood and a FPA spectrum extracted from a cell corner of the FTIR-FPA image, recorded of the solid wood section of beech (see Fig. 3 B). (B) FTIR-ATR spectrum of Grand fir solid wood and a FPA spectrum extracted from a cell corner of the FTIR-FPA image, recorded of the solid wood section of Grand fir (see Fig. 3 A). For the ATR spectrum, the averages of 120 spectra, for the FPA spectrum the average of 5 spectra are given in the wavenumber range from 1800-900 cm^{-1}.

It is obvious that the absorbance of the FPA spectra in the wavenumber region between 1150-900 cm^{-1}, tentative assignable to carbohydrates, is much lower and degenerated, compared to the ATR spectra. This holds true for both tree species and was most likely due to the thickness of the sections. According to our own experience, the quality of the spectra in this region is increasing in thinner sections. However, due to room humidity, such thin sections roll up and undulate, rendering the record of a plane section area impossible. Thus, thicker sections were selected and the area between 1150 and 900 cm^{-1} was excluded for evaluation of the FPA data set for cellulose with the correlation method.

The correlation was accomplished for baseline-corrected ATR and FPA spectra in the fingerprint-region (1800-900 cm^{-1}) by cutting off the adjacent wavenumber range from 1800-3900 cm^{-1} in the FPA spectra and additionally from 900-600 cm^{-1} in the ATR spectra. The intensities of the particular data points of all wavenumbers of the reference ATR spectrum were plotted with those of all 4096 spectra of the FPA data set, generating a scatterplot. A straight line was set through the plot, resulting in a significant slope. The value of this slope corresponded to the value saved as result for the FPA-data set. The higher the value of the particular slope, the higher was the correlation of the FPA-data set and the particular reference spectrum. The scale was open ended and not normalized. The obtained values were illustrated in a color coded image, ranging from blue (no lignin or cellulose content) to pink (high lignin or cellulose content), semiquantitatively illustrating the spatial distribution of lignin and cellulose, respectively.

Since the illustration of the received FPA images is based on two different evaluation methods, the obtained values reflect relative intensities and correlations and therefore the intensities can not be compared directly. However, an assessment of the distribution of lignin and cellulose is possible.

5.3.7   Specimen preparation for Scanning transmission electron microscopy combined with Energy dispersive X-ray spectroscopy (STEM-EDX)

5 specimen (length: 0.5 cm, width: 0.5 cm, height: 0.3 cm) were excised with a razor blade from the same wood block as used for FTIR microscopy and extracted with acetone (300 ml) by Soxhlet-extractor for 8 hours. Then they were treated with a solution of mercuric acetate (and acetic acid at 95 °C with methanol as solvent in a total volume of for 8 hours (according to Westermark et al. 1988). The particular ratios are given in Table 1.

Table 1: *Parameter for mercurization of the specimen excised from Grand fir solid wood for EDX analysis.*

Nr:	Weight of specimen [mg]	Mercuric acetate [mg]	Acetic acid [ml]	Total volume including methanol [ml]
1	16.83	126.2	0.21	10
2	94.47	708.5	1.18	30
3	28.16	211.2	0.35	10
4	26.23	196.7	0.32	10
5	13.73	102.9	0.17	10

After mercurization, the samples were washed by refluxing in boiling methanol (350 ml) for 8 hours. Then the mercurized wood samples were transferred stepwise to anhydrous acetone in a graded methanol-acetone series using 2:1, 1:1 and 100 % acetone, respectively. Each step took 24 h and was accomplished in a dark room.

For embedding the specimen a styrol-methacrylate-medium was utilized, mixed of 2 g dibenzoylperoxide (Peroxid-Chemie GmbH, Pullach, Germany), 50 ml styrol (Merck-Suchardt, Darmstadt, Germany) and 50 ml butyl-methacrylate (Sigma-Aldrich, München, Germany). The dehydrated samples were incubated with anhydrous acetone and styrol-methacrylate in a graded series (2:1), (1:1), (1:2) for 24 h, respectively. Then 100 % styrol-methacrylate was used for incubation for 24 h.

The specimens and pure styrol-methacrylate were put into gelatine capsules (size: 0, Plano GmbH, Wetzlar, Germany) and polymerized in a dryer (II25, Memmert, Schwabach, Germany) for 24 h at 60 °C and for 7 days at 35 °C. Sections of approximately 1µm were cut with an ultramicrotome (Reichert-Jung, Heidelberg, Germany), glued on copper grids (according to Fritz 2007) and coated with carbon under vacuum (Balzers, Bingen, Germany).

5.3.8   STEM-EDX

For the detection of mercurized lignin in wood cell walls, four transmission-electron microscopes were used.

A JEM-2100 HR (JEOL, Eching, Germany) was applied, operating at 120 kV and equipped with a high-angle-annular-darkfield detector (HAADF) for STEM mode imaging. Energy dispersive X-ray spectrometry (EDX) was performed using a 30 mm^2 EDX-detector (JEOL, Eching, Germany).

A Tecnai G^2 Spirit BioTWIN (FEI Company, Eindhoven, Netherlands) was used, operating at 120 kV and equipped with a high-angle-annular-darkfield detector (HAADF) for STEM mode imaging. EDX was performed with a 50 mm^2 EDX-detector (EDAX, Mahwah, USA).

A LIBRA 120 (Carl Zeiss NTS GmbH, Oberkochen, Germany) was applied, operating at 120 kV and equipped with a high-angle-annular-darkfield detector (HAADF) for STEM mode imaging. Energy dispersive X-ray spectrometry (EDX) was performed using a 30 mm^2 EDX-detector (Oxford Instruments Analytical, High Wycombe, England).

An EM 420 (Philips, Eindhoven, Netherlands) was used, operating at 120 kV and combined with a 30 mm^2 EDX-detector (EDAX DX-4, EDAX, Mahwah, USA).

5.4 Results

5.4.1   Analysis of Klason lignin

For a better understanding of the properties of the analyzed wood samples, the lignin contents in stem-wood of Grand fir and beech were analyzed (Table 2). We determined an average lignin concentration of 26.0 % (± 0.7) in Grand fir and 21.2 % (± 3.6) in beech (Tab. 2).

Table 2: *Klason lignin content isolated from beech and Grand fir solid wood and the corresponding N concentrations of Klason lignin. For Klason lignin the average of 6, for N the average of 18 replicates is given, respectively.*

	Klason Lignin	**N**
Beech	21.29 ± 3.6	0.32 ± 0.06
Grand fir	26.01 ± 0.7	0.16 ± 0.02

To our knowledge, the determination for Grand fir Klason lignin has not been made before. The comparison with the lignin percentages of other coniferous trees, such as *Abies alba* Mill. (28.9 %) and *Abies balsamea* (L.) Mill. (27.7 %) (Fengel and Wegener 2003), showed that the determined lignin content of Grand fir is rather similar to those species. This holds true for the averaged value of Klason lignin obtained for beech, given by Fengel and Wegener (2003), who reported a lignin content of 22.2 %. However, the methods of lignin determination can be carried out in many different manners (Fengel and Wegener 2003) and we do not know the methods applied to obtain data. We determined an average N content of 0.32 % ($\pm$ 0.06) in Klason lignin of beech and 0.16 % ($\pm$ 0.02) in that of Grand fir (Tab. 2). These data imply that the N content of beech was twice as high as in Grand fir.

5.4.2   FTIR microscopy

The results of the FTIR microscopic analyses are shown in figures 3-5.

5.4.2.1 *Correlation of beech and Grand fir solid wood ATR spectra with the particular FPA data set*

The mean FTIR-ATR spectra of beech (n=120) and Grand fir (n=120) solid wood (Fig. 2 A, B) were correlated with the FPA data set recorded of the particular wood section, respectively, to determine in which wavenumber range the particular spectra are correlating in the best way. Figure 3 gives the results for the light microscopic images of Grand fir (A) and beech (C) and the corresponding FPA images (B, D). Using a wavenumber range between 1800-1150 cm^{-1}, a high correlation was obtained, indicated by the bright pink color (3 B, D). The complete wood area shows high correlation. The lumen are illustrated in blue color, indicating, as expected, no correlation between the particular FTIR spectrum and FPA data set (3 B, D). If the whole spectrum was used (4200-600 cm^{-1}), high spectral noise (3900-1800 cm^{-1}) and the degeneration of the carbohydrate band around 1100 cm^{-1} (1150-900 cm^{-1}), shown in figure 2, spoiled the correlation between ATR and FPA spectra. This result served as basis for further investigations, especially for the determination of the spatial distribution of cellulose. The analysis also showed that the lumina of fibers were clearly visible for Grand fir but not for beech. This was caused by the small dimensioned cells and lumina in the section of beech, whereas in the section of Grand fir, both were larger in dimension.
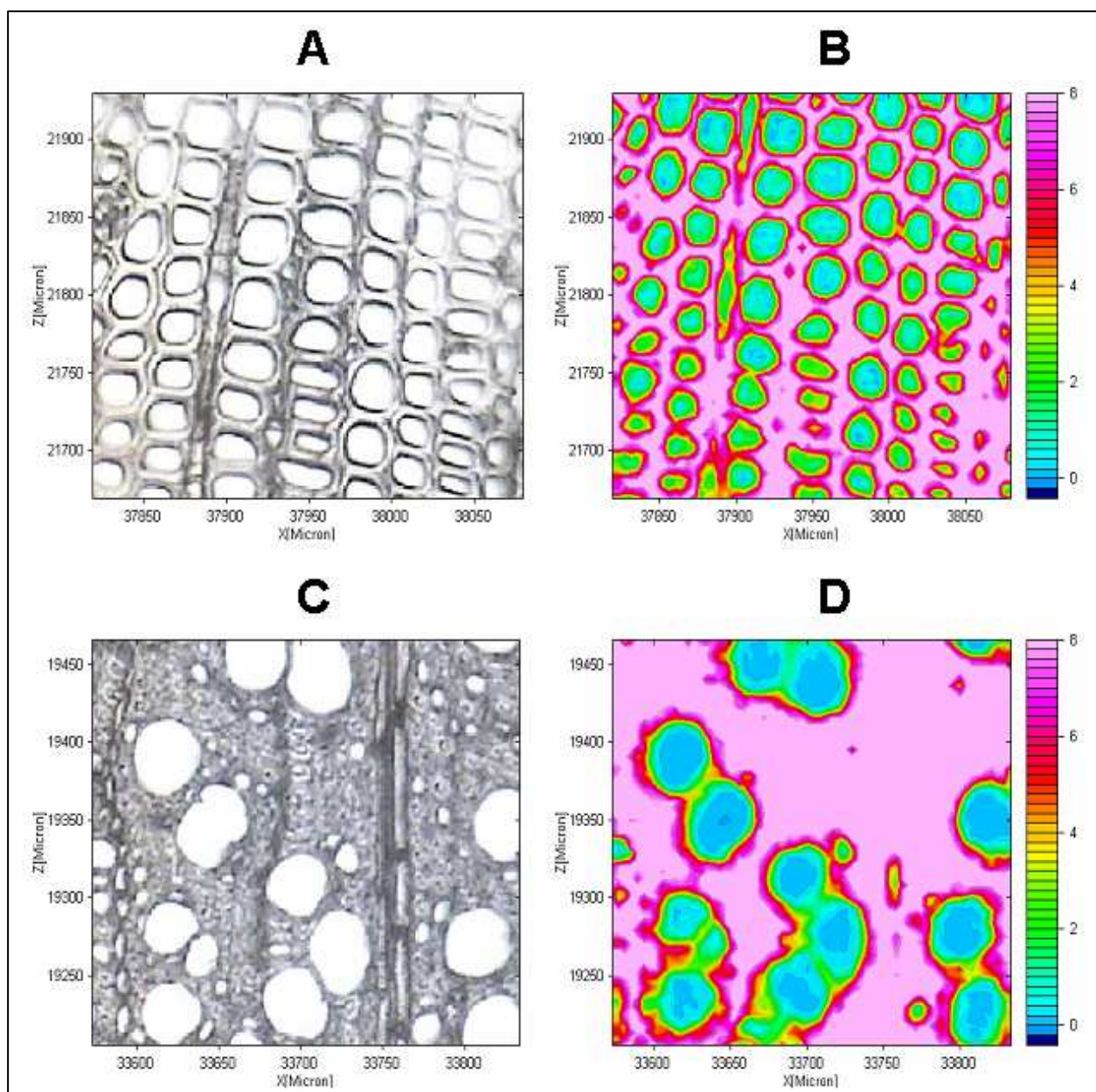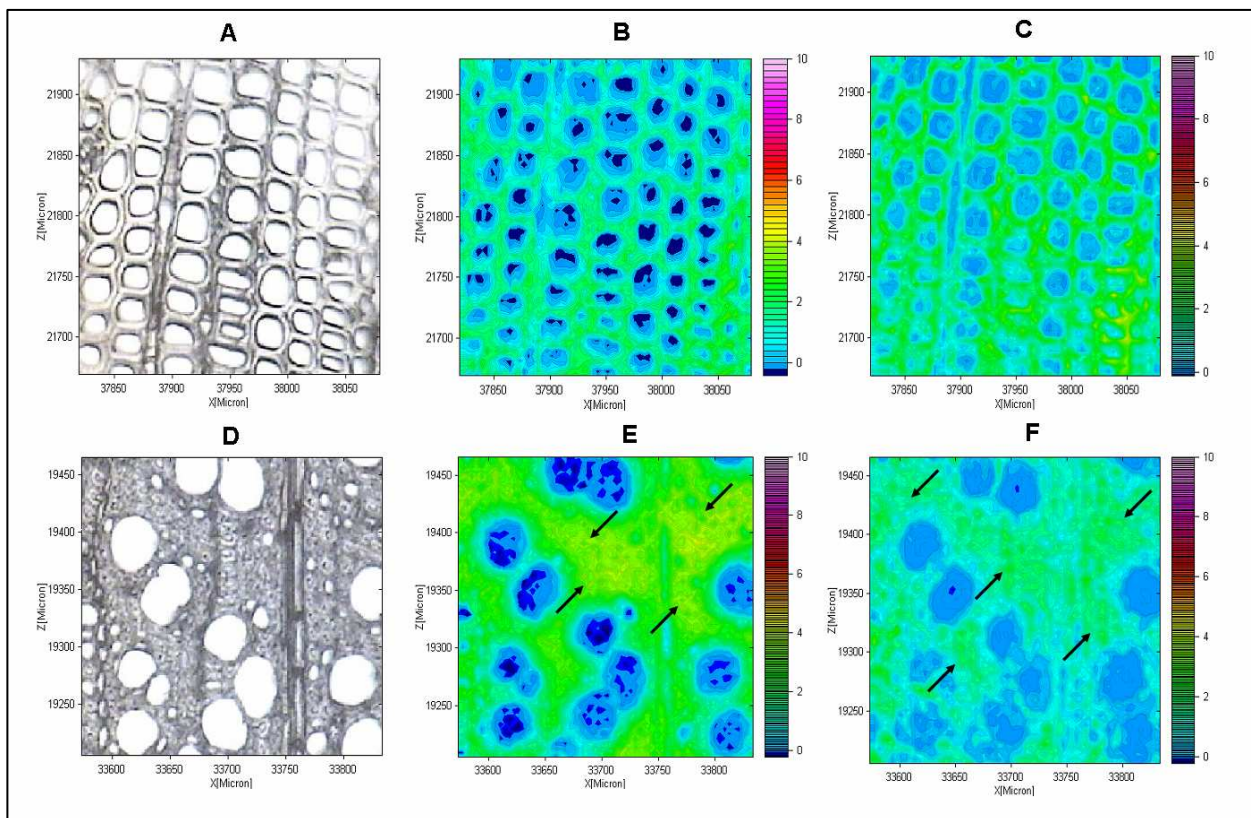
Fig. 3 A-D: Light microscopic view of Grand fir (A) and beech (C) cross-sections. The spectra of the corresponding FPA images are correlated with the averaged FTIR-ATR spectrum of Grand fir (B) and beech (D) solid wood in the wavenumber range of 1800-1150 cm^{-1}. The color scale represents increasing correlation from blue (low) to pink (high).

5.4.2.2 FTIR-FPA imaging of cellulose

Light microscopic images illustrate the anatomy of late wood of Grand fir (Fig. 4 A) and beech (Fig. 4 D). The corresponding FPA images reflect the spatial distribution of cellulose after evaluating all spectra by integration for the wavenumber range between 1390 and 1350 cm^{-1}, tentatively assignable to cellulose (B, E). The images obtained by correlating the FPA data set with the averaged ATR spectrum of cellulose are illustrated in figures 4 (C) and (F). The color scale indicates increasing cellulose content from blue to pink.

The integration of the FPA data set for the latewood area of Grand fir (4 B) and beech (4 E) revealed a homogenous spatial distribution of cellulose over the analyzed wood area. This is visible in the green coloration without any regions of significant cellulose accumulation. However, the cellulose content in the section of Grand fir increases top down (Fig 4 B). This is indicated by blue and slight green coloration in the upper part of the image which is tending to deeper green in the lower part. This might be due to the decreasing distance to the annual growth ring (Fig. 4 B). The lumina are illustrated in blue color, indicative for no cellulose content.

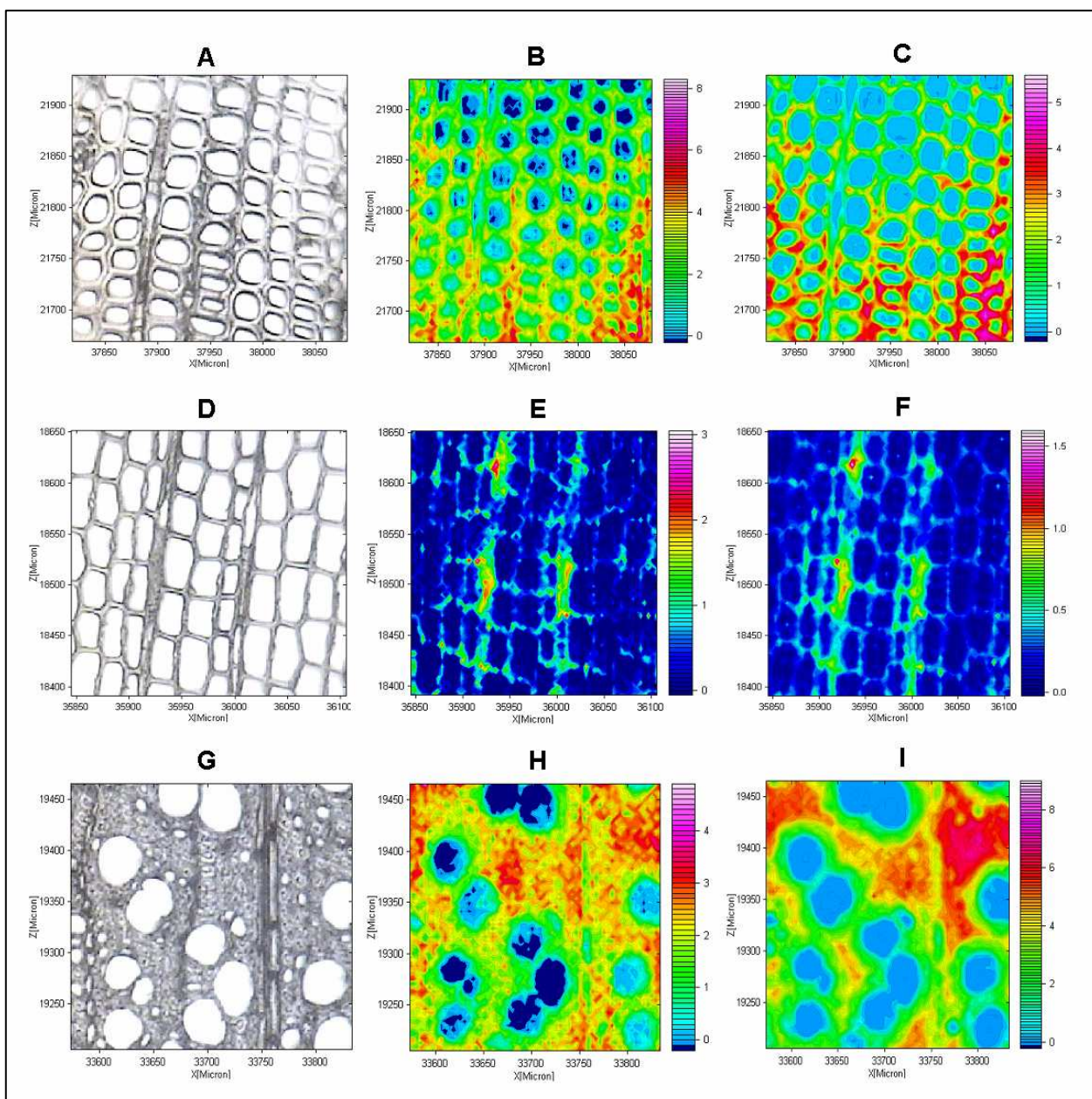*Fig. 4 A-F: Light microscopic view of Grand fir (A) and beech (D) cross-sections. The spectra of the corresponding FPA images are integrated for the wavenumber range considered as typical for cellulose (1390-1350 cm^{-1}) for Grand fir (B) and beech (E), or correlated with the averaged FTIR-ATR spectrum of cellulose in the wavenumber range of 1800-1150 cm^{-1} for Grand fir (C) and beech (F). The color scale represents increasing cellulose content from blue (low) to pink (high). The arrows in figure 4 E and F indicate areas with increased accumulation of cellulose.*

The spatial distribution of cellulose indicated by correlation was homogenous (Fig. 4 C). The gradient top down is still detectable. The coloration of the cell walls in the investigated area is given in the same green coloration with some yellow in the lower part of the image. Furthermore, the image shows a slightly higher contrast compared to 4 (B), enabling a better separation of lumina of tracheids and cell walls, even in the endmost latewood area.

The spatial distribution of cellulose in the section of beech solid wood, obtained by integrating the FPA data set, is illustrated in figure 4 E. The cells were too small to be illustrated separately with the 4 µm x 4 µm detector elements. This prevents a clear separation of single cells. The distribution of cellulose was quite homogenous, visible in largely green coloration. However, an area with slightly higher accumulation of cellulose was verifiable.

This is indicated by the yellow coloration in the image (Fig. 4 E). The lumina are illustrated in blue color, indicative for no cellulose content.

The spatial distribution of cellulose in the solid wood section of beech, obtained by correlation, is shown in figure 4 F. Areas with significant accumulation of cellulose were indicated by green coloration (4 F). The lumina are illustrated in blue color as well as areas with low accumulation of cellulose. Furthermore, the image shows a low contrast, especially in the lower part of the image (4 F), which impedes a clear separation of lumen of vessels and cell walls.

5.4.2.3 FTIR-FPA imaging of lignin

The FPA images in figure 5 (B), (E) and (H) reflect the spatial distribution of lignin after evaluating all spectra by integration for the range between 1530 and 1490 cm^{-1}, tentatively assignable to lignin. The images obtained by correlating the FPA data set with the averaged ATR spectrum of Klason lignin are illustrated in figures 5 (C), (F) and (I). The color scale indicates increasing lignin content from blue to pink.

Fig. 5 A-I: Light microscopic view of Grand fir latewood (A), earlywood (D) and beech latewood (G) cross-sections. The spectra of the corresponding FPA images are integrated for the wavenumber range considered as typical for lignin (1530-1490 cm^{-1}) for Grand fir (B, E) and beech (H), or correlated with the particular averaged FTIR-ATR spectrum of Klason lignin in the wavenumber range of 1800-900 cm^{-1} for Grand fir (C, F) and beech (I). The color scale represents increasing lignin content from blue (low) to pink (high).

The integration of the FPA data set for the latewood area of Grand fir revealed a high accumulation of lignin especially in the area of the middle lamellae and the corners of the cells (Fig. 5 B). However, due to the fact that one spectrum is recorded for each pixel (4x4 μm), the resolution of the FPA image is generally not high enough to assign the

coloration of the corners, either to the interface where the three tracheids adjoin, or to the particular cell wall layer. The upper part of the image largely shows green coloration, indicative of low lignin content. In the underpart high lignin content is detectable, shown in an intense yellow and red coloration. This semiquantitatively indicates an increase of the lignin content top down (Fig. 5 B). The area of the middle lamellae is displayed in green or yellow and partly in red coloration, indicating lower lignin content than in the cell corners, largely illustrated in red color (Fig. 5 B). The lumina of the tracheids are displayed in blue color, indicative of no lignin content. However, in the lower part of the image, the coloration of the lumina tends more and more to green, which impedes a clear separation of lumen and cell wall.

Comparable results were obtained for the earlywood area (Fig. 5 E). Since the lignin content is lower in earlywood than in latewood (5 B), indicated by blue coloration, a different color scale is used. A high lignin accumulation is detectable in the area of the middle lamellae and the angles of the cells. The wood rays reveal lignin content partly higher than in the other earlywood cells, indicated by green or yellow coloration. The lumina of the tracheids are illustrated in blue color, indicative for no lignin (5 B).

Figure 5 (C) displays the correlation between the averaged ATR spectrum of Grand fir Klason lignin and the FPA data set. The image shows a high contrast, enabling a considerable differentiation of the lignin accumulation in dependency of the particular cell compartment. Furthermore, the separation of lumina of tracheids and cell walls is clearly possible. A high accumulation of lignin is displayed especially in the area of the middle lamellae and the angles of the cells, indicated by yellow or red coloration. The content is increasing top down with red or pink coloration of the lower cell compartments. The yellow and partly red coloration of the cell corners indicates a higher content than in the middle lamellae.

The accumulation of lignin in the earlywood area (5 F) is generally comparable to that of the latewood area (5 C). Cell corners show higher lignin content than the middle lamellae. A significant accumulation of lignin is detectable in the rays, visible in yellow or red coloration. The high contrast enables a good differentiation of the lignin distribution in the particular cell compartments. The blue coloration of the lumina is indicative for no lignin (5 C).

The spatial distribution in the solid wood section of beech, evaluated by the integration method, is given in figure 5 (H). As already detected for cellulose, the cells are too small to be illustrated in high resolution with the 4 µm x 4 µm detector elements. This inhibits a clear separation of single cells. High lignin content is illustrated especially in the upper and middle

parts of the image, visible in significant red coloration (5 H). The wood ray is illustrated with varying lignin content whereas the lumina of the tracheids are displayed in blue color, indicative for no lignin (5 H).

Figure 5 (I) shows the spatial distribution of lignin in the solid wood cross-section of beech after evaluation by correlation. Areas with significantly high lignin accumulation are given in the upper and middle parts of the image (5 I), visible in deep red coloration. The lower part of the image is illustrated in yellow with slight red, indicative for decreased lignin content. However, in figure 5 (I), there is a continuous coloration of the particular areas of lignin accumulation and not a clear assignment to particular cell walls. The lumina are colored in blue, indicative for no lignin content.

5.4.2.4 Differences in image illustration depending on the evaluation method

For Grand fir, the images evaluated by integration (4 B; 5 B, E) and correlation (4 C; 5 C, F) illustrate the spatial distribution of cellulose and lignin quite similar. However, the illustration is obviously dependent on the particular evaluation method. Integrating the FPA data set for cellulose (1390-1350 cm^{-1}) a clear gradient top down is detectable (4 B). In the image evaluated by correlating the FPA data set with the mean spectrum of cellulose, a gradient is identifiable, too (4 C). However, the correlation of the FPA data set with an averaged ATR spectrum of cellulose results in a much sharper image illustration than integrating the spectra for a particular wavenumber area (4 B). This holds true especially for lignin of Grand fir (5 B, E and C, F). Differences in the coloration of the cell compartments are detectable. The latewood image evaluated by trace-computation generally shows a higher ratio of red or yellow color (5 C). Several compartments indicate higher lignin content than in the image obtained by integration of spectra (5 B). This is visible e.g. for the cells of the entire right part of the image (5 C), showing an intense red coloration in the cell corners, whereas the same compartments are illustrated in yellow color with slight red in figure 5 (B). A sharper illustration is also visible in the earlywood area. In figure 5 (F) the cell walls can be distinguished very well from the lumina, whereas in figure 5 (E) a disruption of the walls is visible. Thus, correlating the 4096 spectra for Grand fir enables an easy distinction of the areas of lignin accumulation and a better illustration of tracheid lumina, tracheid cell walls and ray cells.

A dependency of the image illustration for lignin and cellulose was also detectable for beech (4 E, F and 5 H, I). For cellulose, image 4 (E), evaluated by integration, shows an accumulation in the middle and upper right part of the image. This was not detectable for the

image evaluated by correlation (4 F), which shows largely green coloration. Furthermore, in the lower part of the image (4 F) quite no cellulose is illustrated, whereas 4 (E) shows green coloration. Additionally, the illustration in 4 (F) is not as sharp as that evaluated by integration 4 (E). This inhibits an easy separation of lumen and cell walls, visible in the lower middle and lower right part of the image. This holds true for the images illustrating the spatial distribution of lignin in the beech section (5 H, I). Though the small cell walls inhibit an easy assignment of lignin to particular cells, it is possible to detect lignin in the cell walls (5 H). This is visible e.g. in the upper right part of the image (5 H). In contrast to that, 5 (I) shows a continuous coloration of areas with significant accumulation of lignin. Though the location of the particular areas is comparable to figure 5 (H), a clear assignment of lignin to single cell walls is not possible.

5.4.3   STEM-EDX

Scanning transmission electron microscopy combined with EDX spectroscopy was used for validation of the results obtained by FTIR microscopy. We labeled lignin with mercury (Hg) and detected it indirectly by determining Hg in early and latewood cells. We analyzed the similar wood areas as by FTIR microscopy with much higher resolution, enabling an exact illustration of lignin in the particular cell compartments. However, the high magnification impedes a direct comparison of larger cell wall areas between FTIR images and EDX-mappings.

The results are displayed in figures 6 and 7. STEM mode images show the cell wall of latewood (Fig. 6 A) and earlywood (Fig. 7 A). The corresponding Hg-EDX-mappings, illustrating the spatial distribution of lignin in the particular cell compartments, are given in figure 6 B for latewood and figure 7 B for earlywood.

The EDX-mapping of latewood (Fig 6 B) shows a dependency of the Hg content on the particular cell compartment. Hg is shown for the entire area of the middle lamellae with significant regions of accumulation. This is visible in the intense blue coloration in the lower right part of image or the cell corner. However, the Hg distribution of the middle lamellae is obviously varying. Regions with a significant accumulation of Hg are detectable, illustrated in bright blue coloration as well as regions with low Hg content, displayed in black color. A pronounced content of Hg is also illustrated in the edge of the S2 layer of the latewood cell wall. With increasing distance from the corner, the accumulation is decreasing. The lumen is well distinguishable from the cell wall. Point measurements confirm these results (see appendix III and Fig. 1 A, B).
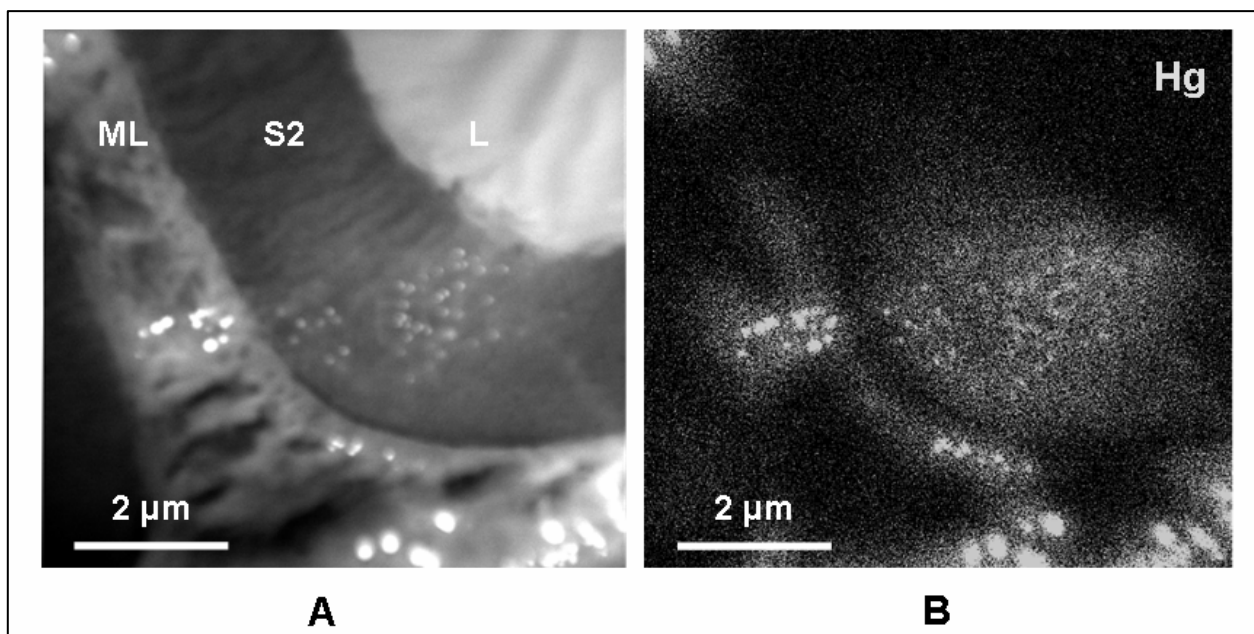
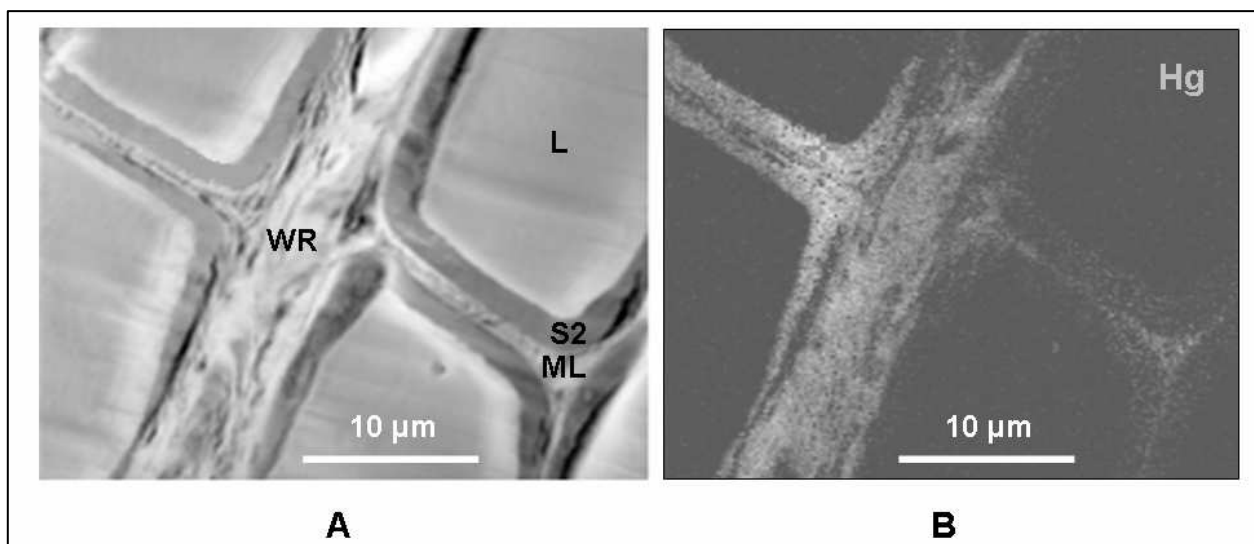*Fig. 6 A, B: STEM mode image (A) of a latewood cell wall with lumen (L), secondary wall (S2) and the compound middle lamellae (ML), analyzed by JEM-2100 HR microscope. The corresponding EDX mapping for mercury (B) is illustrating the lignin distribution in the particular cell compartments.*

The results of the EDX-mapping of the earlywood area (Fig. 7 B) are similar to those of the latewood area (Fig 6 B). There are hardly any differences detectable in the Hg illustration, depending on the particular wood compartment. The highest content is identifiable for the area of the middle lamellae, the cell corners and the wood ray. The ray shows high Hg content, indicated by the continuous green coloration. The lumina are very well distinguishable from the cell walls. Point measurements reveal a generally lower Hg content in earlywood than in latewood. Furthermore, they confirm the increased Hg content in the ray (see appendix III and Fig. 1 C, D).

Fig. 7 A, B: STEM mode image (A) of earlywood cell walls with lumen (L) and secondary wall (S2), the compound middle lamellae (ML) and a wood ray (WR), analyzed by Tecnai G^2 Spirit BioTWIN microscope. The corresponding EDX mapping for mercury (B) is illustrating the lignin distribution in the particular cell compartments.

Line scans were accomplished for analyzing the lignin content in different cell compartments. Figure 8 (A) exemplarily shows a line scan with a longitude dimension of 32 µm in a section of Grand fir. The 10 point measurements range from lumen (L) to lumen over the compound middle lamellae (ML) of a latewood cell of Grand fir. The localization of each point measurement is marked in red color. Figure 8 (B) gives the corresponding mercuric content of the particular point measurements in percent per weight. The significantly highest content of Hg is detectable in the area of the middle lamellae (point measurement Nr: 6 in Fig. 8 B) which is obviously decreasing towards the particular lumen.
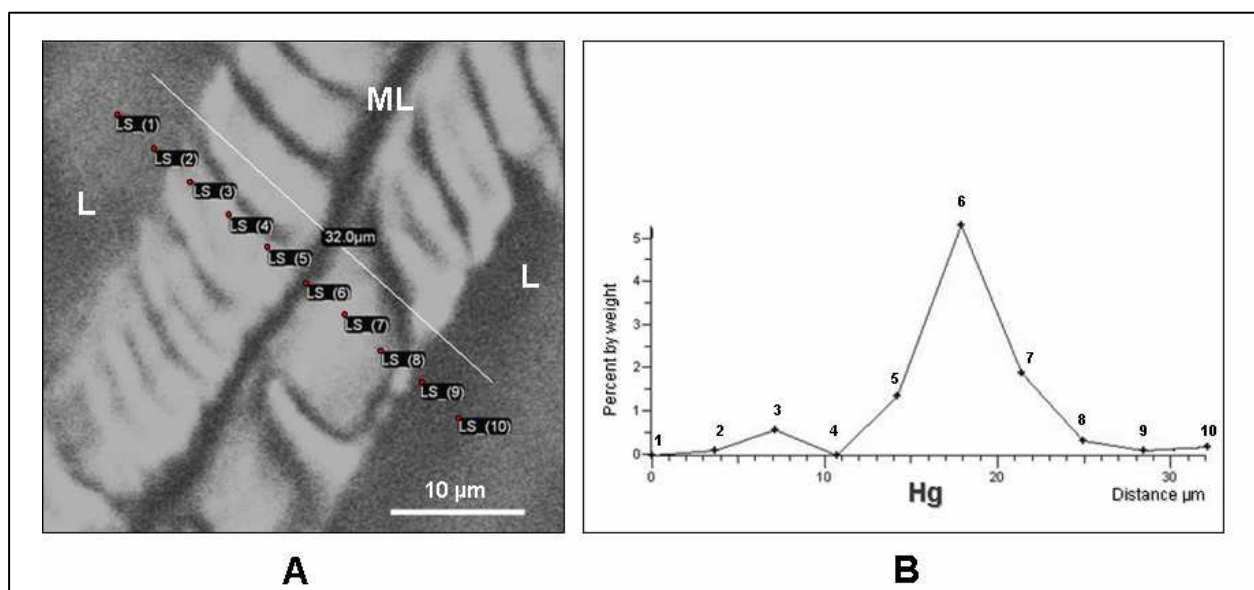
Fig. 8 A, B: STEM mode image (A) of a line scan with a longitude dimension of 32 µm. The 10 point measurements range from lumen (L) to lumen over the compound middle lamellae (ML) of a latewood cell of Grand fir, analyzed by LIBRA 120 microscope. The localization of each point measurement is marked in red color. (B) gives the corresponding mercuric content of the particular point measurement in percent by weight.

Concluding, FTIR microscopy enables the illustration of cellulose and lignin in different cell compartments of late or earlywood of Grand fir and latewood of beech. A pronounced content of lignin is identifiable for the middle lamellae, the angles of the cells and the wood rays of Grand fir. Furthermore, the illustration of the cellulose and lignin distribution is dependent on the particular evaluation method and the tree species. The images, evaluated by correlating the FPA data set with the averaged ATR spectrum of cellulose and Klason lignin, reveal a sharper illustration of the cellulose and lignin distribution for Grand fir. STEM microscopy with indirect lignin labeling by Hg confirms these results with a much higher resolution of EDX-mapping.

However, for beech, the illustration of cellulose and lignin was slightly sharper by using the integration method for image evaluation than correlating the FPA data set with an averaged ATR spectrum of Klason lignin or cellulose.

5.5 Discussion

The cellulose and lignin distribution in Grand fir and beech was illustrated by FTIR-FPA microscopy, using two independent methods for image evaluation. The obtained data for Grand fir lignin were validated with STEM-EDX. To our best knowledge, this combined method was used for the first time to analyze the lignin distribution in cell walls, as well as the FPA imaging of the spatial distribution of cellulose in wood tissue.

The principle questions were, if FTIR-FPA microscopy has the potential to detect and illustrate cellulose and lignin in different cell compartments and if there is a dependency of the image illustration on the particular evaluation method.

For determination of the spatial distribution of cellulose by correlation, the wavenumber range between 1150 and 900 cm^{-1} had to be excluded from spectra evaluation. This was due to the thickness of the sections which lowered the spectral quality in this region. Faix and Böttcher (1992) reported the same phenomenon investigating the influence of the particle size and concentration on transmission spectra of *Guibourtia* sp. Especially the broad band of carbohydrates around 1100 cm^{-1} is strongly dependent on the thickness of the section (Faix and Böttcher 1992). Thinner sections lead to an increasing quality of the spectra in this region. However, due to room humidity, such thin sections roll up and undulate, avoiding the recording of a plane section area. Furthermore, in too thin sections, the absorbance of the bands in the wavenumber range from 1800-1150 cm^{1} significantly decreases, overlapping with the spectral noise and, thus, spectral information is spoiled.

For Grand fir (4 B, C) and beech (4 E, F), the spatial distribution of cellulose was illustrated homogenously. The gradient top down in the section of Grand fir (4 B, C) is also detectable for lignin (5 B, C). The area with higher accumulation of cellulose in the beech cross section (Fig. 4 E, F), visible in the middle and upper part of the images, shows high accumulation of lignin, too (Fig. 5 H, I). This might be due to the close bond of lignin and cellulose in wood tissue (Fengel and Wegener 2003). The three main components of wood, lignin, cellulose and hemicelluloses are linked very closely, generating high stability (Fengel and Wegener 2003). Lignin is polymerizing especially in between the cellulose fibrils (Sjöström 1998; Fengel and Wegener 2003).

For Grand fir, FTIR microscopy identifies a high accumulation of lignin especially in the area of the middle lamellae and the angles of the cells (Fig. 5 B, C and 5 E, F). However, it is not possible to assign the coloration of the corners either to the interface where the three tracheids adjoin, or to the particular cell wall layer. This held true especially for the illustration of the lignin and cellulose distribution in the section of beech

solid wood (Fig 5 H, I). Due to the small dimensioned cells and lumina, a differentiation was quite impossible. The size of the single detector elements (4 µm x 4 µm) defines this limit of resolution (Naumann and Polle 2006). If one detector element measures one cell wall, it seems to have a thickness of 4 µm. However, if the cell wall is measured simultaneously by two detector elements, it seems to have a thickness of 8 µm, which leads to a decrease of the spectral intensity (Naumann and Polle 2006). Thus, due to this overlap, it was impossible to resolve the small lumina in the section of beech solid wood. Additionally, the images were recorded with a resolution of 8 cm^{-1} which might have been undervalued to obtain enough spectral information. Furthermore, the resolution of FTIR images depends on the wavenumber of the radiation (Naumann and Polle 2006). At 900 cm^{-1}, theoretically a maximum spatial resolution of 7 µm is possible. With increasing wavenumbers, the spatial resolution gradually increases. At 1500 cm^{-1} and higher, a local resolution of up to 4 µm is achievable (Naumann et al. 2008).

A dependency of the FPA image illustration on the particular evaluation method is detectable for cellulose and lignin and holds true for both tree species (Fig. 4, 5). For Grand fir, the images evaluated by trace-computation result in a generally sharper illustration, enabling an easy separation of the areas where lignin is accumulating. However, for beech the images evaluated by integration were sharper.

Naumann and Polle (2006) described that the resolution of FTIR images depends on the size of the single detector elements as well as on the wavenumber of the radiation. Since the settings of the device, the analyzed sample areas and the data were the same, the high resolution in the images evaluated by trace-computation is most likely due to the different principals on which both evaluation methods are based on. The integration method calculates the area below each spectrum of the FPA data set for a particular band of the entire wavenumber, analyzing just a cut-out (40 wavenumbers) of the entire wavenumber range. However, the trace-computation correlates the data set with an averaged ATR spectrum for 1800-900 cm^{-1} (lignin) or 1800-1150 cm^{-1} (cellulose), resulting in the coefficient of correlation for each spectrum. Thus, the analysis of the spectra is accomplished for a broader wavenumber range (900 wavenumbers for lignin and 650 for cellulose) and comprises more spectral information.

Lignin is a complex polymer (Boerjan et al. 2003) as well as cellulose (Fengel and Wegener 2003) which is not assignable to a fixed wavenumber. Müller et al. (2007) investigated the bands of different lignin and cellulose types with FTIR-ATR spectroscopy. They detected a dependency of the absorbance units especially on the particular lignin types

but also on the type of cellulose for the entire fingerprint-region. A spectral cut-out does not reflect these deviations. This might be a reason for the sharper illustration in the image obtained by spectra correlation.

Furthermore, the better signal to noise ratio in the image evaluated by trace-computation might lead to a sharper illustration. Since a broad wavenumber range is selected for spectra evaluation, the spectral noise is of less consequence than in a spectral cut-out as used for integrating the spectra. This might lead to a spoiling of the cellulose and lignin illustration.

The images of the latewood area revealed an increasing lignin content top down (5 B, C). This might be caused by the shorter distance of the cells to the boarder of the growth ring. In this region, the thickness of the cell walls is increasing. If one detector element measures only a cell wall, the lignin content in the cell wall seems to be higher as if wall and lumen are measured together (Naumann and Polle 2006).

In the lower part of the latewood images of Grand fir (5 B, C) and in the small cells of beech (5 H, I) the coloration of the lumina tends to green, which impedes a clear separation of lumen and cell wall, especially in the image evaluated by integration. The reason might be that the empty lumina contribute to the signal intensity and lead to an underestimation of chemical components at the intersection of wall to lumen (Naumann and Polle 2006).

STEM-EDX on Grand fir sections was used as an independent technique to confirm the results obtained by FTIR microscopy (Fig. 6-8). Westermark et al. (1988) and Schindel (1998) described the EDX technique as well suited for lignin determination on mercurized wood. High lignin content is detectable in the area of the middle lamellae with STEM-EDX, containing regions with more or less lignin accumulation (Fig. 6). This might be due to slight differences in the thickness of the section in this area, leading to a different scattering of the electrons and thus to another contrast in the image. However, the line-scan significantly determined the highest lignin content in the area of the middle lamellae (Fig. 8).

The determination of lignin, especially in the cell corners and the middle lamellae, is accredited by several studies. Donaldson (1993) received similar results determining lignin in cell walls of *Pinus radiata* using quantitative interference microscopy. This holds true for Fromm et al. (2003), analyzing the lignin distribution in cell walls of spruce and beech with TEM and backscattered SEM techniques. Schindel (1998) detected lignin especially in the cell corners and the middle lamellae, applying TEM-EDX. Möller et al. (2005) identified high lignin concentration in the compound middle lamella with UV-microspectrophotometry. The significant accumulation of lignin in the cell corner and the middle lamellae results from the

enzyme mediated polymerization of monolignols initiated by unknown factors located at the corners of cells and in the middle lamellae (Donaldson 2001).

Furthermore, FTIR microscopy and STEM-EDX revealed a partly higher lignin content in the wood rays of Grand fir (Fig. 5 E, F and 7 B) than in the other earlywood cells. In the section of beech (Fig. 5 H, I) a high lignin content of the ray is verifiable, too. This is accredited by Eriksson et al. (1988) who identified a higher lignin concentration in ray cells than in the secondary cell walls of fibers by SEM and TEM-EDXA analysis on birch. UV-microscopic investigations on spruce by Fergus et al. (1969) revealed a higher content of lignin in the rays than in the secondary cell wall of tracheids.

We showed that FTIR microscopy has the potential to detect and illustrate cellulose and lignin in different cell compartments of European beech and Grand fir. Evaluating the FPA data set by trace-computation is promising for studying the chemical components of wood tissue on the level of single cell walls.

References

Adler, E., Björkquist, J., Häggroth, S. (1948). Über die Ursache der Farbreaktionen des Holzes. Acta Chem. Scan. (2): 93-94.

Agarwal, U. P., Ralph, S. A. (2007). Revealing organization of cellulose in wood cell walls by Raman imaging. Proceedings of the 14th international symposium on wood fiber and pulping chemistry. Durban, South Africa.

Anterola, A. M., Lewis, N. G. (2002). Trends in lignin modification: a comprehensive analysis of the effects of genetic manipulations/mutations on lignification and vascular integrity. Phytochemistry. 61: 221-294.

Boerjan, W., Ralph, J., Baucher, M. (2003). Lignin biosynthesis. Annual Review of Plant Biology. 54: 519-546.

Dence, C. W. (1992). Methods in lignin chemistry. Springer-Verlag, Berlin, pp. 33-61.

Donaldson, L. A. (1985a). Critical assessment of interference microscopy as a technique for measuring lignin distribution in cell walls. N. Z. J. For. Sci. (15): 349-360.

Donaldson, L. A. (1993). Lignin distribution in wood from a progeny trial of genetically selected *Pinus radiata* D. Don. Wood Science and Technology. 27: 391-395.

Donaldson, L. A. (2001). Lignification and lignin topochemistry - an ultrastructural view. Phytochemistry. 57: 859-873.

Eriksson, I., Lidbrandt, O., Westermark, U. (1988). Lignin distribution in birch (*Betula verrucosa*) as determined by mercurization with SEM and TEM-EDXA. Wood Science and Technology 22: 251-257.

Faix, O. (1991). Classification of lignins from different botanical origins by FT-IR spectroscopy. Holzforschung. 45: 21-27.

Faix, O., Böttcher, J. H. (1992). The influence of particle size and concentration in transmission and diffuse reflectance spectroscopy of wood. Holz als Roh- und Werkstoff. 50: 221-226.

Fengel, D., Wegener, G. Wood - chemistry, ultrastructure reactions. Kessel Verlag, Remagen, 2003.

Fergus, B. J., Procter, A. R., Scott, J. A. N., Goring, D. A. I. (1969). The distribution of lignin in sprucewood as determined by ultraviolet microscopy. Wood Science and Technology. 3: 117-138.

Freudenberg, K., Sohns, F., Dürr, W., Niemann, C. (1931). Über Lignin Coniferylalkohol und Saligenin. Cellulosechemie. 12:263-275.

Fritz, E. (2007). Measurement of cation exchange capacity (CEC) of plant cell walls by X-ray microanalysis (EDX) in the transmission electron microscope. Microsc. Microanal. 13: 233-244.

Fromm, J., Rockel, B., Lautner, S., Windeisen, E., Wanner, G. (2003). Lignin distribution in wood cell walls determined by TEM and backscattered SEM techniques. Journal of Structural Biology. 143: 77-84.

Günzler, G., Gremlich, H.-U. IR spectroscopy. Wiley-VCH Verlag. Weinheim, 2002.

Iiyama, K., Pant, R. (1988). The mechanism of the Mäule colour reaction introduction of methylated syringyl nuclei into softwood lignin. Wood Science and Technology. 22: 167-175.

Jensen, W. A. Botanical histochemistry: principles and practice. W.R. Freeman. San Francisco, 1962.

Labbé, N., Rials, T. G., Kelley, S. S., Cheng, Z.-M., Kim, J.-Y., Li, Y. (2005). FT-IR imaging and pyrolysis-molecular beam mass spectrometry: new tools to investigate wood tissues. Wood Science and Technology. 39: 61-77.

Lichtenegger, H., Müller, M., Paris, O., Riekel, Ch., Fratzl, P. (1999). Imaging of the helical arrangement of cellulose fibrils in wood by synchrotron X-ray microdiffraction. Journal of Applied Crystallography. 32 (6): 1127-1133.

Möller, R., Koch, G., Nanayakkara, B., Schmitt, U. (2005). Lignification in cell cultures of *Pinus radiata*: activities of enzymes and lignin topochemistry. Tree Physiology. 26: 201-210.

Müller, G., Naumann, A., Polle, A. (2007). FTIR spectroscopy in combination with cluster analysis as tool for analysis and control of wood properties and production processes. In: The plant cell wall - recent advances and new perspectives. Mitteilungen der Bundesforschungsanstalt für Forst- und Holzwirtschaft Hamburg. Schmitt, U., Singh, A. P., Harris, P. (eds.). Wiedebusch Verlag, Hamburg. 223: pp. 129-136.

Naumann, A., Navarro-González, M., Peddireddi, S., Kües, U., Polle, A. (2005). Fourier transform infrared microscopy and imaging: Detection of fungi in wood. Fungal Genetics and Biology. 42: 829-835.

Naumann, A., Polle, A. (2006). FTIR imaging as a new tool for cell wall analysis of wood. New Zealand Journal of Forestry Science. 36: 54-59.

Naumann, A., Peddireddi, S., Kües, U., Polle, A. (2008). Fourier transform microscopy in wood analysis. In: Wood production, wood technology and bio-technological impacts. Ed. Kües, U. Universitätsverlag, Göttingen. pp. 179-196.

Pandey, K. K., Pitman, A. J. (2003). FTIR-ATR studies of the changes in wood chemistry following decay by brown-rot and white-rot fungi. Intern. Biodeterior. Biodegr. 52: 151-160.

Saka, S., Thomas, R. J. (1982). A study of lignification in loblolly pine tracheids by the SEM-EDXA technique. Wood Sci. Technol. (16):167-179.

Salzer, R., Steiner, G., Mantsch, H. H., Mansfield, J. (2000). Infrared and Raman imaging of biological and biomimetic samples. Fresenius J. Anal. Chem. 366: 712-726.

Schindel, K. (1998). Die Röntgenmikroanalyse von Lignin als Untersuchungsmethode für Holz und Holzwerkstoffe. Dissertation Georg-August-Universität, Göttingen.

Schmitt, U., Frankenstein, C., Singh, A., Möller, R. (2006). Cell wall modifications in woody stems induced by mechanical stress. New Zealand Journal of Forestry Science. 36: 72-86.

Tsuneta, R., Koguchi, M., Nakamura, K., Nishida, A. (2002). A specimen-drift-free EDX mapping in a STEM for observing two-dimensional profiles of low dose elements in fine semicondutor devices. Journal of Electron Microscopy. 51: 176-171.

Westermark, U., Lidbrandt, O., Eriksson, I. (1988). Lignin distribution in spruce (*Picea abies*) determined by mercurization with SEM-EDXA technique. Wood Science and Technology. 22: 243-250.

Wright, P., J., Wallis A. F. A. (1998). Rapid determination of cellulose in plantation eucalypt woods to predict kraft pulp yields. Tappi journal. 81 (2): 126-130.

Appendix III
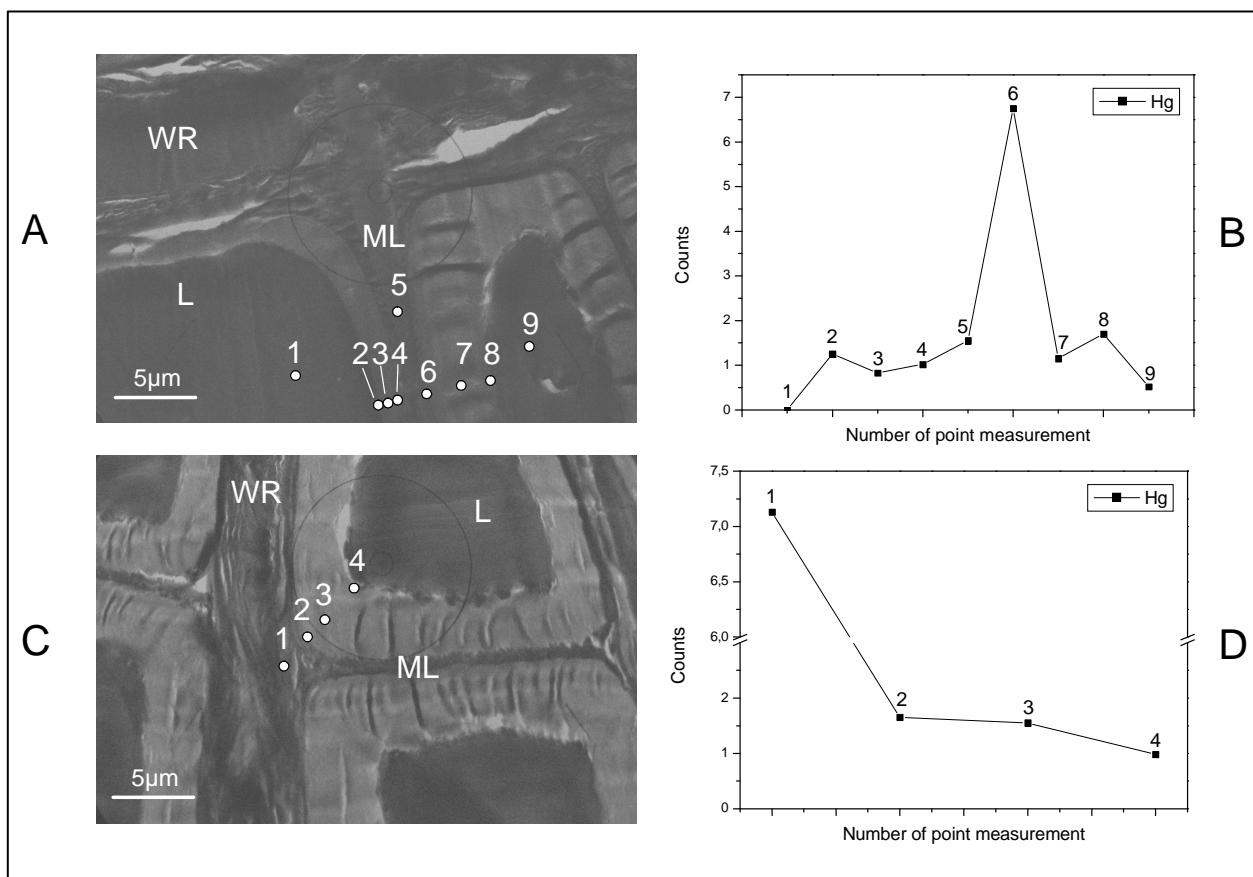
Fig. 1 A-D: TEM point measurements and the corresponding Hg count rates in a section of Grand fir, analyzed by EM 420 microscope. (A) illustrates the localization of the point measurements at the boarder of a growth ring with wood ray (WR), compound middle lamellae (ML) and lumen (L). The corresponding counts for Hg are given in (B), indicating the highest Hg content in the compound middle lamellae. (C) displays the localization of the point measurements in a latewood area with wood ray (WR), compound middle lamellae (ML) and lumen (L). The corresponding counts for Hg are given in (D), indicating the highest Hg content in the wood ray.

Acknowledgements

Declaration

Contributions and some data shown in this thesis have been provided by colleagues:

Chapter 2: *"FTIR spectroscopy in combination with cluster analysis as tool for analysis and control of wood properties and production processes"*

The FTIR-ATR and FTIR-FPA techniques were introduced by Dr. Annette Naumann and the results discussed in detail.

Chapter 3: *"FTIR-ATR spectroscopic analysis of changes in wood properties during particle- and fiberboard production of hard- and softwood trees"*

The investigations of the mechanical and technological properties of the novel and conventional panel boards (Tab. 1) were accomplished by Hubert Vos under the guidance of Prof. Dr. Alireza Kharazipour (Molecular Wood Biotechnology and Technical Mycology, Büsgen-Institute, Georg-August-University Göttingen).

Chapter 4: *"FTIR-ATR spectroscopic analysis of changes in fiber properties during insulating fiberboard manufacture of beech wood"*

The investigations of the raw densities of the insulating wood fiberboards of beech in dependency on the type and amount of binder (Tab. 1) were accomplished by Michael Bartholme under the guidance of Prof. Dr. Alireza Kharazipour (Molecular Wood Biotechnology and Technical Mycology, Büsgen-Institute, Georg-August-University Göttingen).

Chapter 5: *"Imaging of lignin and cellulose in soft- and hardwood species using Fourier transform infrared microscopy and Scanning transmission electron microscopy"*

The STEM mode images, STEM-EDX-mappings and the line scan (Fig. 6, 7, 8) were recorded by Dr. Andrea Olbrich (Forest Botany and Tree Physiology, Büsgen-Institute, Georg-August-University Göttingen).

Curriculum vitae

Personal details

Name	Günter Stefan Müller
Date of birth	06/ 07/ 1978
Place of birth	Oberviechtach, Bavaria, Germany
Nationality	German
Marital status	Unmarried

Education

03/2006-06/2008	Scientific assistant, Faculty of Forest Sciences and Forest Ecology, Department of Forest Botany, University of Göttingen. Research fellow for the Competence Network for the Sustainable Use of Wood (N.H.N. e.V.). Dissertation: "FTIR-ATR spectroscopic and FTIR-FPA microscopic investigations on panel board production processes using Grand fir (*Abies grandis* (Douglas ex D. Don) Lindl.) and European beech (*Fagus sylvatica* L.)". Supervisor: Prof. Dr. Andrea Polle.
11/2005	M.Sc. of Forest Science, Faculty of Forest Science and Resource Management, Technical University of Munich (TUM).
09/2005	Dipl.-Ing. (silv.), Faculty of Forest Science and Resource Management at the Technical University of Munich (TUM). Thesis: „Möglichkeiten einer wildökologischen Raumplanung im Forstamtsbereich Oberammergau". Supervisor: Prof. Dr. Wolfgang Schröder.
09/1999- 02/2001	Business studies, University of Passau, Germany.
09/1989-06/1999	Secondary school, Joseph-von-Fraunhofer Gymnasium, Cham, Germany.
09/1985-07/1989	Primary school, Cham, Germany.

Publications

Müller, G., Bartholme, M., Kharazipour, A., Polle, A. (2008). FTIR-ATR spectroscopic analysis of changes in fiber properties during insulating fiberboard manufacture of beech wood. *Wood and Fiber Science.* (submitted).

Müller, G., Vos, H., Kharazipour, A., Polle, A. (2008). FTIR-ATR spectroscopic analysis of changes in wood properties during particle- and fiberboard production of hard- and softwood trees. *Holzforschung*. (submitted).

Rana, R., **Müller, G.**, Naumann, A., Polle, A. (2008). FTIR spectroscopy in combination with principle component analysis or cluster analysis as a tool to distinguish beech (*Fagus sylvatica* L.) trees grown at different sites. *Holzforschung*. (submitted).

Müller, G., Naumann, A., Olbrich, A., Polle, A. (2008). Imaging of lignin and cellulose in soft and hardwood species using FTIR microscopy and STEM. (draft).

Müller, G., Olbrich, A., Naumann, A., Polle, A. (2007). FTIR spectroscopy and microscopy in combination with cluster analysis as tools for analysis and control of wood properties and production processes. In: *Review of Forests, Wood Products and Wood Biotechnology of Iran and Germany*. Eds. Kharazipour A., Schöpper C., Müller C. pp. 46-57.

Müller, G., Polle, A. (2007). Optimization and control of hardwood processing using FTIR spectroscopy combined with cluster analysis. In: *Proceedings of the 1st International Scientific Conference on Hardwood Processing*. 24-26.09.2007, Québec, Canada. Ed. Blanchet, P. pp.149- 155.

Müller, G., Naumann, A., Polle, A. (2007). FTIR spectroscopy in combination with cluster analysis as tool for analysis and control of wood properties and production processes. In: *The Plant Cell Wall-Recent Advances and New Perspectives*. Mitteilungen der Bundesforschungsanstalt für Forst- und Holzwirtschaft Hamburg (223). Eds. Schmitt, U., Singh, A.P., Harris, P.J. pp.129-136.

Oral presentations

02/2008   3rd German-New Zealand Cell Wall Symposium, 13.-15.02.2008, Auckland, New Zealand.

09/2007   1st International Scientific Conference on Hardwood Processing, 24-26.09.2007, Quebec, Canada.

11/2006   University of Teheran, 01.11.2006, Teheran, Iran.

10/2006   2nd German-New Zealand Cell Wall Symposium. Bundesforschungsanstalt für Forst- und Holzwirtschaft, 04.-06.10.2006, Hamburg, Germany.

Poster presentations

09/2007   „Innovation durch spektroskopisch-bildanalytisch kontrollierte Produktions-
prozesse für Holzwerkstoffe", BMBF- Tagung, Universität Göttingen,
Germany.

05/2007   „FTIR-Spektroskopie und Mikroskopie an *Abies grandis* und *Fagus sylvatica*",
LIGNA, Hannover, Germany.

07/2006   Biologische Analyse von Holz und Holzwerkstoffen (*Fagus sylvatica, Abies
grandis*), „Tag der Niedersachsen", Melle, Germany.